WL-TR-96-4015

CERAMIC BEARING DEVELOPMENT

VOL 1, FATIGUE AND WEAR BEHAVIOR OF NBD-200 SILICON NITRIDE BALLS

HAROLD I. BURRIER, JR.
CHARLES BURK

NORTON ADVANCED CERAMICS
DIV. OF SGNICC
10 AIRPORT PARK ROAD
EAST GRANBY, CT 06026

MARCH 1995

INTERIM REPORT FOR 08/01/92-10/01/94

MATERIALS DIRECTORATE
WRIGHT LABORATORY
AIR FORCE MATERIEL COMMAND
WRIGHT PATTERSON AFB OH 45433-7734

NOTICE

When government drawings, specifications, or other data are used for any purpose other than in connection with a definitely related government procurement operation, the United States Government thereby incurs no responsibility nor any obligation whatsoever; and the fact that the government may have formulated, furnished, or in any way supplied the said drawings, specifications, or other data, is not to be regarded by implication or otherwise as in any manner licensing the holder or any other person or corporation, or conveying any rights or permission to manufacture, use, or sell any patented invention that may in any way be related thereto.

This report is releasable to the National Technical Information Service (NTIS). At NTIS, it will be available to the general public, including foreign nations.

This technical report has been reviewed and is approved for publication.

KARL R. MECKLENBURG, Project Engineer
Nonstructural Materials Branch
Nonmetallic Materials Division

KENT J. EISENTRAUT, Chief
Nonstructural Materials Branch
Nonmetallic Materials Division

CHARLES E. BROWNING, Chief
Nonmetallic Materials Division
Materials Directorate

If your address has changed, if you wish to be removed from our mailing list, or if the addressee is no longer employed by your organization, please notify WL/MLBT, Bldg 654, 2941 P Street, Suite 1, Wright-Patterson AFB OH 45433-7750 to help maintain a current mailing list.

Copies of this report should not be returned unless return is required by security considerations, contractual obligations, or notice on a specific document.

DISCLAIMER NOTICE

THIS DOCUMENT IS BEST QUALITY AVAILABLE. THE COPY FURNISHED TO DTIC CONTAINED A SIGNIFICANT NUMBER OF PAGES WHICH DO NOT REPRODUCE LEGIBLY.

REPORT DOCUMENTATION PAGE

Form Approved
OMB No. 0704-0188

1. AGENCY USE ONLY (Leave blank)	2. REPORT DATE	3. REPORT TYPE AND DATES COVERED
	MAR 1995	INTERIM 08/01/92--10/01/94

4. TITLE AND SUBTITLE CERAMIC BEARING DEVELOPMENT

VOL 1, FATIGUE AND WEAR BEHAVIOR OF NBD-200 SILICON NITRIDE BALLS

5. FUNDING NUMBERS

C F33615-92-C-5917
PE 62712
PR 8355
TA 00
WU 07

6. AUTHOR(S)

HAROLD I. BURRIER, JR.
CHARLES BURK

7. PERFORMING ORGANIZATION NAME(S) AND ADDRESS(ES)

NORTON ADVANCED CERAMICS
DIV OF SGNICC
10 AIRPORT PARK ROAD
EAST GRANBY CT 06026

8. PERFORMING ORGANIZATION REPORT NUMBER

9. SPONSORING/MONITORING AGENCY NAME(S) AND ADDRESS(ES)

MATERIALS DIRECTORATE
WRIGHT LABORATORY
AIR FORCE MATERIEL COMMAND
WRIGHT PATTERSON AFB OH 45433-7734

10. SPONSORING/MONITORING AGENCY REPORT NUMBER

WL-TR-96-4015

11. SUPPLEMENTARY NOTES

12a. DISTRIBUTION/AVAILABILITY STATEMENT

APPROVED FOR PUBLIC RELEASE; DISTRIBUTION IS UNLIMITED.

12b. DISTRIBUTION CODE

13. ABSTRACT *(Maximum 200 words)*

These are the test results of the fatigue and wear performance of NBD-200, silicon nitride balls under conditions of rolling contact in ball bearings. Life testing was done under conditions of load and EHD film thickness equal to or more severe than those to be expected in turbine engine mainshaft applications. The actual temperatures and speeds of those applications were not simulated.

No fatigue failures occurred in a sample of 556 "standard" NBD-200 balls within a test limit of five times the experimentally - determined L-10 life of the AISI 52100 steel balls. Ball failures did occur in a sample of balls identified by a Surface Acoustic Wave NDE technique as being flawed, but the correspondence between the estimated severity of the flaws and the specific ball failures was not good. A Thermal Proof Testing technique for eliminating balls with flaws may possibly have promoted failures of balls that otherwise would have performed satisfactorily. Wear tests, performed under moderate to severe boundary lubrication conditions showed no measurable, "conventional" wear. The life - limiting factor in these hybrid bearings was microspalling of the AISI 52100 and M-50 steel races.

14. SUBJECT TERMS

Wear Coefficient Testing Ferrographic Evaluation of Selected Test Lubricants Wear Modeling Baseline Testing Critical Flaw Size Determination

15. NUMBER OF PAGES 143

16. PRICE CODE

17. SECURITY CLASSIFICATION OF REPORT	18. SECURITY CLASSIFICATION OF THIS PAGE	19. SECURITY CLASSIFICATION OF ABSTRACT	20. LIMITATION OF ABSTRACT
UNCLASSIFIED	UNCLASSIFIED	UNCLASSIFIED	SAR

Table of Contents

Table of Contents (Continued)

List of Figures

List of Figures (Continued)

List of Figures (Continued)

List of Figures (Continued)

List of Figures (Continued)

List of Figures (Continued)

List of Figures (Continued)

List of Figures (Continued)

List Of Tables

Foreword

This work was performed by Harold I. Burrier Jr., in cooperation with and as a subcontractor to Norton Advanced Ceramics, Division of Saint Gobain/Norton Industrial Ceramics Corporation. This report presents the results of seven tasks included in subcontract number 2884 of prime contract F33615-92-C-5917, issued by the United States Department of the Air Force, Air Force Systems Command, WPAFB, Dayton Ohio.

This written report is mainly the work of Harold I. Burrier Jr. The contributing efforts of Michael R. Hoeprich and Teri R. Reese, key to the success of this program, are gratefully acknowledged.

Contributions of the following individuals to the completion of this work are acknowledged: Charles Burk, of Norton Advanced Ceramics, John Lucek, formerly of CERBEC. Inc, Peter Ward and Keith Gordon, of MPB Corporation, Robert Hanson and Clark Griffiths of Split Ball Bearing, Charles Mozden, Mark Frank, Joel Russell, David Lawrentz and Michell, of Timken Research.

Several additions, changes and edits were made to this report at Norton Advanced Ceramics.

1.0 Summary

The fatigue and wear performance of (Norton Advanced Ceramics' NBD-200) silicon nitride balls were investigated in complete ball bearing assemblies under lubrication and loading conditions intended to represent those encountered by components of hybrid ball bearings in turbine engine mainshaft applications. The actual operating temperatures and speed conditions of a mainshaft bearing could not, however, be simulated in this testing. Extensive use was made of scanning electron microscopy, metrology and ferrographic techniques to document the nature of the fatigue and wear mechanisms.

A baseline fatigue life of NBD-200 balls which had passed the N.A.C. "standard" level of inspection for 336 Consumable Electrode Vacuum Melt (CEVM) AISI 52100 steel balls was determined by testing. A total of 336 NBD-200 balls were life tested at the same contact stress as the steel balls and 224 NBD-200 balls at a stress level 20 percent higher than that of the steel ball tests. In five "least-of-four" bearing tests, no failures of the NBD-200 balls occurred within a cutoff limit of five times the L_{10} life of the steel balls. Thus, it appears that NBD-200 balls in hybrid bearings possess a significantly greater fatigue life than that of premium quality bearing steel.

An attempt was made to determine the "critical flaw size" for NBD-200 balls under rolling contact loading conditions. Groups of balls were artificially flawed by indenting with a Vickers diamond hardness indentor at three different load levels. Under life test conditions identical to those of the baseline life tests, only the balls indented with the highest load failed within the 1050 hour cutoff limit. These balls contained surface cracks, as a result the indentations, of 172 μm length. Cracks of 61 μm and 34 μm did not produce spalling. Further analysis, however, indicated that the height of the "shoulders" raised around the indents may have been the critical factor in determining failure, rather than the crack length. A means other than mechanically-indenting for introducing known flaws will be needed in order to determine a true critical size for a general flaw case.

Two novel methods of nondestructive evaluation were then

employed by other N.A.C. subcontractors to produce sets of balls with controlled defect severities for life testing. These balls were life tested under conditions similar to those of the baseline and critical flaw size tests. Two ball failures were encountered in test sets graded through the application of a "Surface Acoustic Wave Technique" at Stanford University. The correlation of the two ball failures with the predicted level of defect severity was, however, not good. Two ball failures were also encountered in life testing of a population which had been inspected using a "Thermal Proof Test" technique developed at the University of Dayton. It appeared that the evaluation technique may, itself, have been the cause of the failures, by increasing the severity of existing flaws, in balls which otherwise may have performed satisfactorily.

The wear behavior of NBD-200 balls was investigated by running them in races made of AISI 52100 steel and M-50 steel. The tests were conducted in MIL-L-23699 lubricant under fairly severe film thickness to surface roughness conditions of $\lambda = 1.0$ and 0.3. Under the test conditions used, wear, in the conventional sense, was not measurable. The observed degradation of the bearings, in all cases, was in the form of microspalling of the steel race surfaces. Wear was not detected on the NBD-200 balls, except in the instance where macro-scale spalling of the races had previously occurred. There were indications that the hybrid bearings caused more change to the bond structure of the MIL-L-23699 lubricant during running than did the all-steel bearings. This chemical change may have been related to the temperatures in the ceramic ball contact area reaching higher levels, due to the lower thermal conductivity of the silicon nitride balls.

The result of a search of the literature on the tribology of silicon nitride in hybrid contacts is included. Actual wear modelling could not be performed, since no wear data was produced in the test runs. An adaptation of the Archard wear model to the geometry of a ball bearing was formulated for the case of either the formation of a general wear track or the loss of material from grain pull-out.

2.0 Introduction

The great potential for the use of ceramic materials, specifically high quality silicon nitride, in rolling element bearings has been stated many times. Its hardness, chemical inertness, light weight, electrical resistivity and nonmagnetic nature provide an excellent combination of properties to the designers of bearings for aerospace, chemical processing, machine tool, and other demanding applications. Progress in implementing silicon nitride into either hybrid, steel / ceramic, or all-ceramic bearings has been impeded, however, by several factors. Of these, cost, undefined reliability, and a lack of engineering design data on the wear, fatigue, and fracture toughness properties of the available materials are paramount.

Specific statements of these needs were presented by experts in the fields of silicon nitride manufacturing, bearing design and manufacturing and potential users, at a NIST / DARPA Ceramic Bearing Workshop held April 17-18, 1991 in Gaithersburg, MD. The proceedings were published as NIST Special Publication 824, Said Jahanmir, Editor. As a result of this input, a DARPA (now ARPA) program on Ceramic Bearing Technology was instituted with Dr. William S. Coblenz as the Program Manager.

Prime Contract No. F33615-92-C-5917 was awarded to CERBEC, Inc., now Norton Advanced Ceramics, a Division of Saint-Gobain / Norton Industrial Ceramics Corporation, for the "Characterization of Si_3N_4 Balls". Functionally, the statement of work was divided into ten different tasks, briefly described as follows:

- Task 3.1.1 Determine the critical flaw size in artificially-flawed NBD-200 balls
- Task 3.1.2 Determine the fatigue life of all-steel bearings for the same conditions.
- Task 3.1.3 Determine the fatigue life of "standard" NBD-200 balls.
- Task 3.1.5 Develop and utilize a Surface Acoustic Wave NDE technique.

- Task 3.1.6 Determine the effectiveness of a Surface Acoustic Wave NDE technique.
- Task 3.2.1 Develop and utilize a Thermal Proof Test NDE technique
- Task 3.2.2 Determine the effectiveness of a Thermal Proof Test NDE technique.
- Task 3.3.1 Find the wear rate for hybrid bearings with different steel race materials.
- Task 3.3.2 Develop a wear model for hybrid bearings.
- Task 3.4 Develop Tribochemical finishing techniques for silicon nitride.

Fatigue life testing and wear testing, with analysis of results, was accomplished by the Timken Co., in fulfillment of tasks 3.1.1, 3.1.2, 3.1.3, 3.1.6, 3.2.2, 3.3.1 and 3.3.2. This work is reported in chapter one of this document. Work performed under tasks 3.1.5, 3.2.1, and 3.4 are reported in volumes two, three, and four of this document.

The ball-life testing performed for tasks 3.1.1, 3.1.2, 3.1.3, 3.1.6 and 3.2.2 will be discussed in a different order, so that the results can be related to the baseline of performance observed in the all-steel bearings. The procedures used for these five tasks will be described, followed by discussions of the results for each individual task. Details of the ferrographic analysis are contained in Appendix form, as are the findings of the literature survey on silicon nitride tribology.

3.0 Procedures

3.1 Baseline, Critical Flaw Size and NDE Verification Testing

The fatigue life testing portions of each of the tasks were performed in identical manners. The procedures will be discussed as a group, with the pertinent differences highlighted in the following sections.

3.1.1 Life Test Bearings

The selection of a bearing configuration in which to evaluate the properties of NBD-200 balls in this program was based on several factors. The most important factor was the size of the ball complement. In order to lend some statistical significance to the test results, it was important to test the largest practical number of balls in each condition, while minimizing the expenditure of test machine time.

The 019-series, angular contact bearing chosen (Figure 1) accommodates 28 balls per assembly, while utilizing a test housing size most readily available at Timken Research. The essential geometric characteristics of the test bearings are listed in Table 1. All of the dimensions were held constant among the various tests, with the exception of the race curvatures. The curvatures of the races for the hybrid bearings were adjusted to yield the same maximum Hertzian contact stress in both the all-steel and the hybrid versions when the same thrust load was applied to each. The material of the races was consumable electrode vacuum-melted (CEVM), AISI-52100 type steel. For the relatively low test temperatures used, this material was expected to have the greatest potential race fatigue life of the possible material choices. A metallurgical examination of sample races and of the steel baseline-test balls (Figure 2) verified that the microstructural and hardness

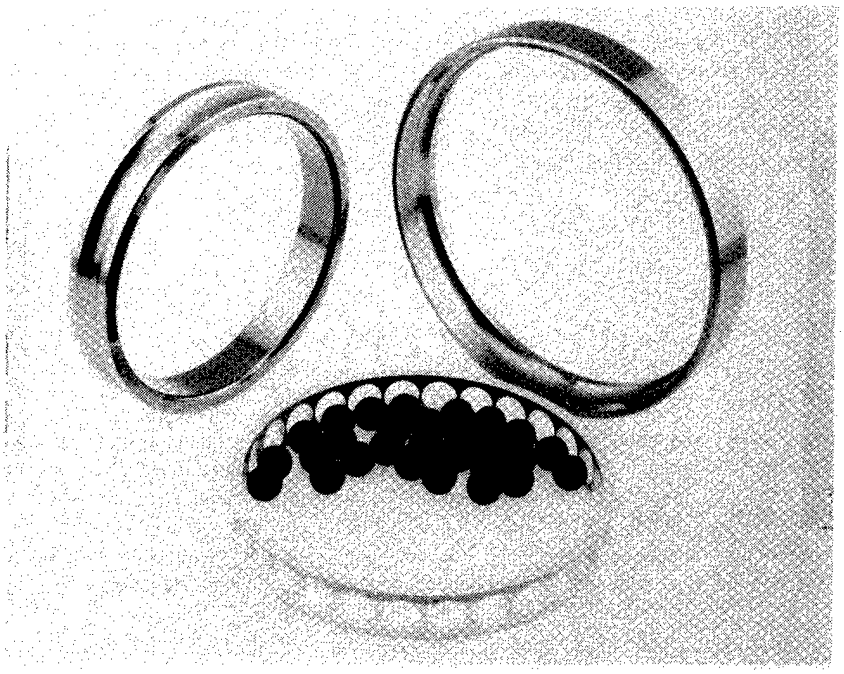

Figure 1 Components of 019-Series Test Bearing Races, Silver-plated AISI 4340 Steel Retainer, Complement of 28 NBD-200 Balls

properties were satisfactory and typical of properly-treated AISI 52100 material. The retainers for these bearings were made of silver-plated 4340 steel.

The test races were designed, manufactured, and assembled by Split Ballbearing Division of MPB Corporation, Lebanon, NH, a subsidiary of The Timken Company. Twelve bearing assemblies were supplied for each of the five tasks. In addition, 20 sets of spare races were manufactured for replacements, in the event of race rather than ball failure in the hybrid bearings.

Table 1
Description Of 019-Series Life Test Bearings

SBB PART No.	26-HADH-019-A26	26-HADH-019-26
Race Material	CEVM, AISI 52100 Steel	Same
Ball Material	Silicon Nitride, NBD-200	CEVM, AISI 52100 Steel
Number Of Balls	28	28
Ball Size 7/16" Grade 10	0.43750" (11.112mm)	Same
Outer Race O.D.	5.1181" (130.00mm)	Same
Inner Race I.D.	3.7402" (95.00mm)	Same
Bearing Width	0.7087" (18.00mm)	Same
Pitch Diameter	4.4291" (112.50mm)	Same
Contact Angle	25°	Same
Outer Race Curvature	0.5165	0.5270
Inner Race Curvature	0.5220	0.5200

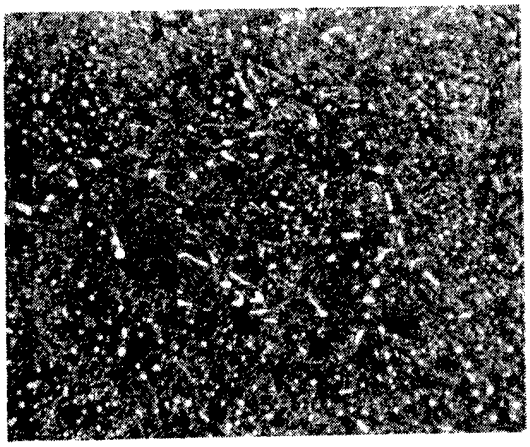

Outer Race

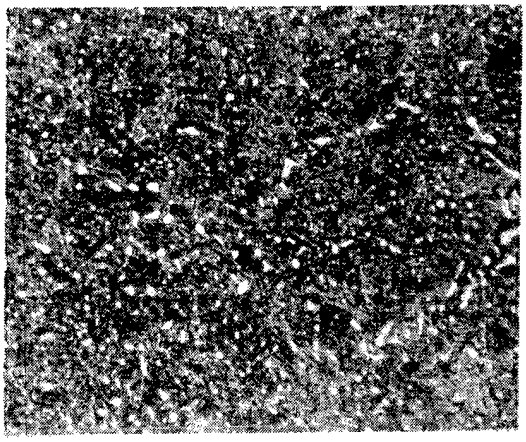

Inner Race

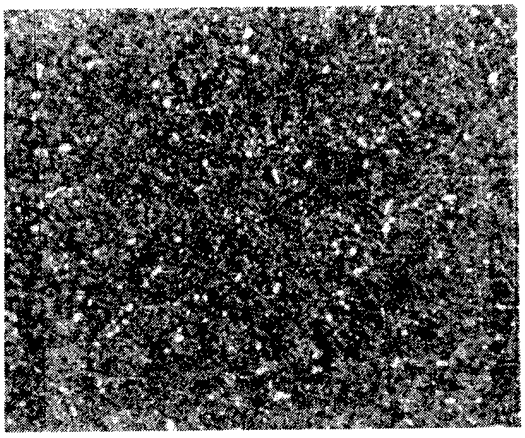

7/16 Diameter Ball

Figure 2 Microstructure of AISI-52100 Material Nital Etched 1000X Magnification.

The silicon nitride NBD-200 balls for the hybrid bearing tests were supplied by Norton Advanced Ceramics Division of Saint-Gobain / Norton Industrial Ceramics Corporation, East Granby, CT. At the inception of this program and at the time of manufacture of the test balls, Norton Advanced Ceramics was known as CERBEC, Inc. The balls were all from one manufacturing lot (powder lot and hot isostatic-pressing run) but were from three different finishing lots as enumerated in the Results section. They were produced to 7/16 inch diameter (11.113 mm), AFBMA Grade 10, "zero gage increment".

3.1.2 Bearing Life Test Equipment

The configuration of the Timken Company-designed, "5-inch" (approximate maximum outer ring diameter) life test housings used for these tests is illustrated in Figure 3. Four different housings were employed for reasons of availability at various times during the test programs. Thrust loading of four bearings at a time was accomplished through a coaxially-mounted hydraulic cylinder. The load value was verified through the use of an electronic load cell. In these purely thrust tests, the radial loading cylinder shown below the bearings in Figure 3 was not used. Lubrication of the test bearings was supplied at a constant rate from a temperature-controlled system through a nominal 41-micron filter to the three inlet positions shown.

3.1.3 Life Testing Parameters

The test lubricant for all of the life tests was EXXON "Turbo Oil-2389", to Spec. MIL-L-7808, Rev. J. A flow rate of 0.016 l /s / bearing (2 pt / min / bearing) was maintained throughout the tests.

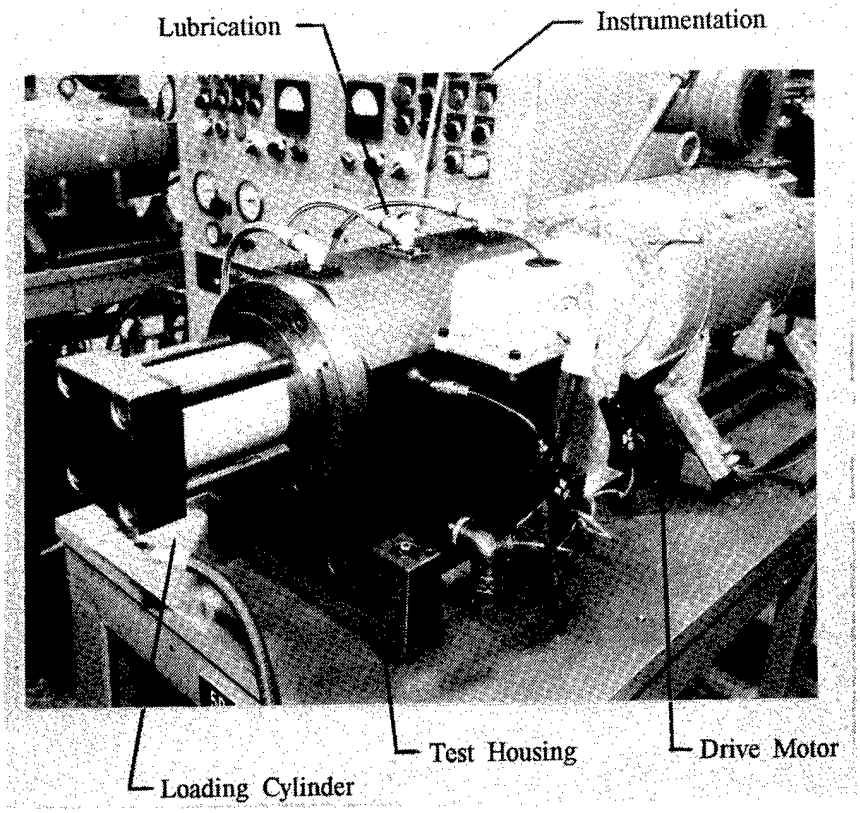

Figure 3 "5-Inch" Bearing Life Test Machine Used To Test 019-Series Bearings.

The inlet lubricant temperature was controlled at 66°C (150°F). All of the tests were run at a rotational speed of 2700 rpm. The load-up procedure for new bearings in each of the tests consisted of increasing the load linearly from zero to one-half of the intended full load over an 8-hour period, followed by a 16-hour hold at half load. The load was then increased linearly to its full value over an additional 8-hour period.

Three sets of four bearings each were run in the steel baseline tests, the critical flaw size tests, and the NBD-200 baseline tests. Each of these tests were run at a maximum Hertzian contact stress of 2.41 GPa (350 Ksi). The applied thrust load to achieve this stress was 30.248 KN (6800 lbf). Under these test conditions, the calculated ball / race EHD film thickness was on the order of 0.13 μm (5.1 μ-in).

Because no ball failures were obtained in the NBD-200 baseline test, two additional sets of four bearings, were run at an increased maximum Hertzian stress condition of 2.88 GPa (420 Ksi). The additional bearing sets were obtained from the bearing sets used for the NDE verification tasks. An applied thrust load of 53.824 KN (12100 lbf) was required to produce this stress level. The film thickness was essentially unchanged by the increase in load.

3.1.4 Critical Flaw Size Specimen Preparation

Balls for the tests to determine the critical flaw size in NBD-200 material were artificially flawed by indenting with a Vickers diamond hardness indentor. The severity of the defect, the crack length, was controlled by changing the load at which the indentations were made. Six impressions were made on each of the 112 balls per test, located on the "poles" and at 90° spacings on the "equator" of the balls. The loading conditions used for indenting were an infeed rate of 200 microns / second (0.008 in/sec.), with a 10 second dwell time at load. Balls for the initial test were from CERBEC manufacturing lot No. 932766.01, and were indented at a load of 5.0 Kg (49.0 N). Indentation loads for the subsequent tests were selected on the basis of fatigue life results from the preceding tests.

3.2 Wear Coefficient Testing

The initial plan for conducting the investigation into the wear rate coefficients of hybrid bearings called for testing four bearings of each of three steel types for various lengths of time and under two different film thickness / roughness ratios (λ). Due to several experimental difficulties, the original plan was modified to eliminate one of the steel types, and to include additional load and film thickness conditions.

3.2.1 Wear Test Bearing Selection

The bearings used for this test, Figure 4, were manufactured by MPB Corporation, Keene, NH. They were of an R-8 size, made to ABEC 7P tolerances. The pertinent dimensions are shown in Table 2. Each bearing contained 10 balls, 5/32" (3.969 mm) in diameter, enclosed in crown-type, snap-in, phenolic laminate retainers. The NBD-200 balls were supplied from CERBEC manufacturing lot No. 912449.10, to AFBMA Grade 5.

The race materials which were tested were CEVM AISI-52100 steel and VIMVAR M-50 type steel. The third test material was to have been the high-temperature carburizing steel M-50NiL. Difficulties with manufacturing and heat treating races of this small size from M-50NiL, however, proved unsolvable within the time frame of this program, and these races were not available for testing.

3.2.2 Wear Test Equipment

Wear coefficient testing was performed in a Timken Company-designed, single bearing lubricant and wear test machine, Figure 5. The machine applies a pneumatically-controlled thrust load to a single bearing as the inner race is rotated at variable speeds, up to about 3000 RPM. Lubrication is applied as an initial, fixed quantity of the chosen lubricant which is maintained at the selected test temperature by resistance heating elements. Provisions are made to monitor and record the bearing test temperature and torque. Shut-down of the machine occurs if either of these parameters varies outside of their set range.

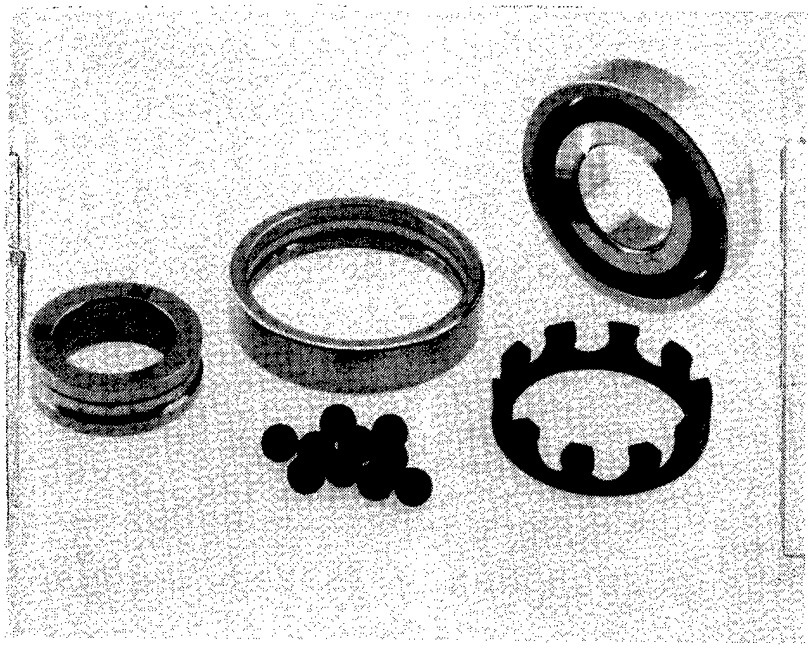

Figure 4 R-8 Bearing And Components For Hybrid Bearing Wear Testing: Steel Races, Phenolic Laminate Retainer, Ten NBD-200 Balls.

Table 2
Description Of R-8 Sized Wear Test Bearings

CHARACTERISTIC	DATA
Race Materials	CEVM AISI 52100 Steel Vimvar M-50 Steel
Ball Materials	Silicon Nitride, NBD-200 Vimvar M-50 Steel
Retainer Material	Phenolic Laminate
Number Of Balls	10
Ball Size 5/32" Grade 5	3.9687mm (0.15625")
Outer Race O.D.	28.575mm (1.1250")
Inner Race I.D.	12.700mm (0.5000")
Bearing Width	6.350mm (0.250")
Contact Angle	15°
Pitch Diameter	21.6344mm (0.85175")
Race Curvature, Outer	0.5300
Race Curvature, Inner	0.5200

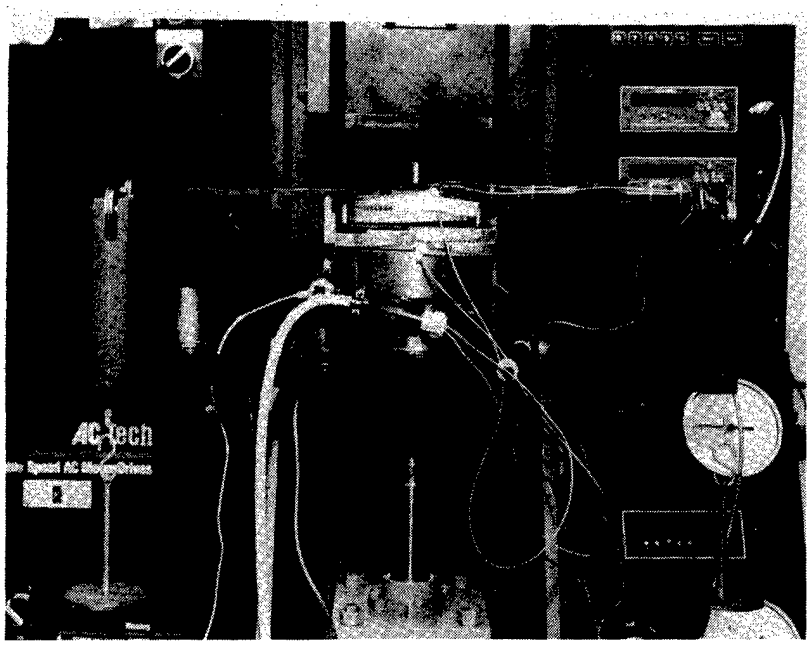

Figure 5 Single-Bearing Wear And Lubricant Test Machine For R-8 Bearings.

3.2.3 Wear Test Operating Parameters

As originally conceived, the wear rate testing was to have been carried out at EHD film thickness / surface roughness ratios of 1.0 and 2.0 in the same type MIL-L-7808 lubricant that was used in the life test tasks. To achieve the necessary film thicknesses of 0.05 μm (2.1 μin) and 0.11 μm (4.2 μin) at a bearing speed of 3000 RPM would have required unrealistically-low bearing operating temperatures; as low as 24°C (75°F). A change of lubricant was made, therefore, to the somewhat higher viscosity MIL-L-23699 fluid (MOBILJET II). Operating temperatures for the film thickness / roughness ratios of 1.0 and 2.0 were thereby raised to the somewhat more reasonable levels of 60°C (140°F) and 38°C (100°F), respectively. At these temperatures, MIL-L-23699 was expected to have viscosities of 13.5 centistokes and 32 centistokes. The humidity during the wear tests was not specifically controlled, and was typical of the building air conditioning. This was recorded to have ranged from 22 to 47% at various times throughout the test program. The fact that the bearings were submerged in heated oil during testing was considered to have largely mitigated any influence from the room humidity condition.

The planned maximum Hertzian contact stress for these tests was 2.76 Mpa (400 Ksi), requiring an axial load of 965 N (217 lbf). Based on the outcome of the early rounds of testing, some tests were also conducted under conditions of lower stress 2.61 GPA (379 Ksi) and lower film thickness / roughness ratio, λ = 0.3, obtained by lowering the axial load to 765 N (172 lbf) and increasing the temperature to 121°C (250°F).

For each of the test conditions, the pretest-documented bearing (see pretest procedure below) was installed into the machine and a lubricant charge of 3.0 ml was added. The bearing temperature was brought to the selected value and stabilized prior to start-up. The loads and speeds were increased, stepwise, over a period of about 5 minutes, to their final values.

3.2.4 Evaluation Procedures

Prior to each wear test, the test bearing was documented by cleaning, weighing, SEM characterization, and tracing of the components for profile and surface finish. These steps were

essentially duplicated at the end of each wear test run for comparison.

For cleaning, the components were immersed in heptane in a "Branson 2200" ultrasonic cleaner and agitated for 30 minutes at a temperature of 40°C (104°F). The solvent was removed by drying in a vacuum dessicator for 30 minutes at 60°C (140°F), and the bearing then cooled to room temperature in a separate dessicator. The steel components were demagnetized prior to weighing. The outer race, inner race, ball set, and retainer were weighed separately on a Mettler Model AE200 balance to the nearest 0.1 mg. The average of three determinations was used to specify the weight.

The scanning electron microscope observations were made with a Cambridge "Stereoscan 250" unit, operated at an accelerating voltage of 20 Kv. The NBD-200 balls and, in some instances, the steel components were sputter-coated with palladium for enhanced imaging.

Profile and surface finish tracing was done with a "Form Talysurf", Model S-5, made by Rank, Taylor and Hobson.

4.0 Results and Discussion

4.1 Baseline Testing

There were two objectives of the "baseline" life tests: to provide an all-steel bogey to compare with the performance of the hybrid bearings, and to provide a benchmark of performance of "standard" NBD-200 balls against which the benefit of the NDE techniques could be assessed.

4.1.1 All-steel bearings

Each of the three tests of a group of four bearings with CEVM 52100 steel balls was terminated by the fatigue failure of one or more of the balls. The "first-in-four" lives of the three groups were, in millions of revolutions: 28.833, 35.967 and 81.820. In the analysis of the results of "first-in-four" testing, each failure represents an estimate of the L-15.9 life of the population. The results of the "median ranks" Weibull analysis of the data for the population is shown in Table 3.

Table 3
Weibull Analysis of "Median Ranks" for
CEVM 52100 All Steel Bearings

PARAMETER	LIFE, Million Rev's	LIFE, HOURS
L-15.9 Life	46.518	287
upper 90% Conf. Limit	89.722	554
lower 90% Conf. Limit	17.670	109
L-10 Life	34.172	210
Weibull Slope	1.613	---

The previously agreed-upon suspension bogey for the hybrid bearings, in the event of no ball failures, was 5 times the L-10 life of the all-steel bearings. Therefore, a run-out limit of 1050 hours for the NBD200 hybrid bearings was established from these results.

The appearance of the spalling damage which occurred on the 52100 steel balls is illustrated in Figure 6. Figure 6d shows the detail of an apparent origin of the spalling damage in the steel balls. Spalling of the races did not occur in the all-steel bearings.

Figure 7 compares the appearances of areas of tested races which were either inside or outside the loading track. The primary difference is in the smoothed or blunted nature of the surface texture in the area over-run by the balls. The surface finish traces and measurements displayed in Figures 8a and 8b also show that the races were somewhat smoother (Ra) in the loading track than in the original surface finish. The finish of the steel balls, on the other hand, became marginally rougher, due to scratches or debris dents which were incurred with running.

4.1.2 NBD-200 Hybrid Bearings

Three sets of four bearings assembled with "standard" inspection NBD-200 balls from CERBEC manufacturing lot # 932766.01 were tested under conditions identical to those of the all-steel baseline tests. Each of these sets of 112 balls achieved the selected run-out bogey of 1050 hours with no ball failures. Thus, it appears that the fatigue durability of standard NBD-200 balls under these test conditions

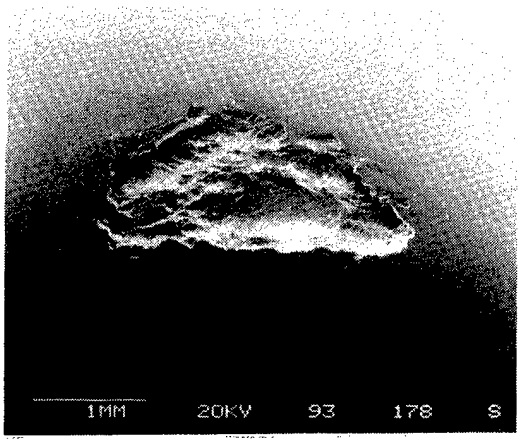

(a)

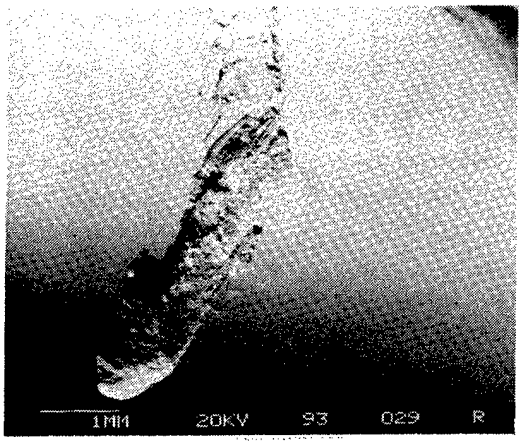

(b)

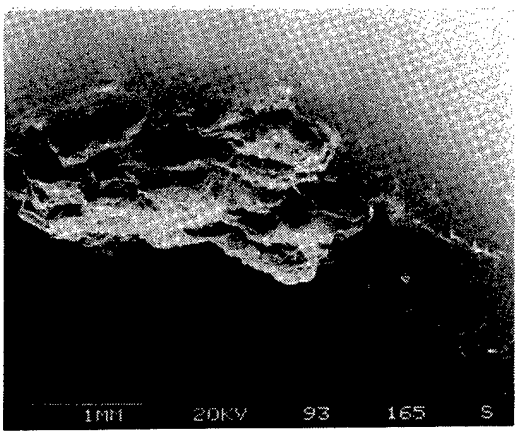

(c)

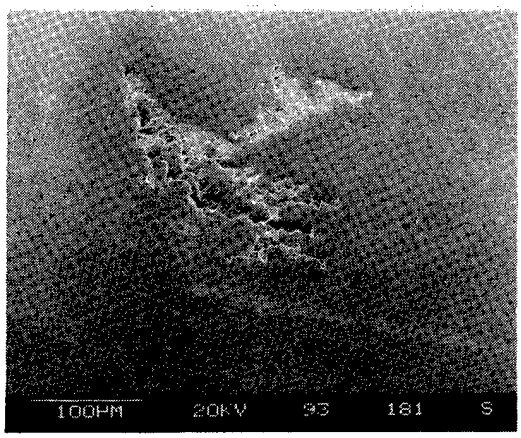

(d)

Figure 6 Appearance Of Spalling Damage On Tested AISI 52100 Steel Balls: (a) Bearing 0002 178 Hr., (b) Bearing 0007 222 Hr., (c) Bearing 0010 505 Hr., (d) Bearing 0002 Second Spall, Origin.

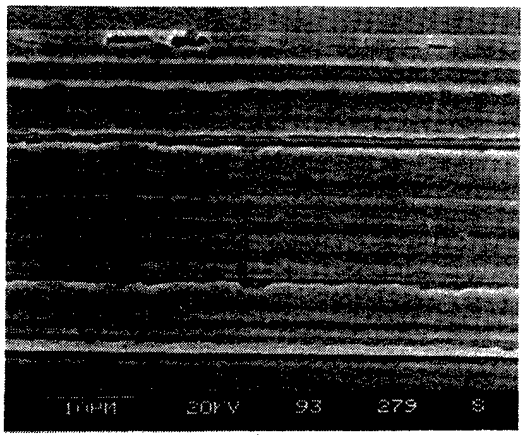

(a)

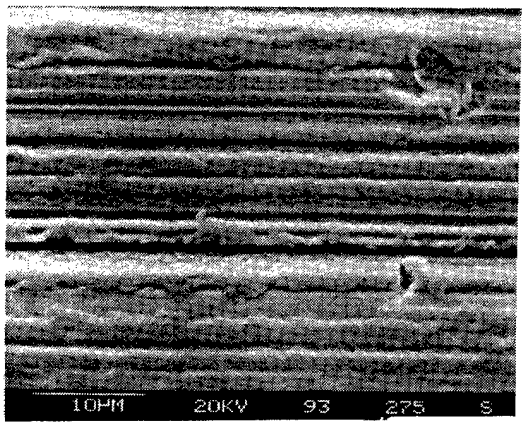

(b)

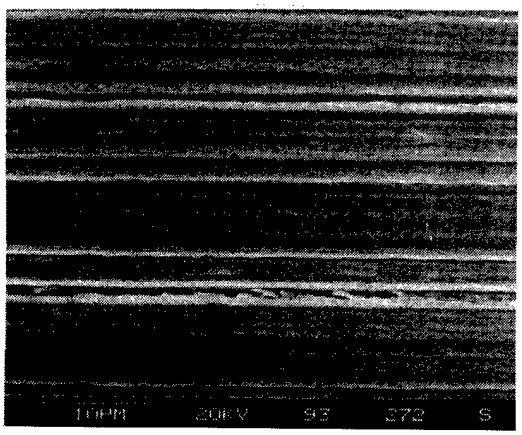

(c)

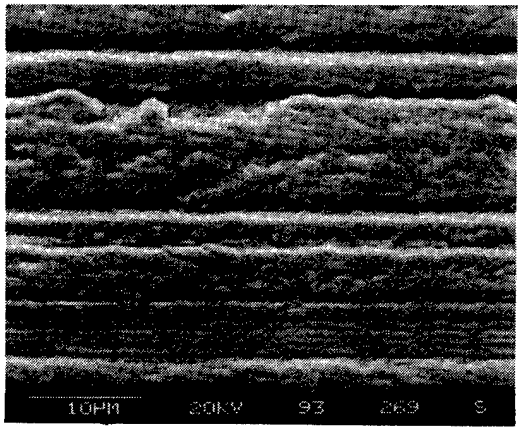

(d)

Figure 7 Changes In Surface Of Races Run With Steel Balls For 222 Hours: (a) Outer Race, Out Of Ball Track, (b) Outer Race, In Ball Track, (c) Inner Race, Out Of Ball Track, (d) Inner Race, In Ball Track.

Outer Race

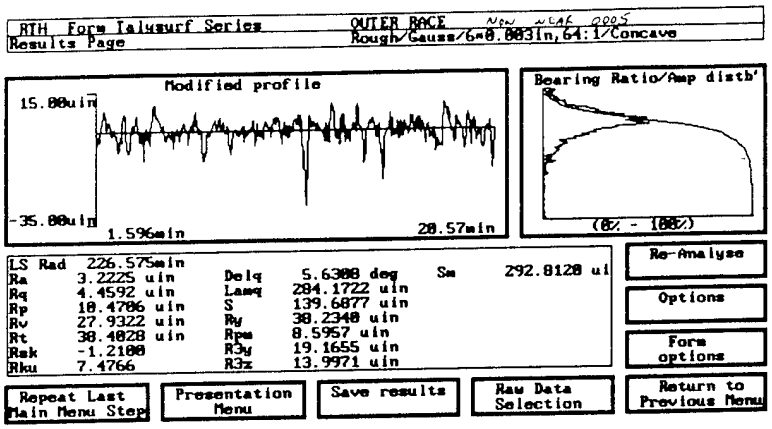

Inner Race

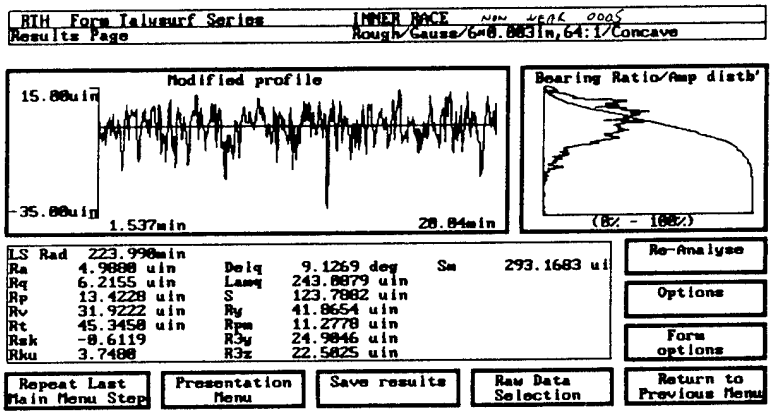

Ball

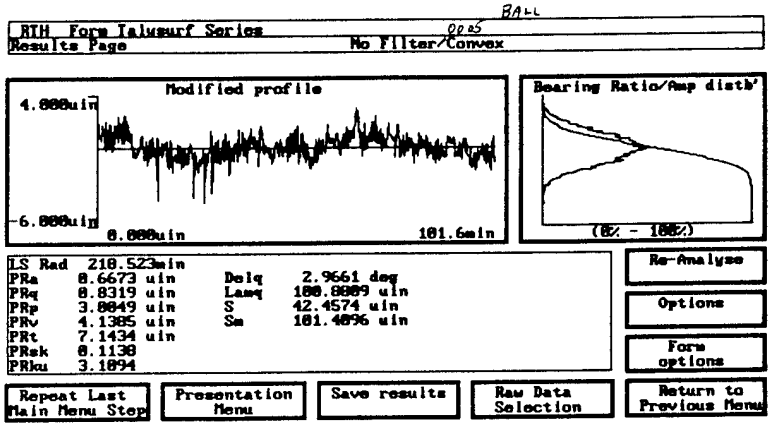

Figure 8a Surface Finish Of AISI 52100 Steel Bearing Components In Areas Outside Wear Tracks.

Outer Race

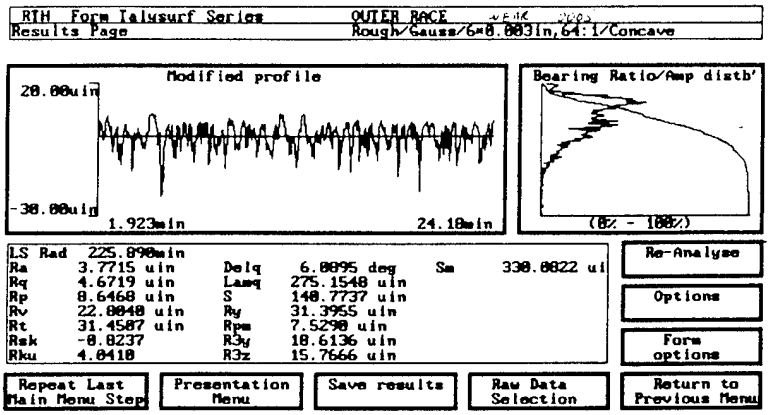

Inner Race

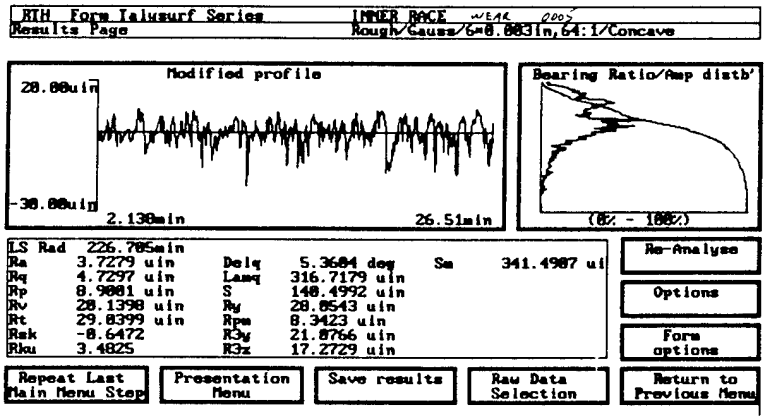

Ball

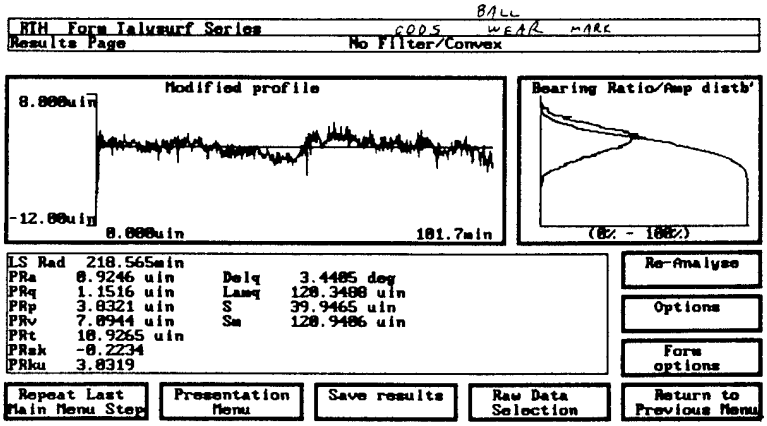

Figure 8b Surface Finish Of AISI 52100 Steel Bearing Components In Wear Tracks After 222 Hours (Bearing No. 0005).

is significantly greater than that of CEVM-52100 steel balls. Since no NBD-200 ball failures were produced under the initial test conditions, two additional four-bearing sets were assembled from races that had been intended for the NDE verification tests. Balls for these bearings came equally from CERBEC manufacturing lots #932766.02 and 932766.03. These bearings were tested at an increased maximum Hertzian contact stress level of 2.88 GPa (420 ksi). These two sets of bearings reached or surpassed the stress-adjusted, run-out bogey of 250 hours, also with no failures among the standard NBD-200 balls.

Table 4 summarizes the results of the baseline testing of both the all-steel bearings and the hybrid, NBD-200 bearings. It is apparent that the NBD-200 balls are significantly superior to CEVM-52100 steel balls in this test. A comparison of the race lives in bearings assembled with either steel balls or NBD-200 balls suggests that no difference in race life is to be expected as a result of the type of balls used. Since no race failures were produced in the all-steel bearings within the life of the balls, however, it can only be considered an estimate that no significant difference exists. The races with all-steel balls would have needed to continue running for about twice the life of the steel balls themselves, for a significant difference to have been shown between steel and ceramic-mated races.

Traces and surface finish measurements made on the races run with NBD-200 balls are illustrated in Figure 9. While the differences are slight, it appears that the surface roughness, Ra, is slightly greater on races tested with NBD-200 balls than on those tested with steel balls. Figure 10 shows the surface texture in the loading track and out of the track for races tested to suspension at 1050 hours with NBD-200 balls. These may be compared with those of Figure 7 from an all-steel bearing.

The difference in the surface texture of an NBD-200 ball in and out of the wear track is shown in Figure 11. The area within the wear track is apparently smoother than that outside of the track, although the difference could not be detected with surface finish measurements.

During the baseline tests of NBD-200 at a contact stress of 2.41 GPa (350 Ksi), any damage to the balls as a result of race failure was undetectable with low power optical microscopy. Balls

which were involved in race failures in the higher stress 2.88 GPa (420 Ksi) tests, however, were found to have surface damage in the form of shallow "scratches" or lines of grain pull-out. Figure 12 shows the typical nature of this damage. The scratches were on the order of 400 μm (0.016in) in length. It is significant that balls with this "natural" damage were run until suspension, with no propagation of the damage in an additional 138 hours of operation of the bearing.

Table 4
Results Of Baseline Testing of AISI 52100 and NBD-200 Balls

AISI 52100 Balls	Max. Stress	Time	Result
Brgs. 0001-0004	2.41 GPa (350ksi)	178 Hr.	Ball Spall, Brg. 0002
Brgs. 0005-0008	2.41 GPa (350ksi)	222 Hr.	Ball Spalls, Brg. 0007
Brgs. 0009-0012	2.41 GPa (350 ksi)	505 Hr.	Ball Spall, Brg. 0010
Race Life L_{10}	2.41 Gpa (350 ksi)	> 89Hr.	No Race Failures
Brgs. 0016-0019	2.41 GPa (350ksi)	105 Hr.	Inner Race Spall, Brg 0016
		1049 Hr.	Suspended, Limit
Brgs. 0020-0023	2.41 GPa (350 ksi)	1047 Hr.	Suspended, Limit
Brgs. 0024-0027	2.41 GPa (350 ksi)	288 Hr.	Inner Race Spall, Brg. 0027
		368 Hr.	Inner Race Spall, Brg. 0026
		494 Hr.	Inner Race Spall, Brg. 0026
		594 Hr.	Inner Race Spall, Brg. 0024
		775 Hr.	Inner Race Spall, Brg. 0025
		1050 Hr.	Suspended, Limit
Brgs. 1-4	2.88 GPa (420 ksi)	159 Hr.	Inner Race Spall, Brg. 3
		297 Hr.	Inner Race Spall, Brg. 3
		297 Hr.	Suspended, Limit
Brgs. 5-8	2.88 GPa (420 ksi)	250 Hr.	Inner Race Spall Brg. 7 Suspended, Limit
Race Life L_{10}	2.41 Gpa (350 ksi)	119 Hr.	
Race Life L_{10}	2.88 Gpa (420 ksi)	95 Hr.	

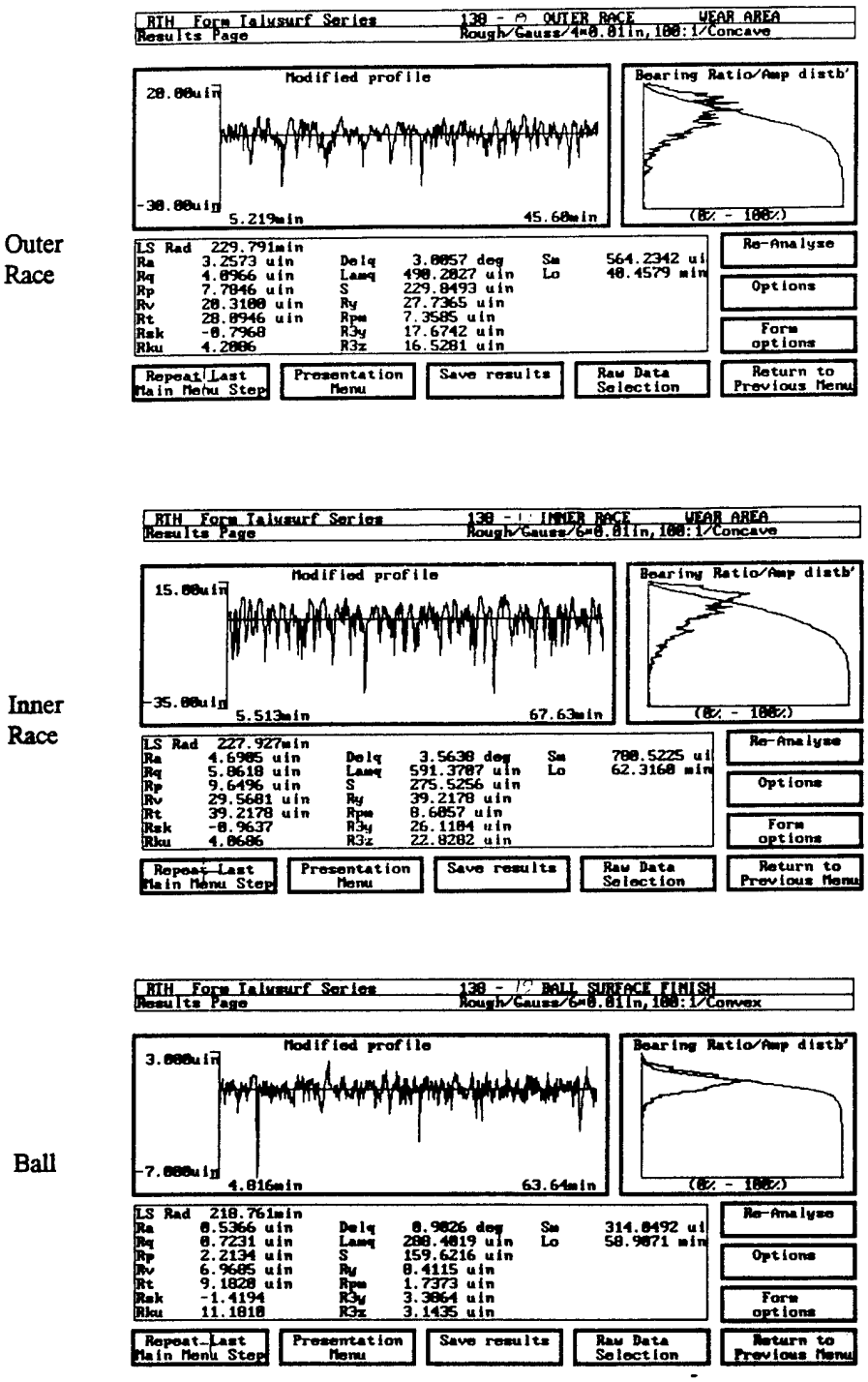

Outer Race

Inner Race

Ball

Figure 9 Surface Finish Of 52100 Steel/NBD 200 Balls In Wear Tracks After 1049 Hr. (Bearing No. 0019).

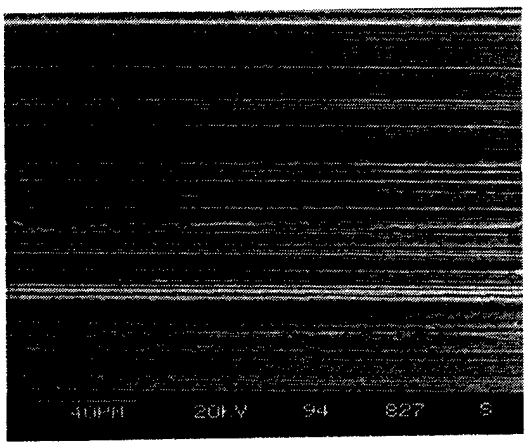

(a)

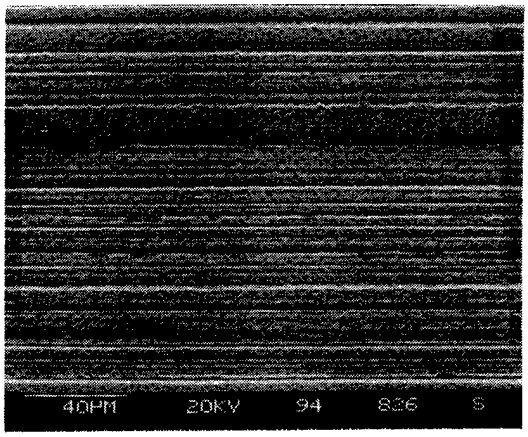

(b)

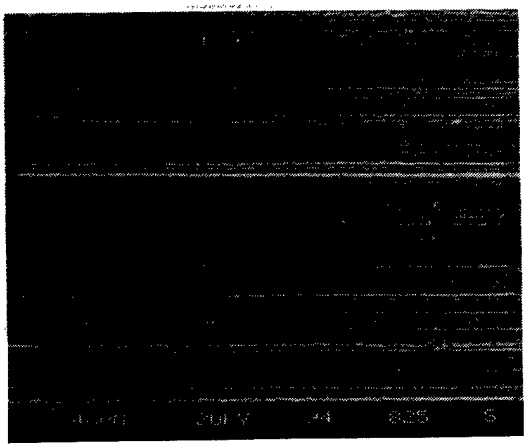

(c)

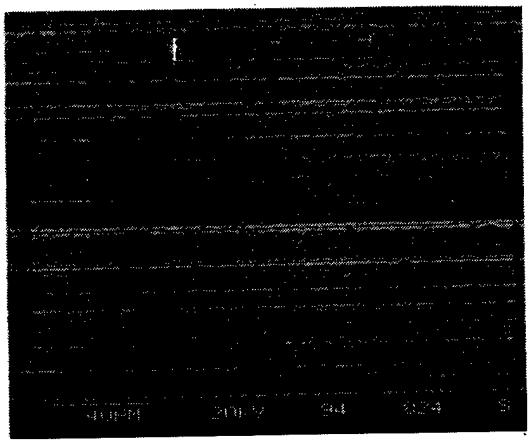

(d)

Figure 10 Changes In Surface Of Races Run With NBD-200 Balls Suspended After 1049 Hr. Running (a) Outer Race, Out Of Ball Track, (b) Outer Race, In Ball Track, (c) Inner Race, Out Of Ball Track (d) Inner Race, In Ball Track.

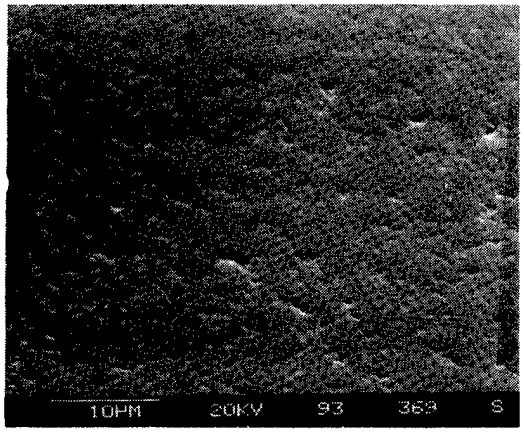

(a)

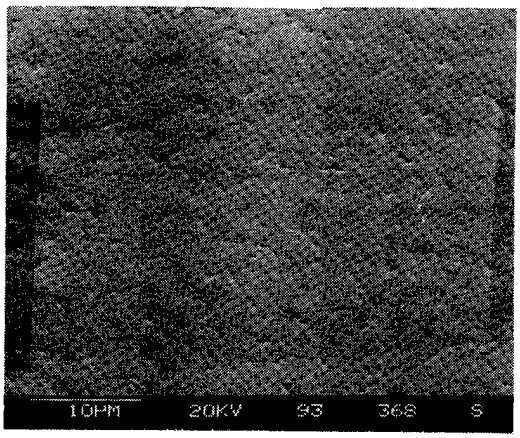

(b)

Out Of
Wear Track

Wear Track

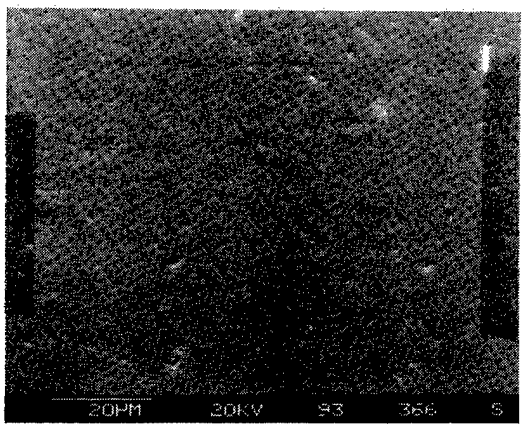

(c)

Figure 11 Surface Of NBD-200 Ball Suspended After 1049 Hrs.:(a) Out Of Wear Track, (b) In Wear Track, (c) Transition.

4.2 Critical Flaw Size Determination

The NBD-200 balls for the critical flaw size tests were produced as CERBEC manufacturing lot #932766.01 (5.0 Kg and 0.5 Kg indents) and #932766.03 (1.0 Kg indents).

4.2.1 Life Test Results

Using a "staircase"-type approach, three levels of Vickers hardness indentations were selected to produce the artificial defects in NBD-200 balls for this task. Since only three sets of bearings were allotted to the task, the steps to bracket the "critical" flaw size were necessarily coarse. The flaw dimensions resulting from each load and the typical appearance of the corresponding flaws are presented in Figure 13. For comparison, the appearance of normal surface flaws on the NBD-200 balls is included. All of the intentionally-produced flaws are very much larger than the normal, occasional grain pull-out seen on the surface of an acceptable ball. Only the largest of the artificial defects was able to produce rolling contact fatigue failures of the balls under the conditions of this test.

In testing balls with indents produced at 5.0 Kg Vickers load, i.e. 172 μm crack length, ball failure occurred even before the intended full load had been reached. The load-up cycle for these tests includes an 8 hour ramp-up to 50% of the test load, followed by a 16 hour hold at 50%, and an 8 hour ramp-up to the full load. After 23.4 hours into the load-up, 15.4 hours at 50% load, failure of balls in two of the bearings occurred. The maximum Hertzian stress at failure, then, was only 1.92 GPa (278 Ksi).

Following these failures, the next set of balls was indented at a lower load of 0.5 Kg, producing an average crack length of 34 μm. Testing of these balls was suspended after a second race spalled at 998

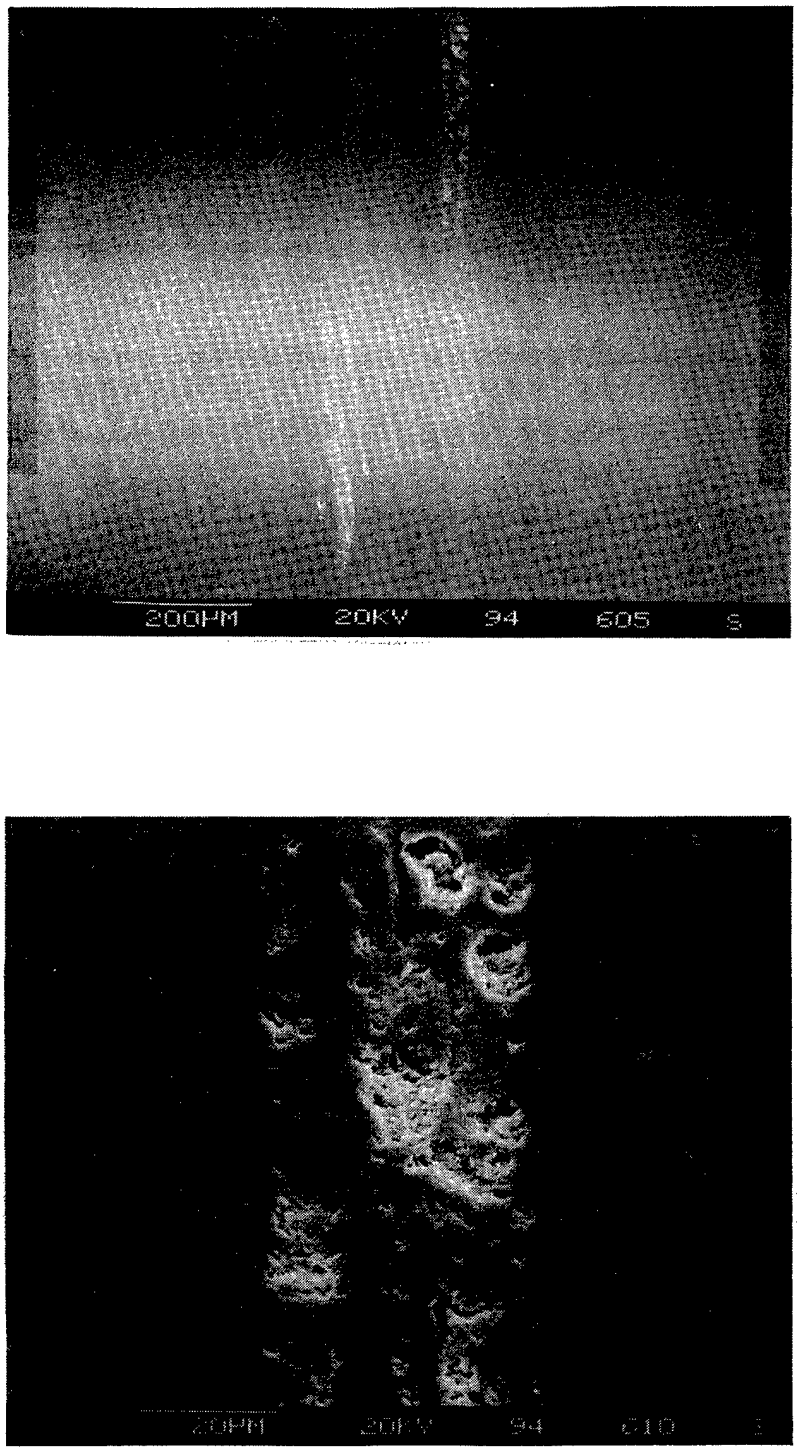

Figure 12 Damage To NBD-200 Ball Resulting From Race Spalling.

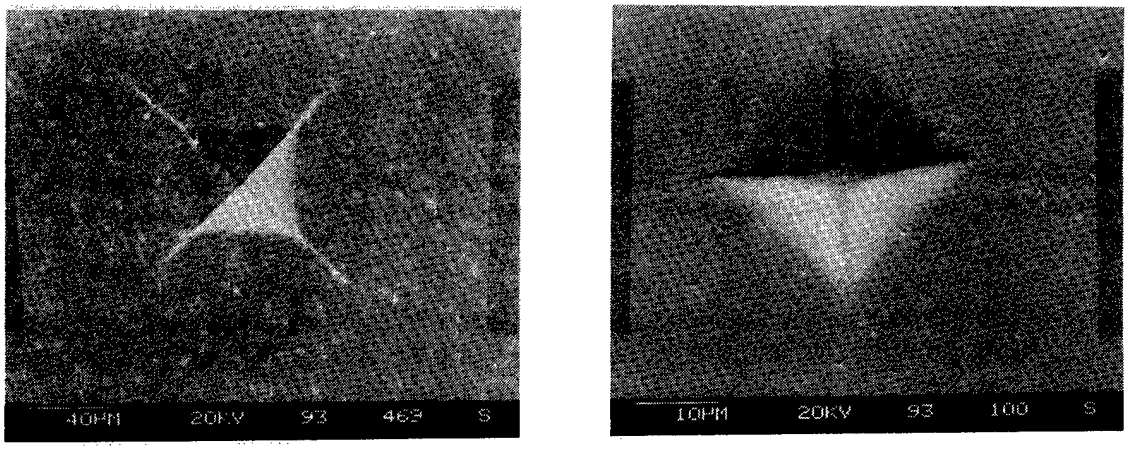

(a) (b)

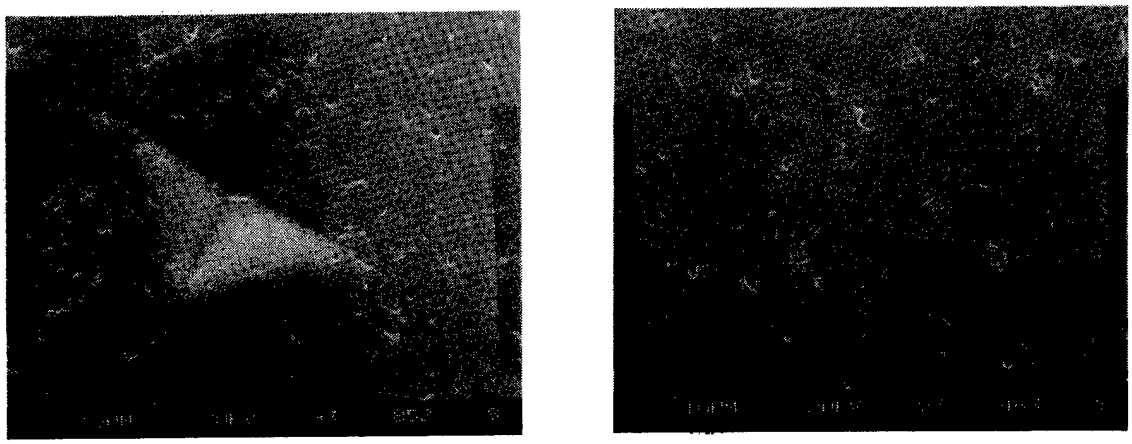

(c) (d)

Figure 13 Artificial Flaws Produced With Vickers Diamond Indentor: (a) 5.0 Kg Indent Load, Average Crack Length 172 μm, (b) 1.0 Kg Indent Load, Average Crack Length 61 μm (c) 0.5 Kg Indent Load, Average Crack Length 34 μm, (d) Typical "Natural" Flaws On Ball Surface.

hours. No ball failures occurred in this test. The indenting load was increased to 1.0 Kg for the final set of balls. The average crack size in these balls was 61 μm. Testing of the four bearings containing these balls was suspended at the bogey life of 1049 hours. No ball or race failures occurred within this time.

4.2.2 Defect Characterization

On the basis of tests of 112 balls (containing 672 total possible failure sites) per defect size, was concluded that the critical flaw size in NBD-200 under these test conditions was between 61 and 172 μm. However, the nature of the defects and of the failures was also an important consideration in applying this conclusion. Details of the spalls produced at indents made with a 5.0 Kg Vickers load are shown in Figures 14-16. The indents are clearly the origins of each of the spalls. The mode of propagation of the spalling was not that which might have been expected, however. The concept of a critical flaw size was typically one of a crack propagating from a semi-circular surface notch in a Mode I, tensile-opening manner. The critical flaw size would then be defined in terms of the stress intensity at such a flaw of measured length, "2c" and depth, "a". The cracking which grew into spalling in these tests did not appear to be related to the size of the cracks at the diagonals of the indents. It was more of a "flaking" of a section of material defined by a quadrant of the indentation and cracks which developed, by progressive fracturing, into the final spall configuration.

The results of an investigation of the effect of running over indents made with the 1.0 Kg load, less than the "critical" size, for 1049 hours are shown in Figure 17. The shoulders raised around the indentations by the displacement of material are shown to be worn smooth by repeated contact with the races. This action would tend to relieve the stress concentration effect of the raised shoulders. A critical-sized indent, then, could be one in which the level of stress generated by the shoulders was great enough to cause fracturing in the material below, rather than wear of the shoulders at the surface.

Figures 18 and 19 show, quantitatively, the difference in height after running of the shoulders remaining around indents made with 5 Kg and 1.0 Kg loads. These studies were made with

the use of an interferometric microscope ("MicroXAM", manufactured by Phase Shift Technology, Inc.). Alternatively, the critical indentation could have been one in which subsurface, lateral cracks were formed. Tested balls were sectioned on a plane that would nearly intersect several indentations. The cut surfaces were then progressively ground and polished to reveal subsurface crack configurations as they were intersected. Results are shown in Figure 20. Unfortunately, it was not possible to relate the position of the plane of polish to a specific location relative to the indent on the ball outside surface. Thus, the exact configuration of the crack network was not revealed. An apparent difference between the critical-sized 5.0 Kg indent and the non-critical 1.0 Kg indent was the presence of a median crack about 76 μm (0.003") deep associated with the critical indent. A median crack was not intersected in polishing through the smaller indents. Given the difficulty of this technique, however, this observation may not be conclusive.

The observations of the spall propagation mode would seem to favor the "critical shoulder height" explanation of the results of these tests. Naturally-occurring flaws, such as from porosity or inclusions would not be expected to have associated shoulders. Thus, the observation of a critical defect size may be very test-specific, and relate more to a critical Vickers indent size than to the case of a general flaw.

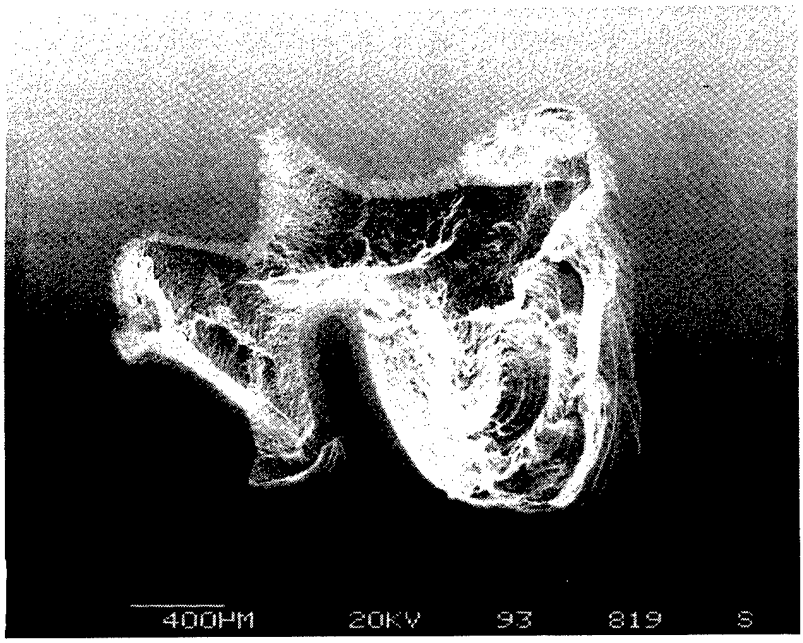

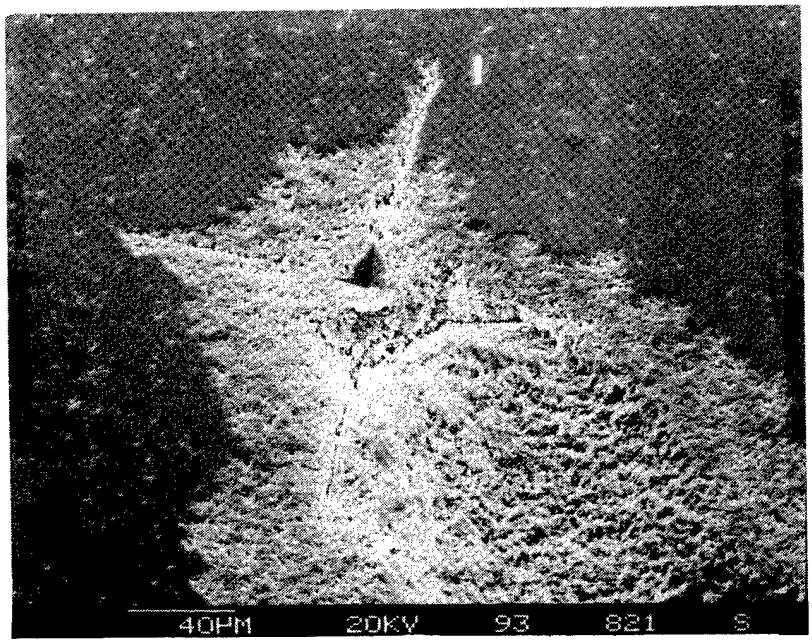

Figure 14 Spalling Of NBD-200 Ball At 5.0 Kg Indent (Bearing 0029).

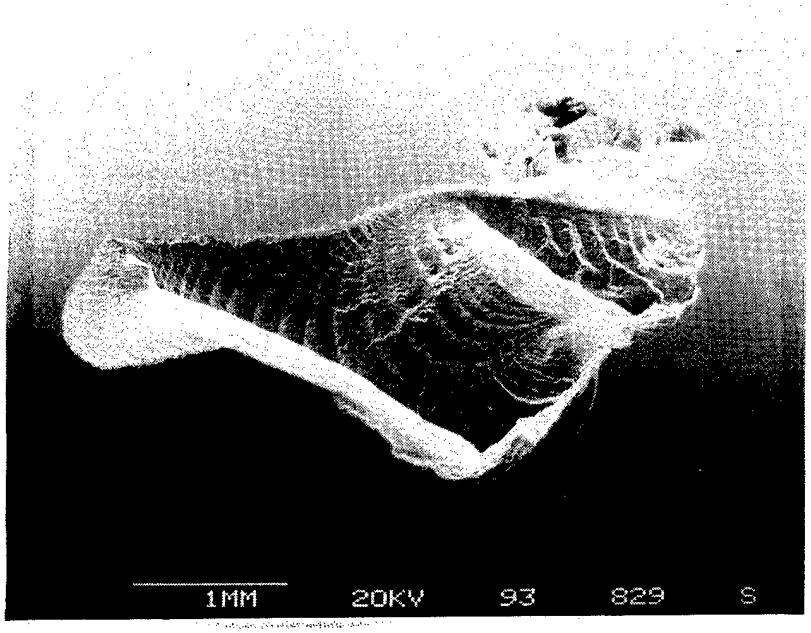

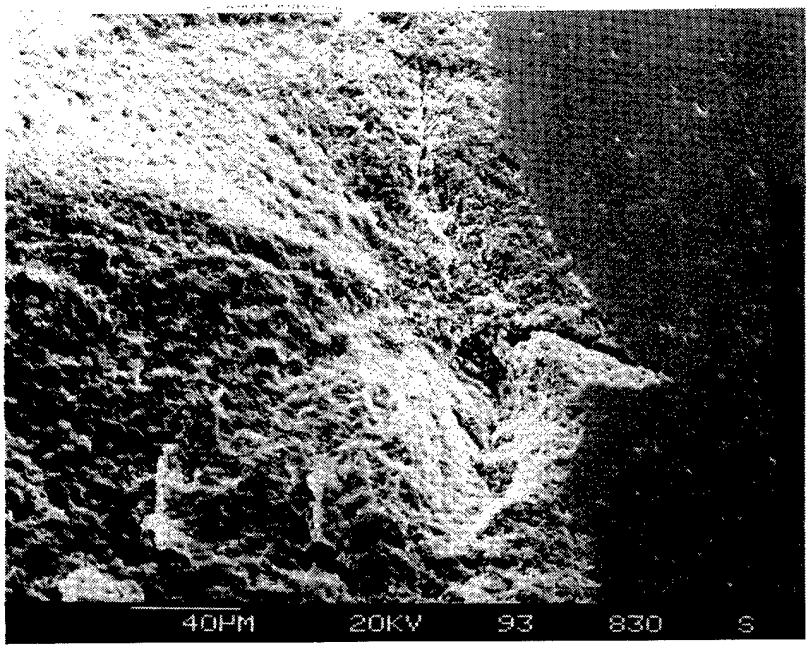

Figure 15 Spalling Of NBD-200 Ball At 5.0 Kg Indent (Bearing 0028).

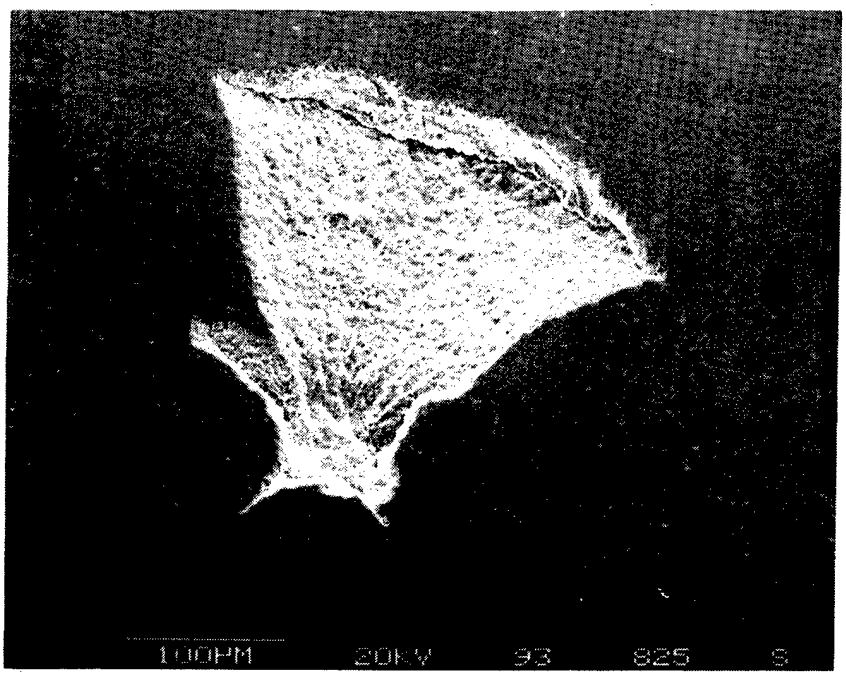

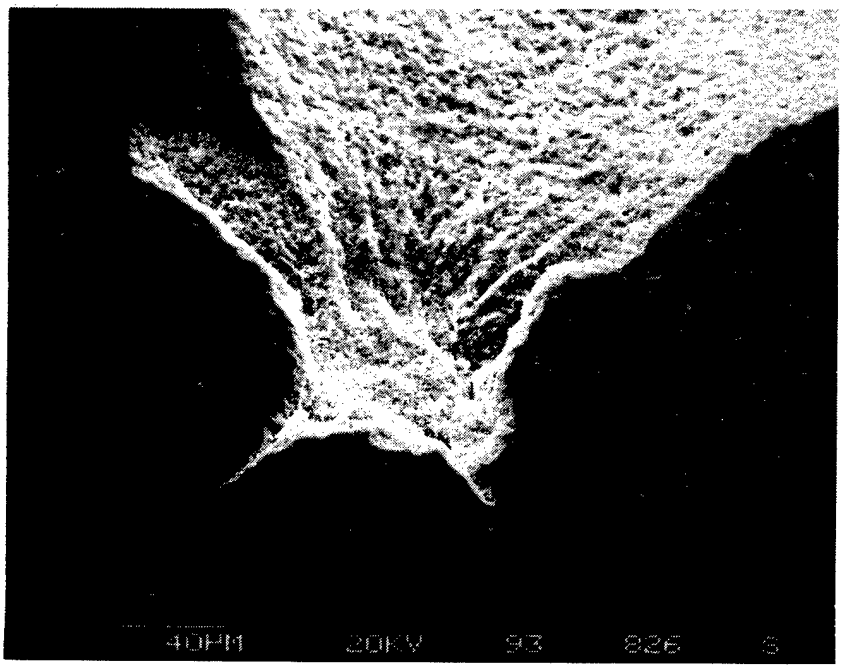

Figure 16 Spalling Of NBD-200 Ball At 5.0 Kg Indent Bearing 0028, Spall "B".

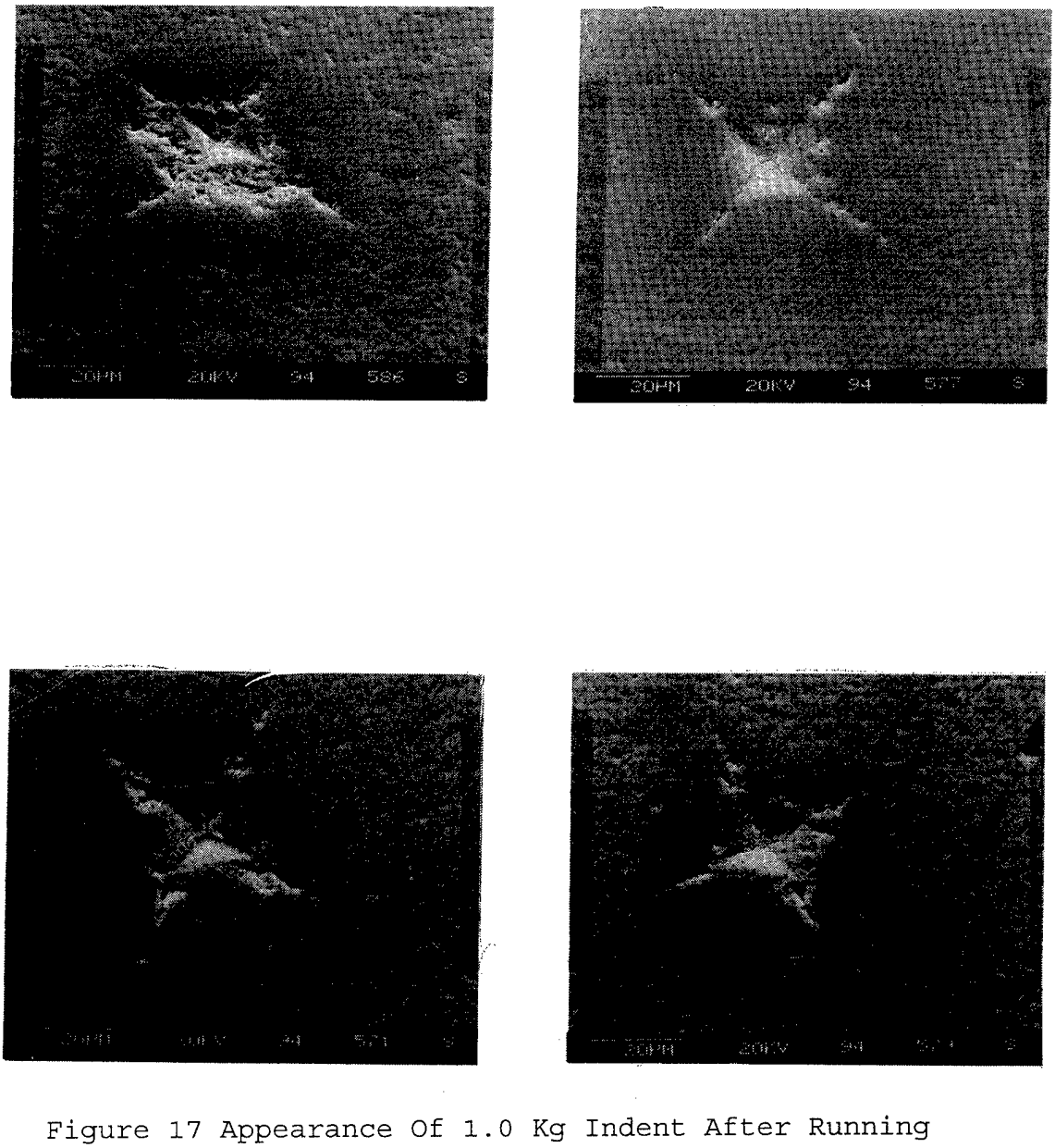

Figure 17 Appearance Of 1.0 Kg Indent After Running 1049 Hr. Shoulders Are Worn Smooth By Repeated Contact With Races.

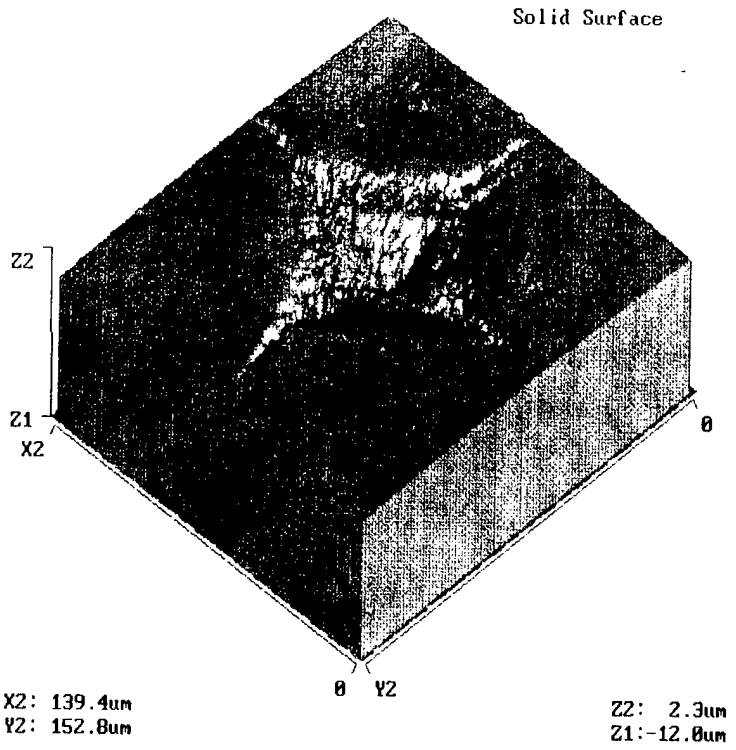

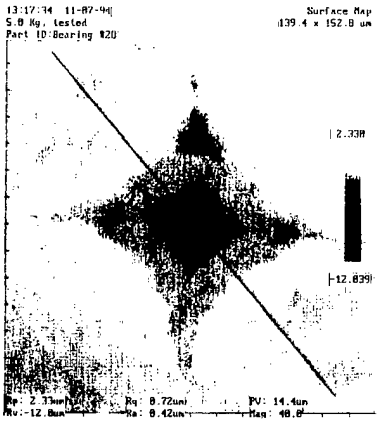

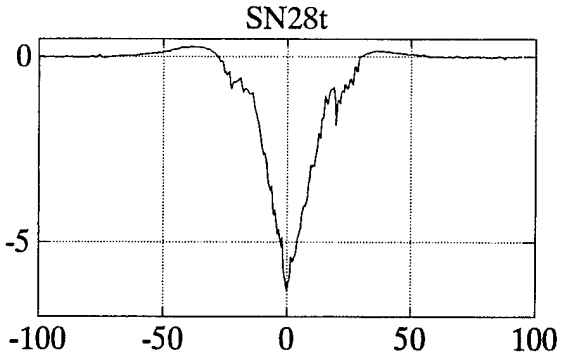

Figure 18 Profile Of Shoulders Of 5.0 Kg Indent After Wear Testing (generated from interferometric microscope image). Height Of Shoulders Has Resulted In Fracture Of Material Around Indent.

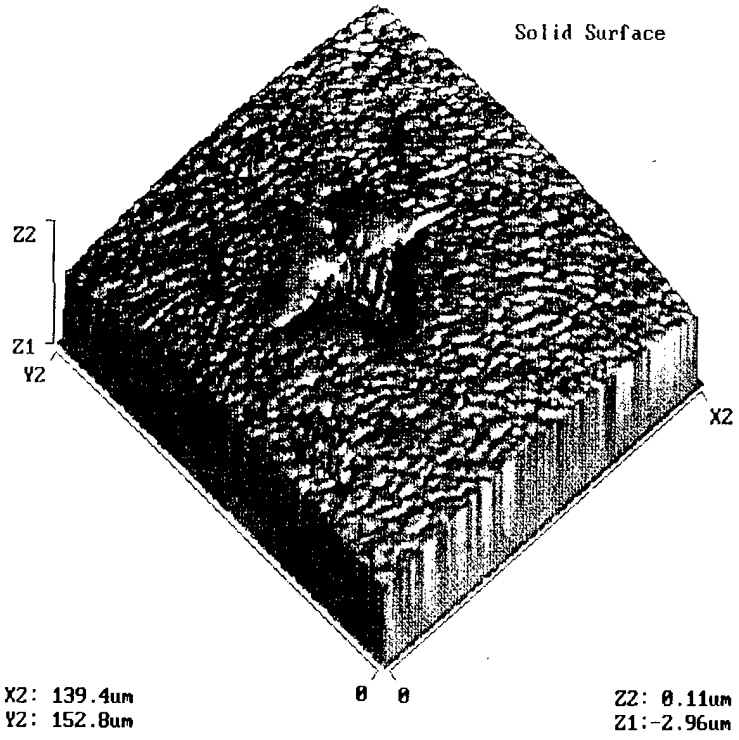

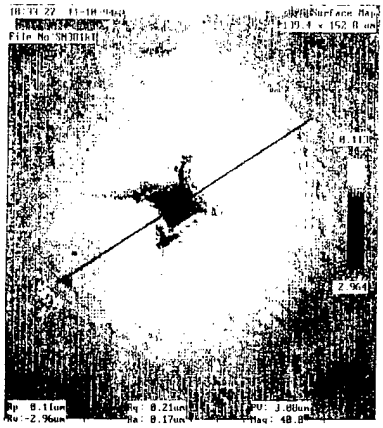

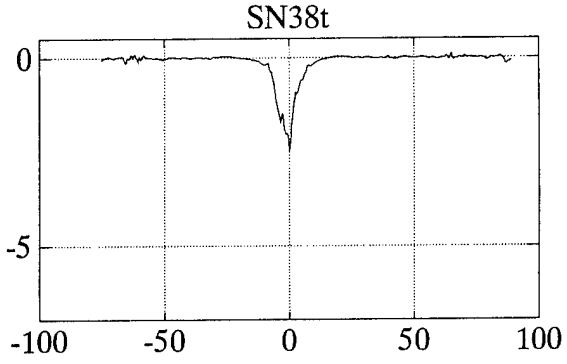

Figure 19 Profile Of Shoulders Of 1.0 Kg Indent After Wear Testing. (generated from interferometric microscope image). Shoulders Have Been Worn Back To Original Base Profile.

4.3 Determination of Effectiveness of NDE Methods

4.3.1 Silicon Nitride Ball Inspection by Surface Acoustic Wave Method

Balls for this test were all from CERBEC manufacturing lot #933766.02 and were selected from a population inspected by the Surface Acoustic Wave (S.A.W.) technique developed by Prof. B. T. Kuri-Yakub at Stanford University. Details of the test method development and inspections are given in Volume two of this report. During this work and related investigations, it was determined that many of the balls in this lot contained small compression type cracks. Given the cost and time constraints of this program, a decision was made to sort the balls by degree of defect severity, as determined by the SAW testing. The balls were graded for quality according to degree of asphericity and defects. Table 5 summarizes the attributes of the balls used for the eight test bearings. (This is described in detail in Volume two). The sorting was an attempt to group by degree of defect severity from low (bearing 1), to high (bearing 8). Bearing 7 was included in group two because that ball complement was tested at a different frequency.

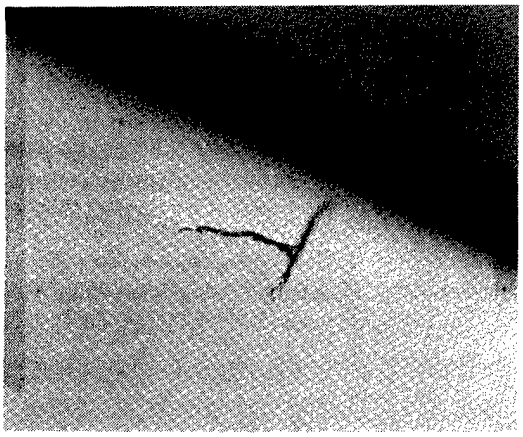

(a)

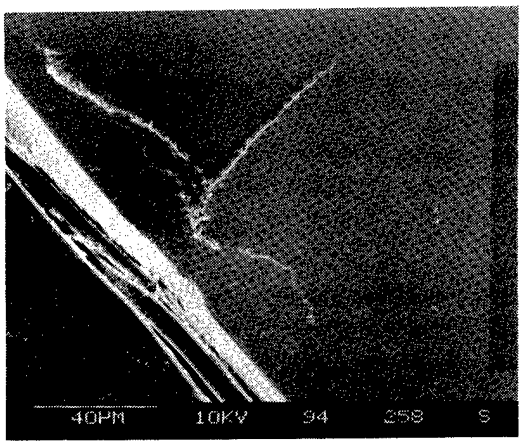

(b)

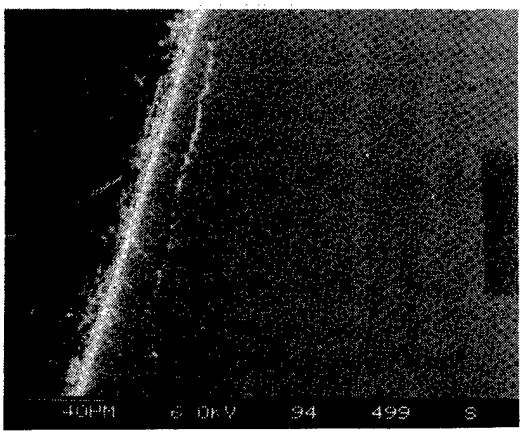

(c)

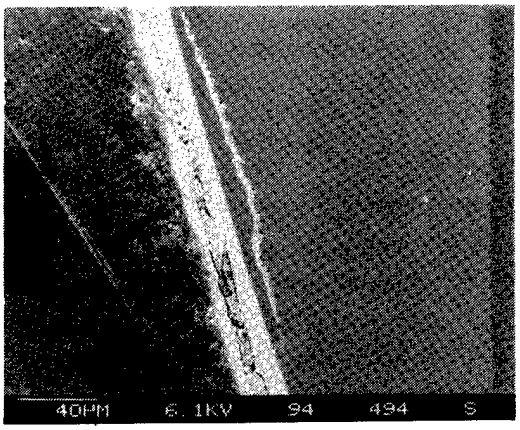

(d)

Figure 20 Cross-Sections Of Balls Through Indents After Being Test Run: (a) 5.0 Kg Indent #4 Median Crack 76 μm Deep Cone Crack 38 μm Subsurface, (b) 5.0 Kg Indent #1 SEM Image Median Crack and Cone Crack, (c) 1.0 Kg Indent "A" Cone Crack 15 μm Subsurface, (d) 1.0 Kg Indent "B" SEM Image Cone Crack.

Table 5
Surface Acoustic Wave Rating of Test Balls By Bearing Set

	Degree of Defect				Degree of Asphericity			
	None	Slight	Mod.	Sev.	None	Slight	Mod.	Sev.
Set One, Bearing 1	X				X	X	X	
Set One, Bearing 2	X	X	X		X	X	X	
Set One, Bearing 3			X			X	X	
Set One, Bearing 4			X				X	
Set Two, Bearing 5			X				X	
Set Two, Bearing 6			X				X	X
Set Two, Bearing 7[a]	X		X		X		X	
Set Two, Bearing 8				X			X	

[a] Bearing 7 of set two was tested at a frequency of 17 MHz.

Two sets of four bearings were life tested at a maximum Hertzian contact stress of 2.88 GPa (420 Ksi). One ball failed from each four bearing set. Ball set No. 1 had a failure of one ball after a running time of only 21.6 hours. This failure occurred during the load-up sequence, at an estimated contact stress of 2.54 GPa (368 Ksi). The features of the spalling are shown in Figures 21 and 22. No definite origin for this spall could be assigned, but the feature shown in Figure 22b was similar to one which was associated with that of Hertzian "cone" cracks known from associated work at Norton Advanced Ceramics to be present in this ball lot. Note that ball set No. 1 was one in which no defects were reported from the S.A.W. inspection.

The second ball failure, in ball set No. 5, occurred at 101.4 hours, at the full contact stress of 2.88 GPa (420 Ksi). The nature of the spalling on this ball is illustrated in Figures 23 and 24. The suspected origin of this spall is, again, cone cracking. Examination of the spall area in Figure 24 showed specific evidence of cone cracks in the immediate vicinity of the spall. Ball set No. 5 did contain balls which were selected as

cracking. Examination of the spall area in Figure 24 showed specific evidence of cone cracks in the immediate vicinity of the spall. Ball set No. 5 did contain balls which were selected as containing S.A.W.-detected defects.

To summarize the results of these life tests, the effectiveness of the Surface Acoustic Wave technique was not verified. The first, very short-lived, ball failure occurred in a group of balls in which no defects had been identified by the technique. The second ball failure occurred in a group of balls with "moderate" defects, rather than defects rated as severe.

4.3.2 Thermally Proof-Tested Balls

The NBD-200 balls for this test were produced from CERBEC manufacturing lots #932766.03 (bearing nos. 1 and 2) and #932766.02 (bearing nos. 3-8). They were subjected to the thermal proof test procedure developed by Professor Leon Chuck at the University of Dayton Research Institute. None of these balls were felt to have suffered crack extension due to thermal proof testing.

Two sets of four bearings with balls which had been thermally proof-tested were life tested at a maximum Hertzian contact stress of 2.88 GPa (420 Ksi). One set of bearings began to sound "noisy"

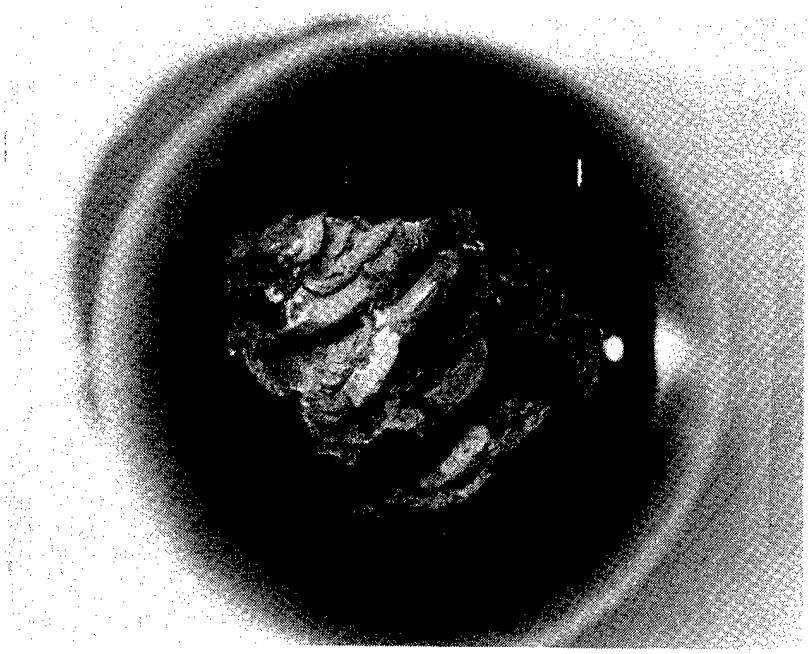

Figure 21 Spall On S.A.W.-Tested Ball From Set #1, Failed During Load-Up Sequence, At Contact Stress Of Approximately 2.54 GPa (368 Ksi) (optical photo 8X magnification).

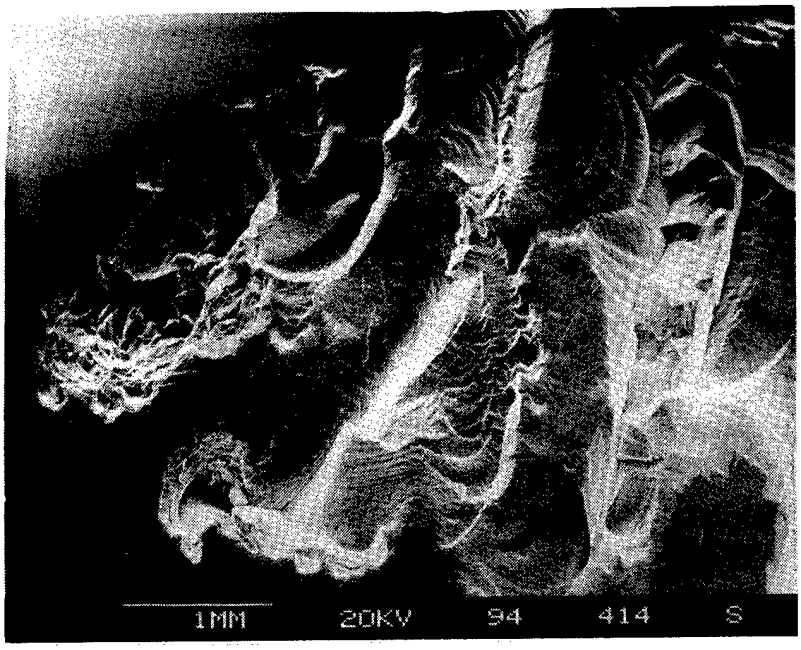

(a)

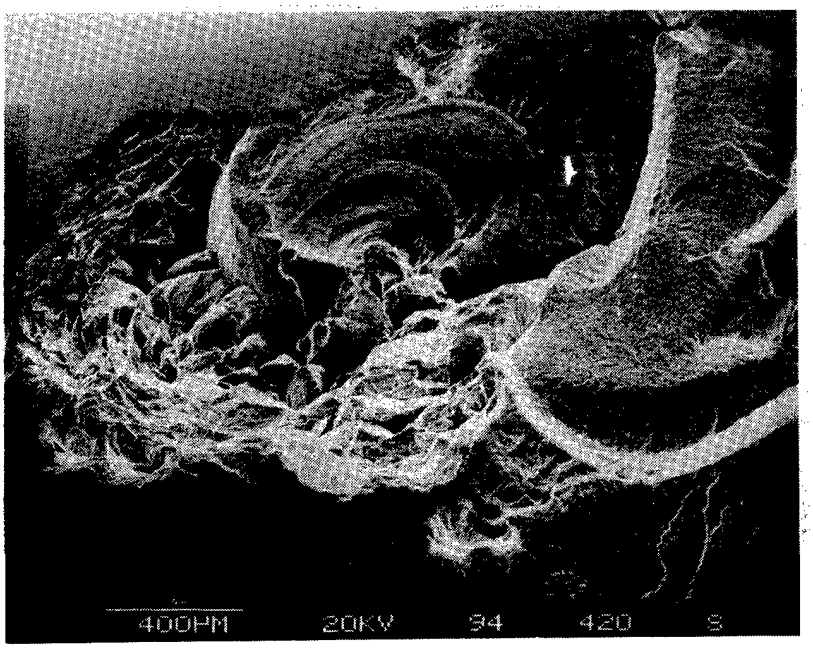

(b)

Figure 22 SEM Photos Of Spall From Ball Set #1. Possible Origin From Cone Crack: (a) Suspected Origin At Left Side, (b) High Magnification Of Suspected Origin.

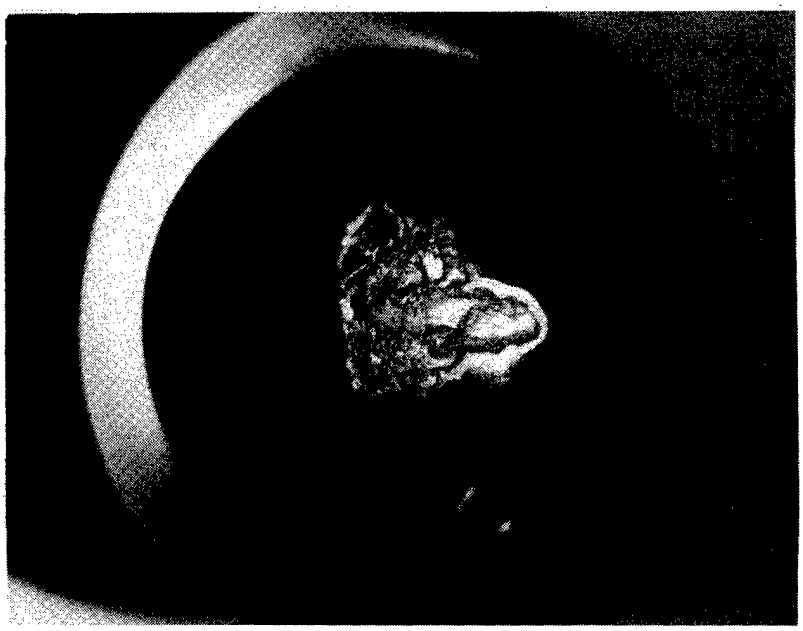

Figure 23 Spall On S.A.W. Tested Ball From Set #5, Failed At 101.4 Hrs. Contact Stress Of 2.88 GPa (420 Ksi) (optical photo 8X magnification).

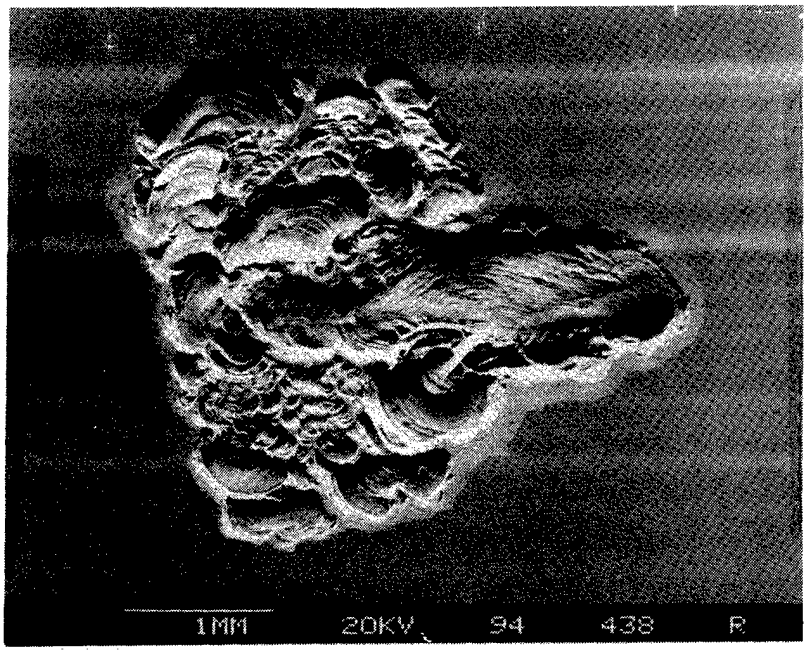

(a)

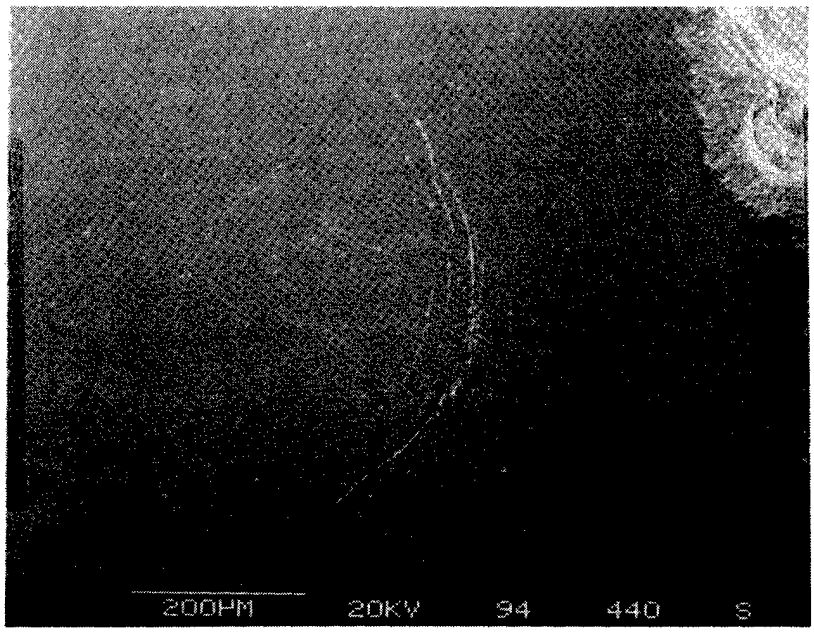

(b)

Figure 24 SEM Photos Of Spall From Ball Set #5: (a) SEM Photo Of Spall, (b) Hertzian Cone Cracks In Spall Vicinity (Below and to the Left of the Spall in 24 a).

after only a few hours into the load-up schedule. They were allowed to run until, at 11.8 hours, a sudden increase in vibration caused the test to shut down. One ball from bearing number 7 was found to have failed catastrophically, fracturing into several pieces. The maximum contact stress at that point in the loading-up sequence would have been on the order of 2.53 GPa (367 Ksi). Details of the fracture surface shown in Figure 25 show clearly that the failure was due to a crack which had propagated in the proof test, but the ball had not been removed in the second stage of the inspection. Remnants of the 60% Sn / 40% Bi low melting point alloy that was used as the thermal transfer medium in quenching the balls are visible to a depth of 1-1.5 mm. The apparent origin of the thermal crack was of a size similar to the cone cracks known to have been present in this lot of balls.

Because this initial life test result did not fully test the capability of the thermal test procedure, the failed ball and races of bearing no. 7 were replaced and the testing continued. At a total of 182.3 hours on the remaining balls, a second ball failure occurred. This ball was from the same ball set in which the early, catastrophic failure had taken place. The appearance of the failure is shown in Figure 26.

The other set of four bearings (brgs. 1-4) containing thermally proof-tested balls was suspended after a total of 353.5 hours, well beyond the 250 hour bogey, with no ball failures.

4.4 Wear Coefficient Tests

The objective of this Task was to compare the overall rates of wear of the components of hybrid bearings containing races made of AISI-52100 steel and M-50 steel. Both are high carbon, through-hardening type bearing steels. For the purposes of this wear test, the essential difference between AISI-52100 steel and M-50 steel is in the amount and distribution of the alloy carbides within the microstructures. M-50, because of the nature and amount of its alloying elements, contains a larger volume fraction of hard, wear resistant carbides than 52100 steel. There is also a tendency for the carbides in M-50 to be larger, as can be seen by comparison of the microstructures in Figure 27. Thus, there may be a potential difference in the way the steels react

to bearing wear conditions, as well as in the way they affect the wear of the NBD-200 balls. A third steel, the carburizing grade M-50-NiL, was to have been included for its still different microstructure and carbide content. M-50-NiL is difficult to process, at best, and manufacturing problems with this small bearing race size made it impossible to manufacture test bearings in this material.

Table 6 is a summary of the conditions under which each of the completed wear tests were run. The post-test data gathered from each run will be discussed on a bearing-by-bearing basis in the following sections.

4.4.1 Tests on AISI-52100 Steel Races with NBD-200 Balls

Figure 28 shows the surface conditions typical of the 52100 steel races prior to testing. The surface appearance typical of the as-received 5/32" NBD-200 balls common to all of the hybrid bearing tests is shown in Figure 29.

The first test of an AISI-52100 bearing was run at the lower of the two originally-planned film thickness / roughness conditions (λ = 1.0) to establish a boundary, "worst-case" condition. The test was to have run for 300 hours, from which point the running times for future tests would be adjusted to provide a wear versus running-time relationship. In this first test, however, the inner race sustained major spalling damage after about 295 hours, shown in Figure 30. As a wear test, then, much of the useful data was lost, since changes to the component weights and profiles could not be related to a simple wear mechanism.

Figure 31 is a summary of the measurements of profiles, surface finishes and weights made on bearing 52100-A-1. Shown are the profiles of the inner and outer races, the arithmetic mean roughness, Ra, the total peak-to-valley roughness, Rt, before and after testing, and the change in weight of the individual components. Note that the profile traces were corrected for the concavity of the races, i.e. in this plot a perfectly-radiused part would appear as a straight line. The profile traces show that very little change from the original profiles of the races occurred, in spite of the major damage to the inner race and the associated debris which subsequently passed through the bearing.

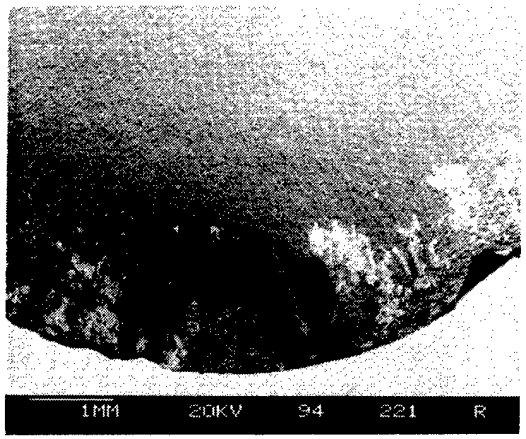

(a)

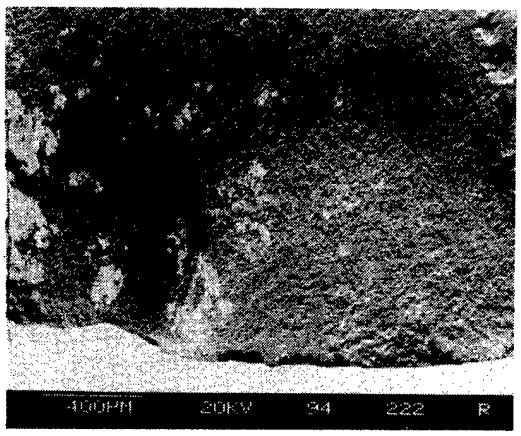

(b)

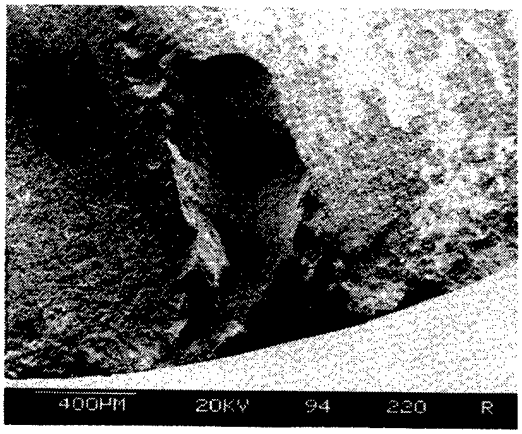

(c)

Figure 25 Fractured Ball From Thermally-Proof Tested Set No.7: (a) Fracture Surface With Remaining Sn/Bi Alloy, (b,c) Details Of Possible Crack Origin.

(a)

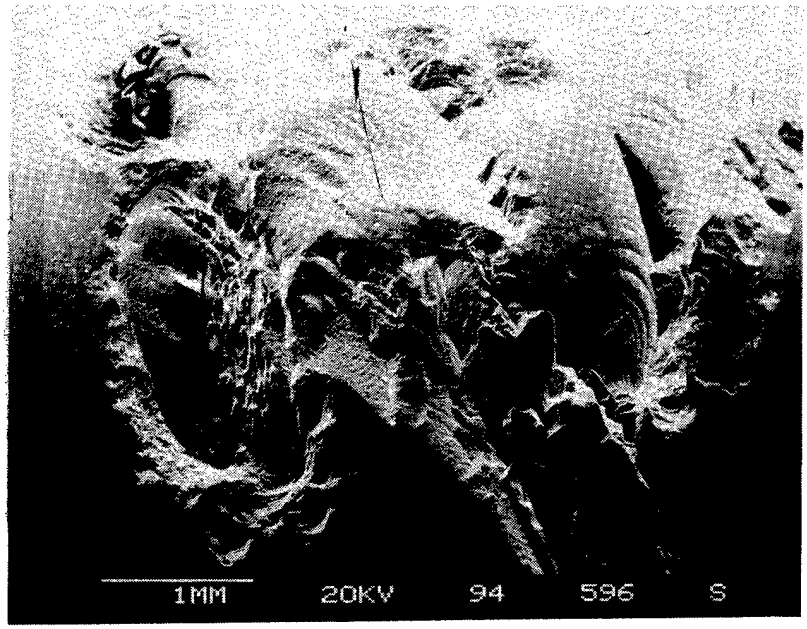

(b)

Figure 26 Spall On Second Ball From Thermally Proof Tested Bearing Set No.7. Failed After 182.3 Hrs., At Contact Stress Of 2.88 GPa (420 Ksi): (a) Optical Photo 8X Magnification, (b) SEM Photo Of Area Of Spall Origin (lower left area of 26 a).

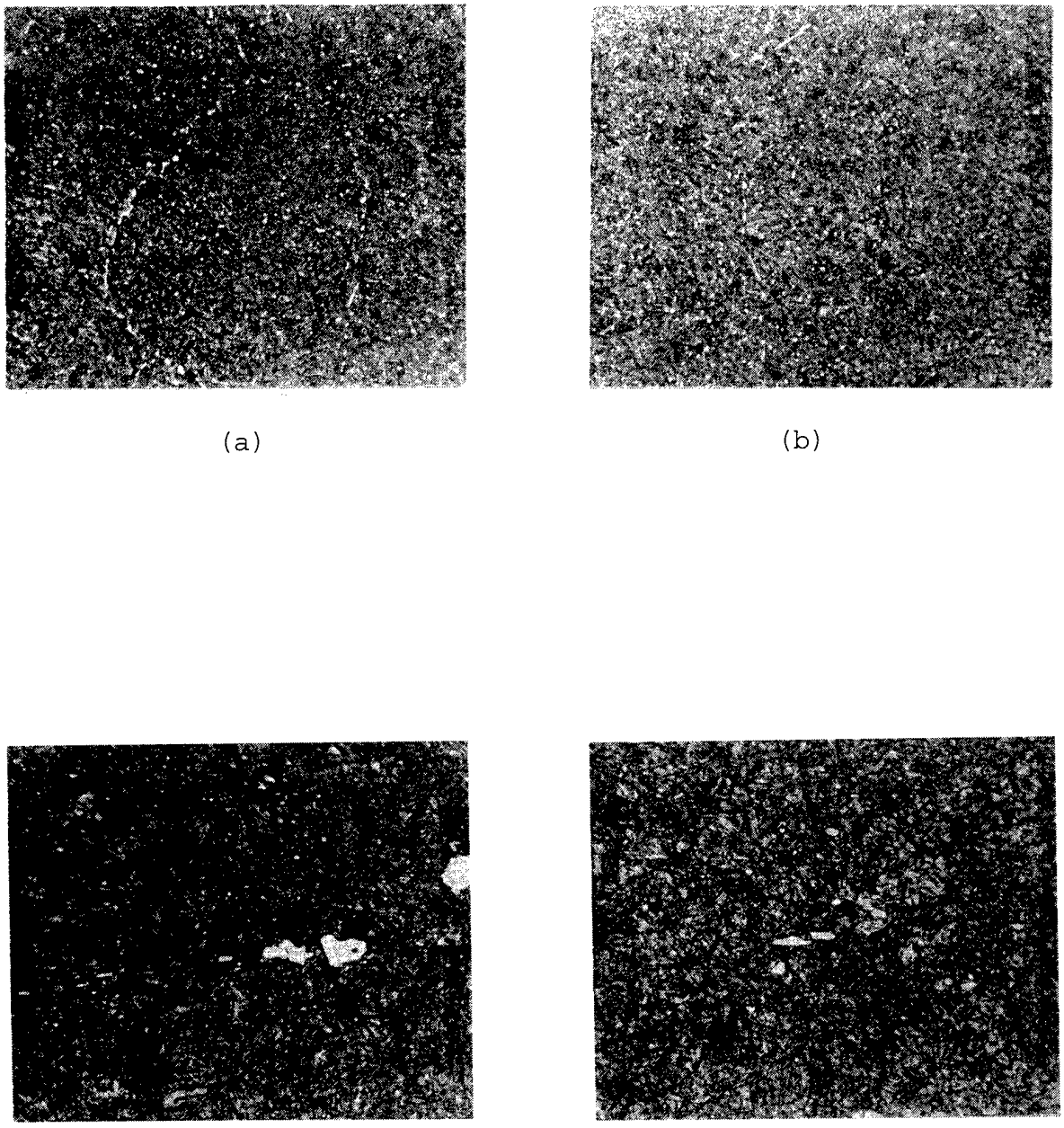

Figure 27 Typical Microstructures Of Wear Test Bearing Races (500X Magnification): (a) AISI 52100 Steel Outer Race, (b) AISI 52100 Steel Inner Race, (c) M-50 Steel Outer Race, (d) M-50 Steel Inner Race.

Table 6
Summary Of Conditions Of Wear Test Runs

Bearing Identification	Race Material	Ball Material	Maximum Contact Stress	Temperature	λ_Ratio	Run Time
A-1	52100 Steel	NBD-200	2.76 GPa	60° C	1.0	295 Hr.
A-2	52100 Steel	NBD-200	2.76 GPa	60° C	1.0	147 Hr.
A-3	52100 Steel	NBD-200	2.76 GPa	60° C	1.0	305 Hr.
B-1	M-50 Steel	NBD-200	2.76 GPa	60° C	1.0	300 Hr.
B-2	M-50 Steel	NBD-200	2.76 GPa	121° C	0.3	150 Hr.
B-3	M-50 Steel	NBD-200	2.61 GPa	121° C	0.3	830 Hr.
X-1	M-50 Steel	M-50 Steel	2.27 GPa	121° C	0.3	500 Hr.

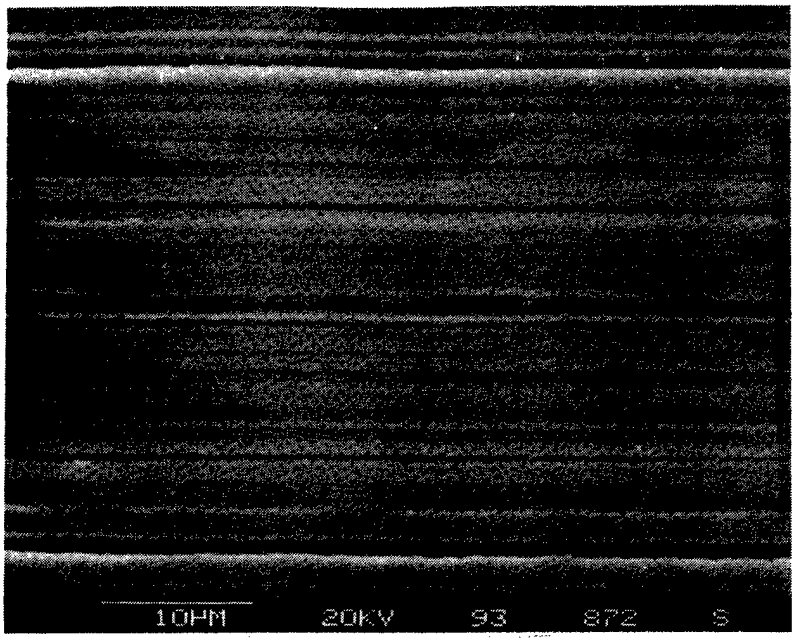

(a)

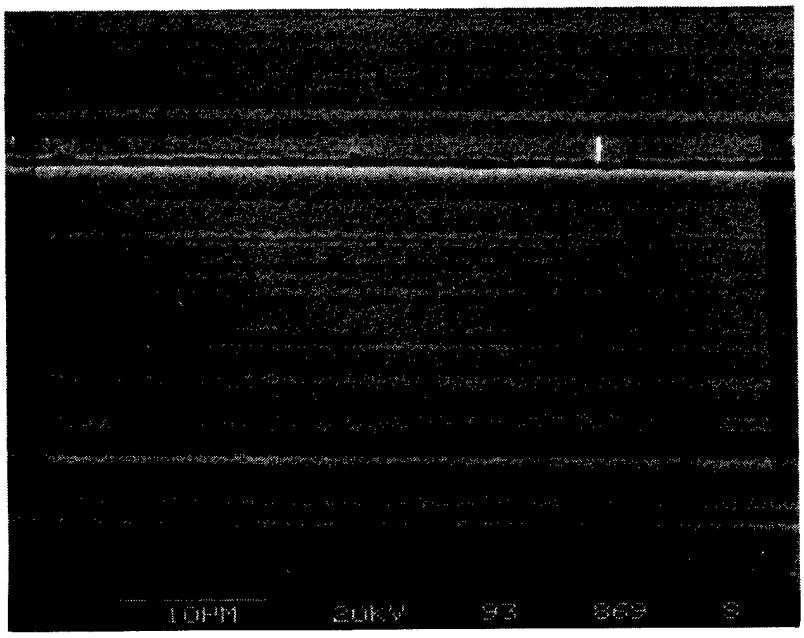

(b)

Figure 28 Pretest Surface Finish Of AISI 52100 Steel Races: (a) Outer Race, (b) Inner Race.

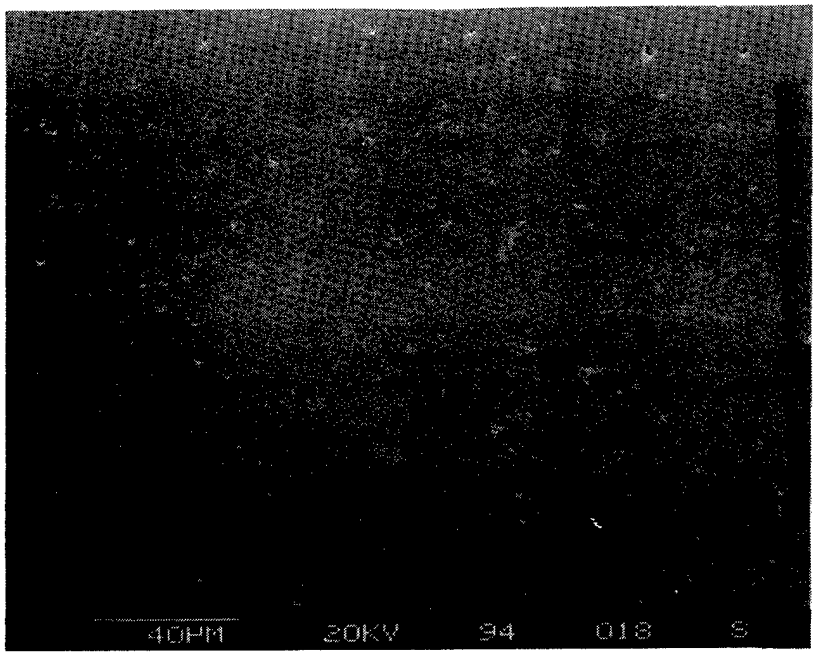

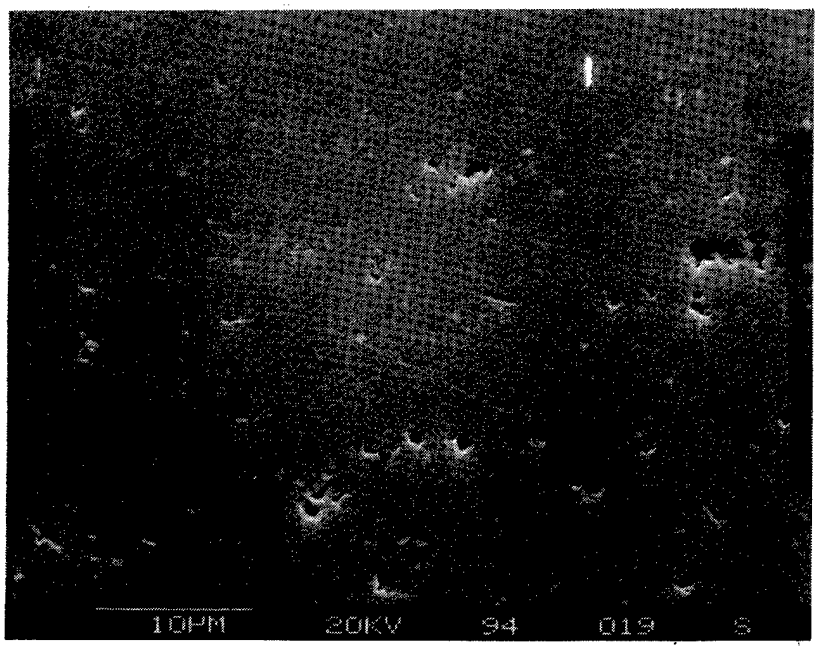

Figure 29 Pretest Surface Condition Of 5/32" NBD-200 Balls.

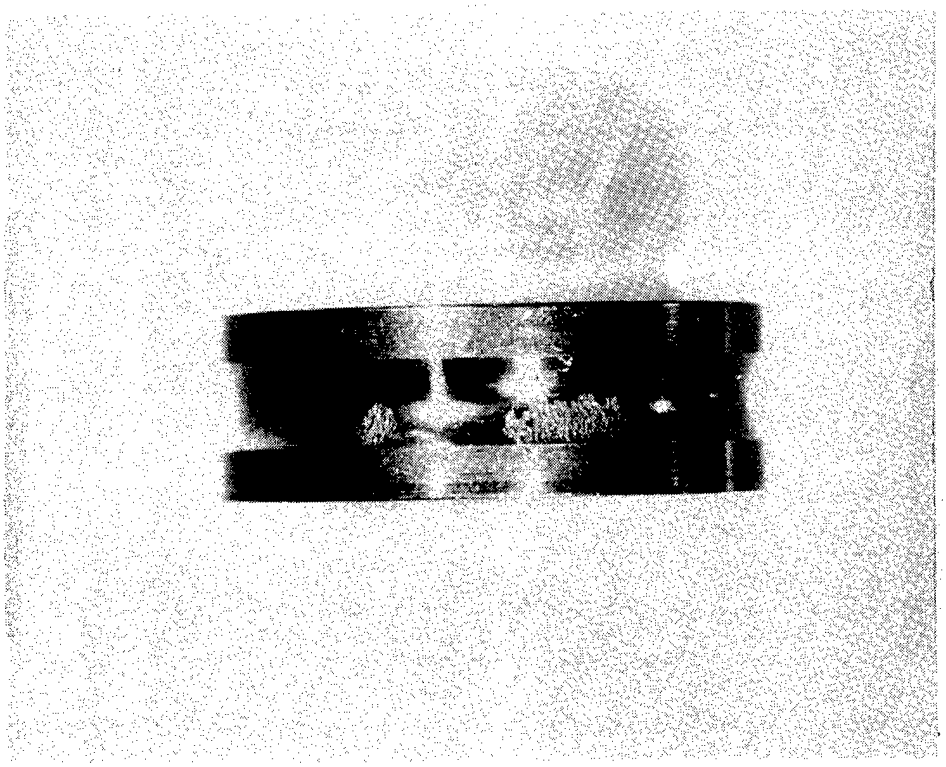

Figure 30 Inner Race Spalling of AISI 52100 Bearing A-1 Failed at Approximately 295 Hrs. at a Maximum Contact Stress of 2.76 Gpa (400 Ksi).

Before Testing

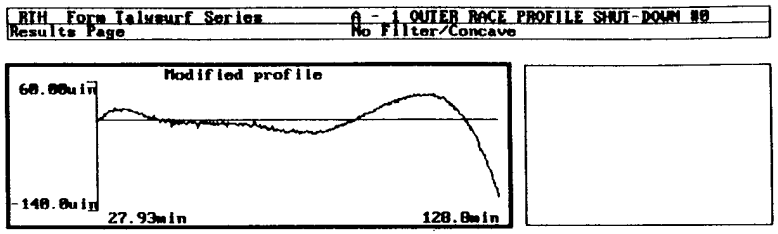

After Testing

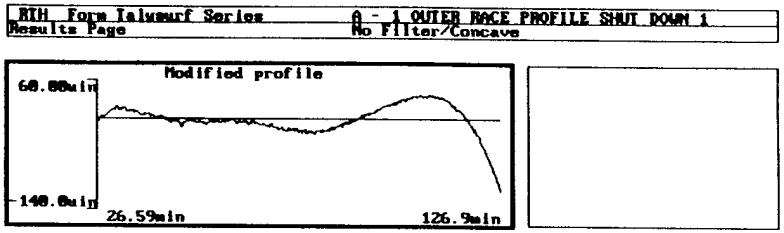

Outer Race

Ra Init = 1.1459 μ in Ra Final = 0.9649 μ in

Rt Init = 11.1919 μ in Rt Final = 8.0440 μ in

Wt. Change -0.0004 gm

Before Testing

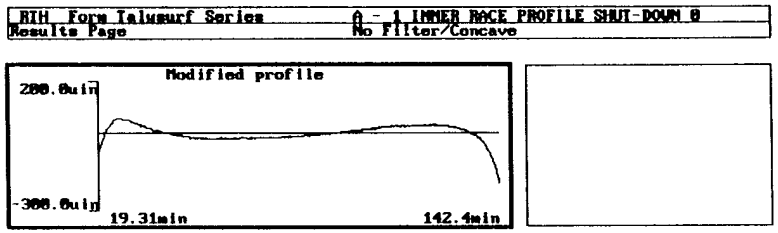

After Testing

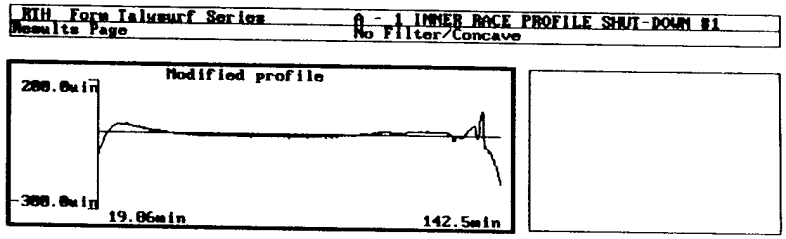

Inner Race

Ra Init = 0.4671 μ in Ra Final = 1.2188 μ in

Rt Init = 6.7906 μ in Rt Final = 13.2575 μ in

Wt. Change -0.00215 gm

Balls

Ra Init = 0.2428 μ in Ra Final = 0.2498 μ in

Rt Init = 3.8602 μ in Rt Final = 4.1564 μ in

Test Conditions

276 Hrs. 54.091 X 10^6 Revs

2.76 GPa (400 Ksi)

$\lambda = 1.0$ T = 60° C (140° F)

Figure 31 Wear Test Results For AISI 52100 Steel Race Bearing "A-1".

The traces of the tested inner races to be discussed show a slight modification of the profile which extends about 500 μm (0.020 in) onto the race. This appears to be a slight plastic deformation of this portion of the race at the edge of ball contact. The measured surface finish of the outer race actually became slightly smoother during running. The inner race finish, as a result of extensive debris bruising, became rougher. The finish of the NBD-200 balls, in the area measured, was essentially unchanged. The change in weight of the components, while essentially meaningless in this run, were qualitatively similar to the degree of change in profile and finish. The inner race showed a net loss of about 2 mg, in spalled-out material, while the outer race and the balls lost much less.

Figure 32 shows the general condition of the inner and outer races after the test. In comparison to Figure 28, the races have a much smoother appearance, with little of the original grinding texture remaining. The balls showed a definite circumferential line of damage in the form of "peeling" or shallow grain pullout, Figure 33. The depth of the peeling damage was measured at less than 0.25 μm. This material removal appears to have been caused by the stress concentrations associated with over-running the debris bruises and pits in the failed races. Figure 34 shows the commonly-observed "cloud" of silicon nitride particles impressed into the steel surface at the outlet side of race discontinuities. A potential wear mechanism in hybrid bearings could be one which starts with a pit or bruise in the races, from micro-spalling due to fatigue or from an inadvertent debris particle. Wear could then proceed by progressive removal of grains from the silicon nitride surface and corresponding damage to the steel races from the roughened balls and the debris generated in the process.

The wear measurements on bearing 52100-A-1 were obscured by the macro-spalling which occurred, so the next run was scheduled for one-half the running time of the first test, to avoid fatigue failure of the races. Bearing 52100-A-2 was run for 147 hours prior to inspection. Figure 35 summarizes the dimensional traces and weight change measurements which were made on the components of this bearing. The profile traces indicate very little change, with the exception of some roughening due to pitting and denting.

The change in the measured surface finish is not felt to be significant. The change in weight is also not significant, actually indicating an apparent weight gain by the races.

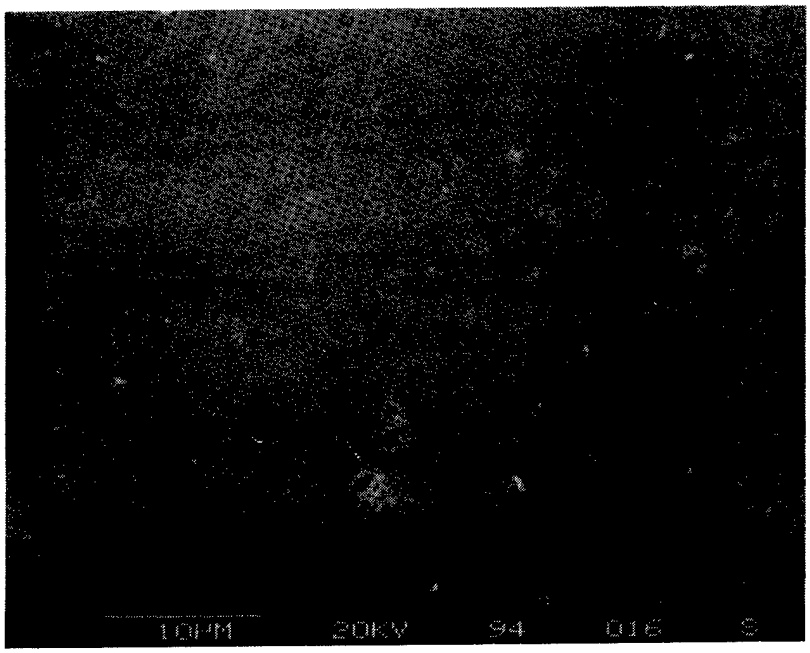

(a)

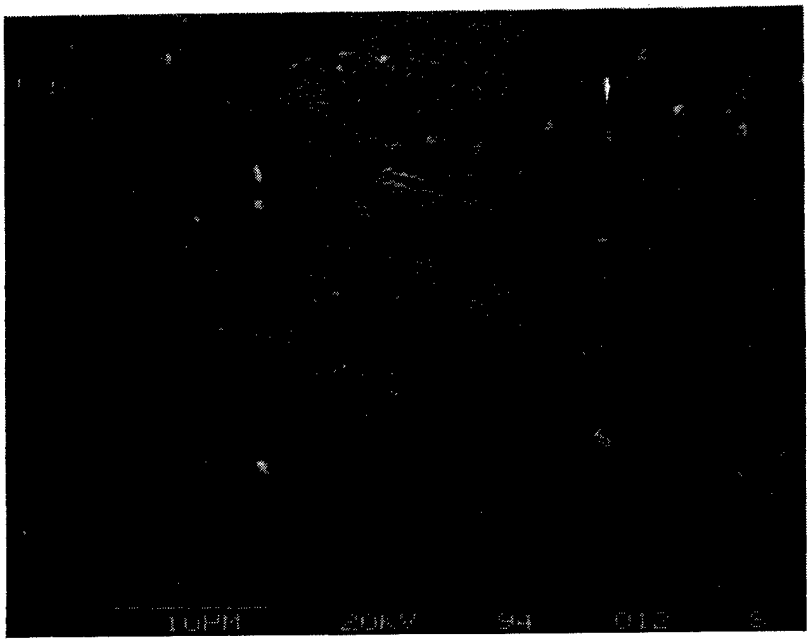

(b)

Figure 32 Surface Of Ball Track Of AISI 52100 Bearing After Test: (a) Outer Race, (b) Inner Race.

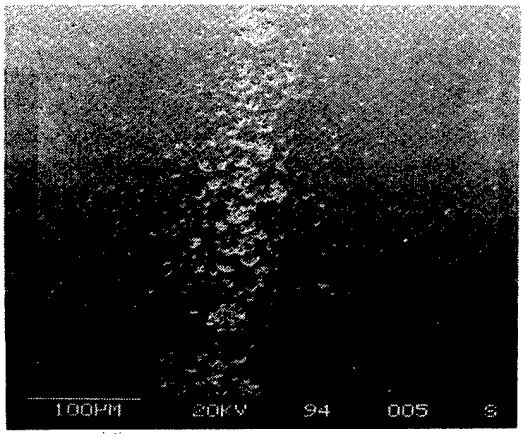

(a)

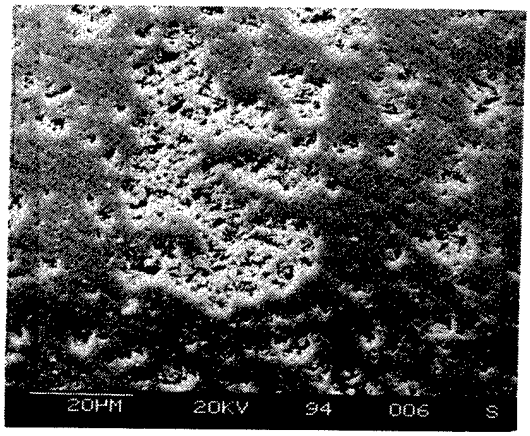

(b)

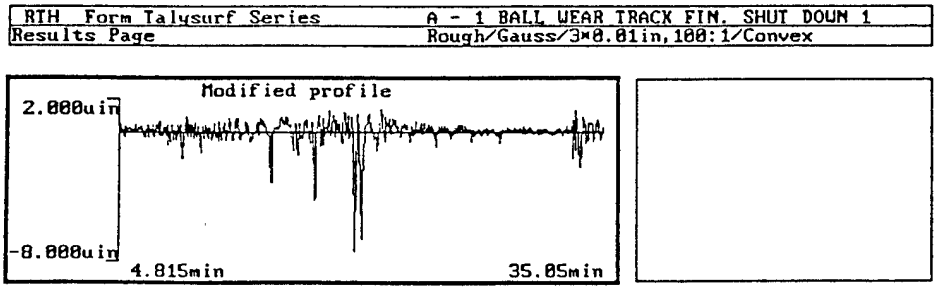

(c)

Figure 33 Damage To NBD-200 Ball From Spalling Of 52100 A-1 Race: (a) Wear Track, (b) Detail Of Shallow Surface Damage, (c) Trace Across Damaged Wear Track.

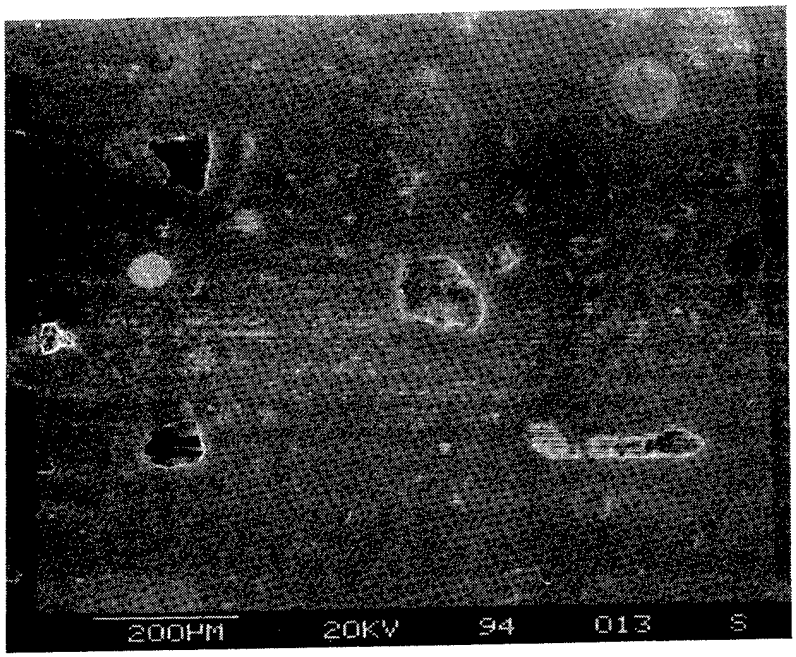

(a)

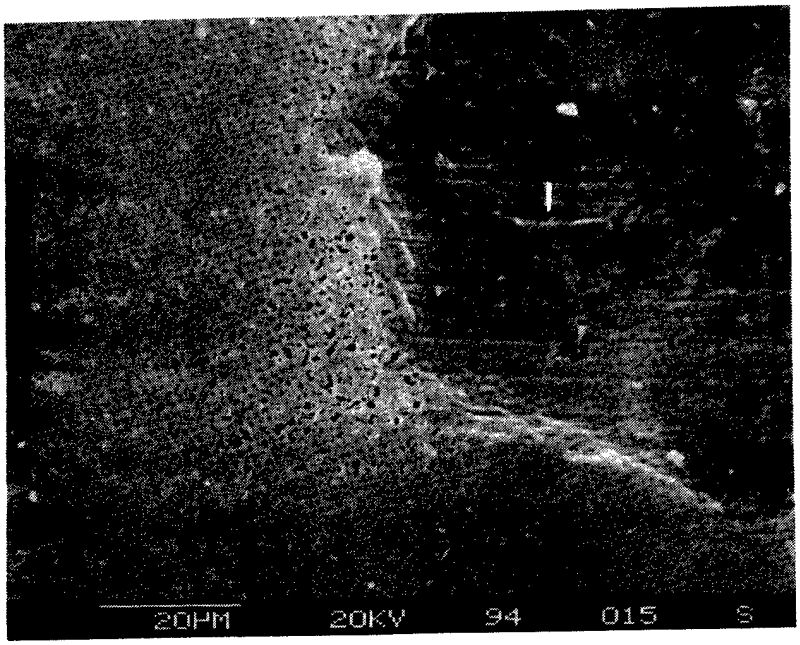

(b)

Figure 34 Damage To Bearing 52100 A-1 Outer Race From Debris: (a) General Bruising And Pitting, (b) Detached Si_3N_4 Particles Impressed Into Race At Bruise.

Before Testing

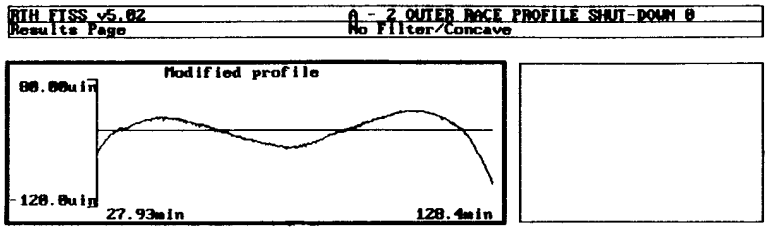

After Testing

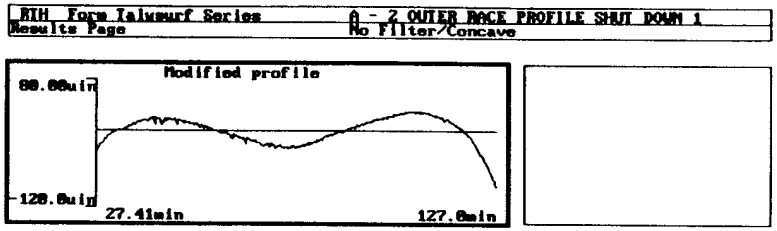

Outer Race

Ra Init = 0.6771 μ in Ra Final = 0.6602 μ in

Rt Init = 6.6289 μ in Rt Final = 5.6444 μ in

Wt. Change +0.0006 gm

Before Testing

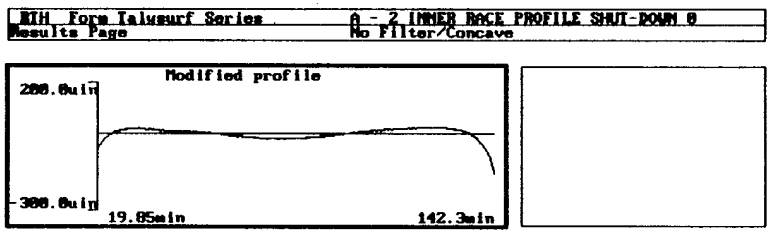

After Testing

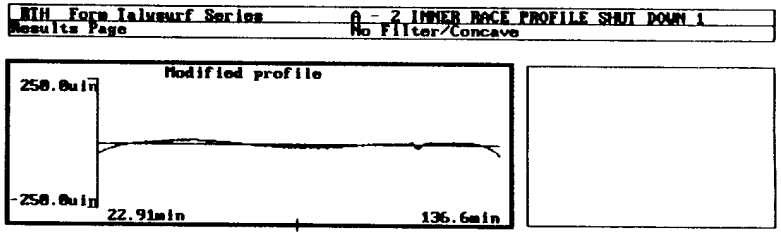

Inner Race

Ra Init = 0.5361 μ in Ra Final = 0.8270 μ in

Rt Init = 4.4414 μ in Rt Final = 8.2624 μ in

Wt. Change +0.0002 gm

Balls

Ra Init = 0.2428 μ in Ra Final = 0.2316 μ in

Rt Init = 3.8602 μ in Rt Final = 3.7721 μ in

Wt. Change 0.0000

Test Conditions

147 Hrs. 26.476 X 10^6 Revs

2.76 GPa (400 Ksi)

λ = 1.0 T = 60° C (140°F)

Figure 35 Wear Test Results For 52100 Steel Bearing "A-2".

Figure 36 shows the typical appearance of the races after testing. As indicated by the surface finish traces, the small-scale roughness of the finish has been reduced somewhat by plastic blunting of the grind texture, but some discrete points of roughness were produced by micropitting and denting. As shown in Figure 37, the microspalling is sometimes associated with near-surface nonmetallic inclusion material-aluminum oxide particles of micron size (the presence of aluminum oxide was verified by EDAX). The ball surface, shown in Figure 38, appeared essentially the same as it did in the pretest condition. The wear process in this bearing appeared to be one of small scale fatigue damage to the steel races.

Bearing 52100-A-3 was run in an attempt to achieve a longer running time under the film thickness conditions of $\lambda = 1.0$. A run of 305 hours was completed on this bearing without fatigue failure of the races. Figure 39 presents the results of the pre-test and post-test measurements on the components of bearing A-3. The traces indicate a slight modification of the profiles of the races, primarily due to denting on the outer race, while the inner race became more nearly a perfect radius with running, due to small plastic deformations of the surface. No net removal of material was indicated, however. No wear tracks were visible on the balls, and the surface finish measurements were essentially identical before and after the test. The weight change measurements also showed no significant changes. Some features of the race appearance after test are shown in Figure 40. They consisted, as in the previous test, of some blunting of the grinding texture, along with denting and micro-spalling.

In summary, the wear tests of hybrid bearings with NBD-200 balls and CEVM-melted, AISI-52100 steel races thus failed to show any measurable wear of the components under the relatively severe film thickness / roughness condition of $\lambda = 1.0$. The primary mode of damage to the races was fatigue micro-spalling associated with extremely small, non-metallic inclusions. In the absence of fatigue spalling of the races, no change in the NBD-200 balls was detected in these tests.

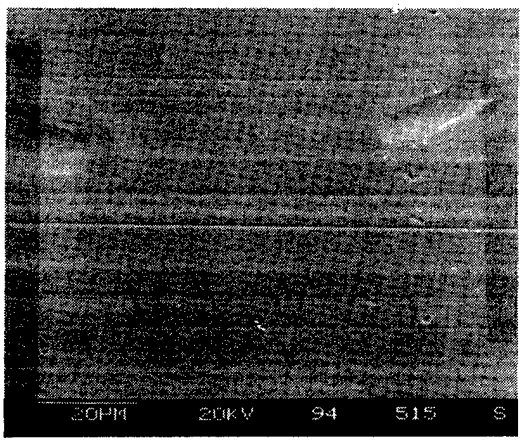

(a)

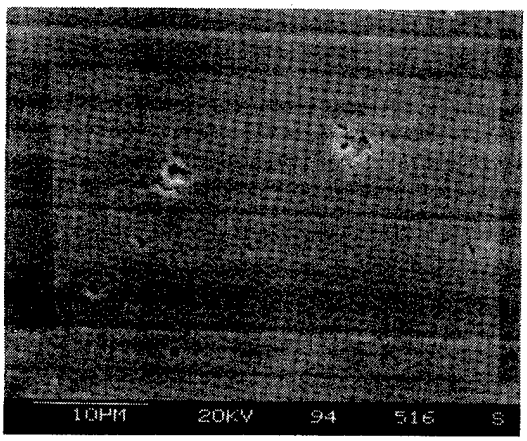

(b)

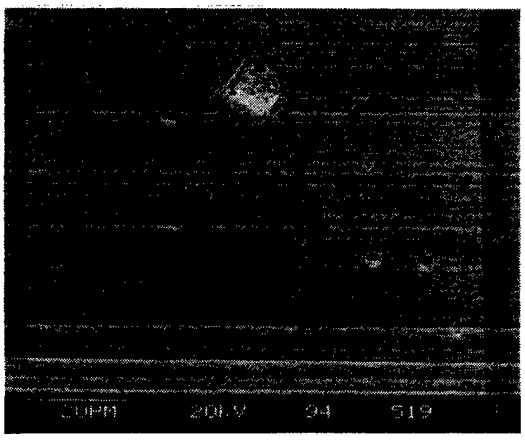

(c)

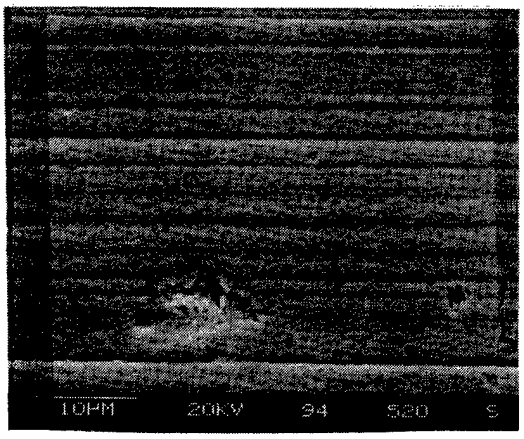

(d)

Figure 36 Post-test Condition of AISI 52100 Races, Bearing A-2 Plastic Blunting of Grind Texture, Pitting and Debris Denting (a,b) Outer Race, (c,d) Inner Race.

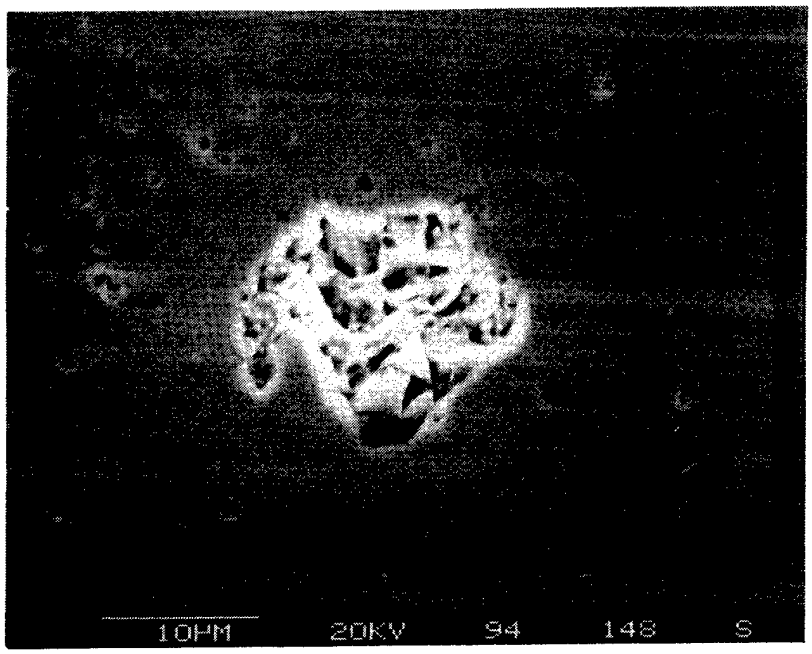

(a)

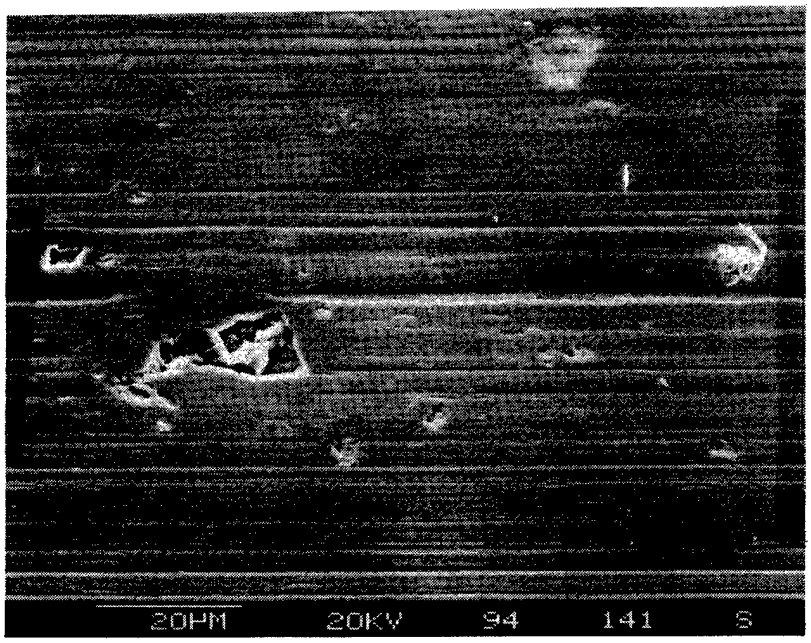

(b)

Figure 37 Micropitting Of AISI 52100 Races and Bearing A-1 At Near-Surface Al_2O_3 Non-Metallic Inclusion Particles: (a) Outer Race, (b) Inner Race.

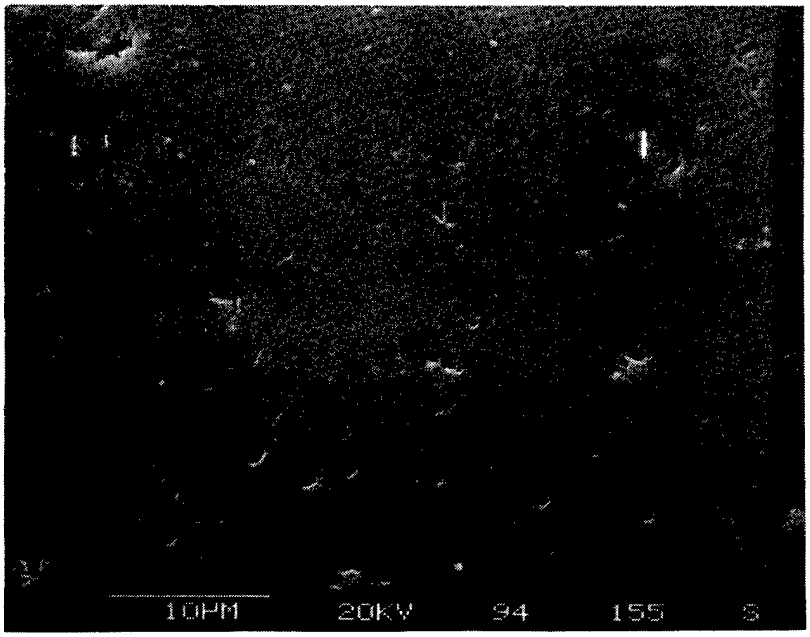

Figure 38 Post-Test Surface Condition Of NBD-200 Ball From AISI 52100 Races and Bearing A-2, Run 147 Hr. at 2.76 GPa (400 Ksi), λ = 1.0.

Before Testing

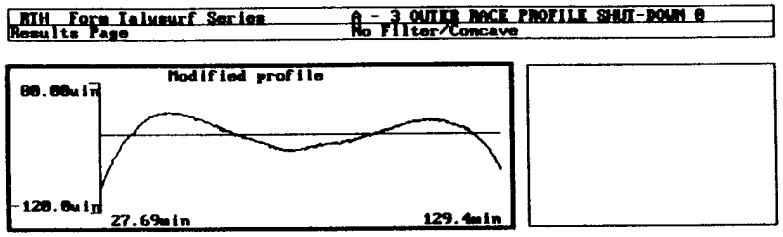

After Testing

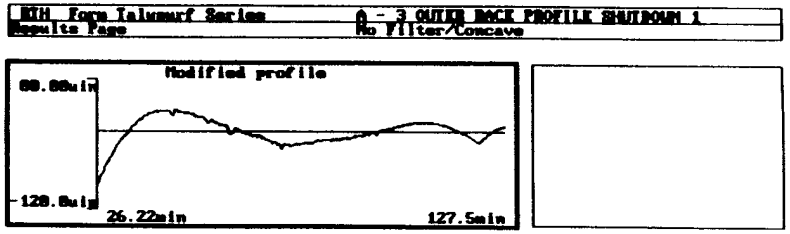

Outer Race

Ra Init = 0.6846 μ in Ra Final = 1.3305 μ in

Rt Init = 8.1215 μ in Rt Final = 12.6155 μ in

Wt. Change -0.0001 gm

Before Testing

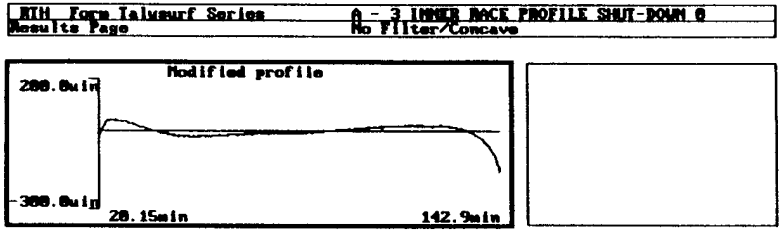

After Testing

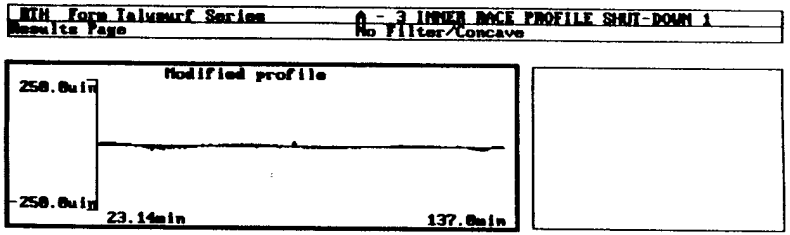

Inner Race

Ra Init = 0.4374 μ in Ra Final = 0.9021 μ in

Rt Init = 4.3311 μ in Rt Final = 23.9476 μ in

Wt. Change +0.0001 gm

Balls

Ra Init = 0.2428 μ in Ra Final = 0.2345 μ in

Rt Init = 3.8602 μ in Rt Final = 4.4404 μ in

Wt. Change -0.0003 gm

Test Conditions

305 Hrs. 55.000 X 10^6 Revs

2.76 GPa (400 Ksi)

$\lambda = 1.0$ T = 60° C (140°F)

Figure 39 Wear Test Results For AISI 52100 Steel Races and Bearing "A-3".

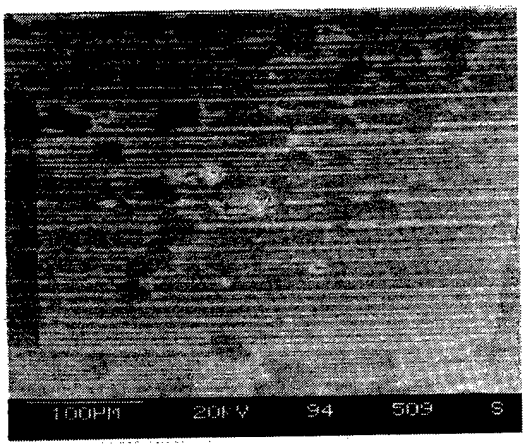

(a)

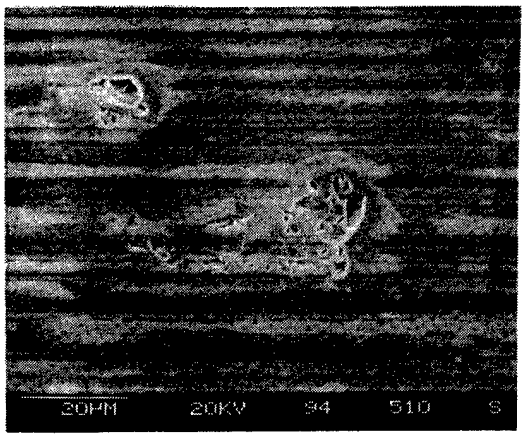

(b)

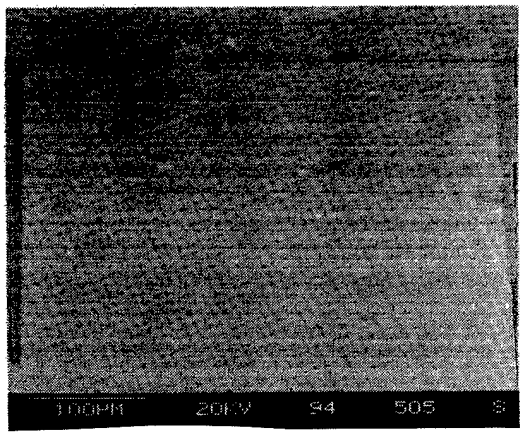

(c)

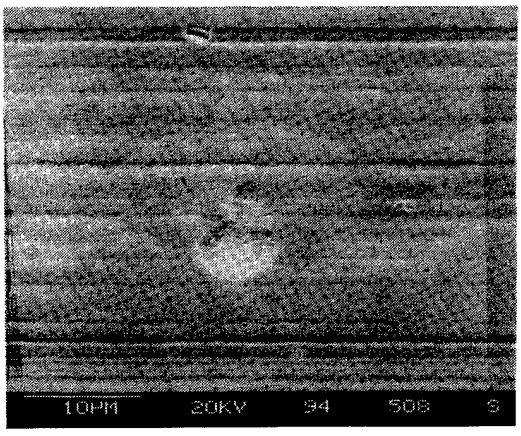

(d)

Figure 40 Post-Test Condition of AISI 52100 Steel Races and Bearing A-3, Run 305 Hrs., At 2.76 Gpa (400 Ksi), λ = 1.0: (a) Outer Race General Appearance, (b) Outer Race Micropitting, (c) Inner Race General Appearance, (d) Inner Race Bruising.

4.4.2 Tests on M-50 Steel Races with NBD-200 Balls

The pretest surface condition typical of the M-50 steel races is shown in Figure 41. The effect of the intersection of the large carbides with the race surfaces on the surface integrity is very apparent in these photos.

Bearing M50-B-1 was tested under conditions identical to those of bearing 52100-A-1, which failed by fatigue spalling just short of the intended 300 hour test time. The M-50 bearing completed 300 hours of running without fatigue failure on a macro-scale. Figure 42 summarizes the dimensional and weight data on the components of bearing B-1. The results were similar to those observed on the 52100 bearings. Essentially no measurable differences were detected between the profiles and surface finishes measured before and after running. Figure 43 shows, however, that fatigue microspalling had occurred on both the inner and outer races. These spalls appeared to have propagated from the large carbides described above. While the spalls were very small, less than 100 μm or less at the time of termination of the testing, they would have eventually led to the failure of the races. No wear track was detectable on the NBD-200 balls after the test.

In an attempt to run a bearing under conditions which would produce wear rather than fatigue, the second M-50 hybrid bearing was run at a temperature of 121°C (250°F). This reduced the calculated EHD film thickness to 0.016 μm (0.62 μin) to give a film thickness to roughness ratio of $\lambda = 0.3$. The contact stress was maintained at 2.76 Mpa (400 Ksi).

The test results for bearing M-50-B2 are shown in Figure 44. Even under these conditions of boundary lubrication, no measurable wear of the components occurred.

The SEM examinations of the tested races in Figure 45 show that the basic appearance of the finish was unchanged. An adherent coating, thought to be a product of degradation of the lubricant, was particularly evident on the surface of the outer race. No distinct wear tracks were visible on the balls from this test. The appearance of the ball surface in Figure 46 suggests that some of the original pits resulting from grain pull-out were filled in by surface film material.

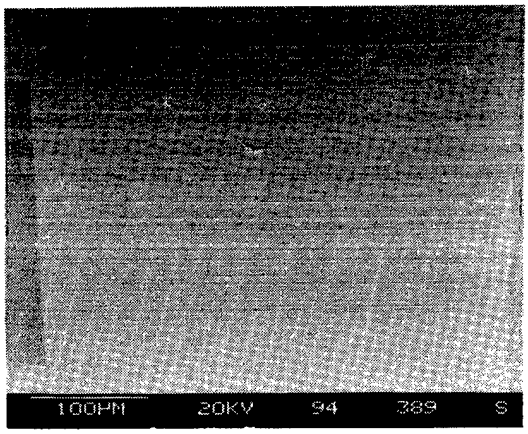

(a)

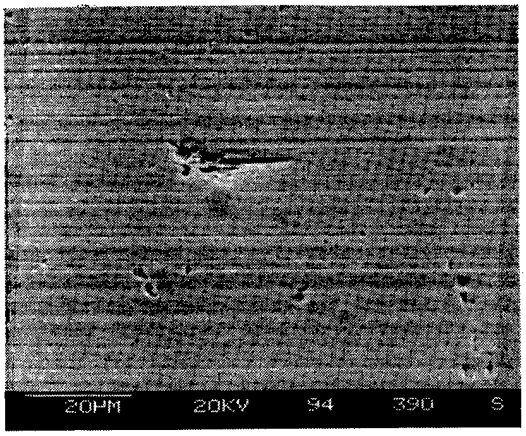

(b)

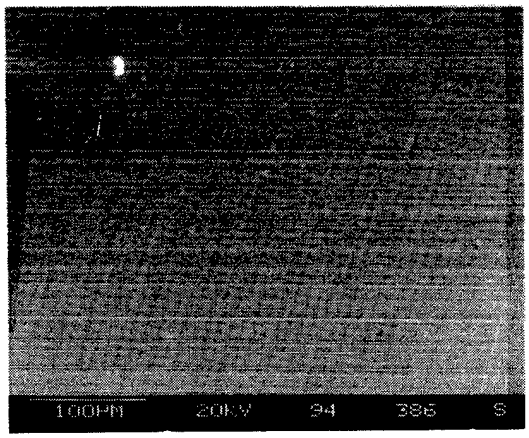

(c)

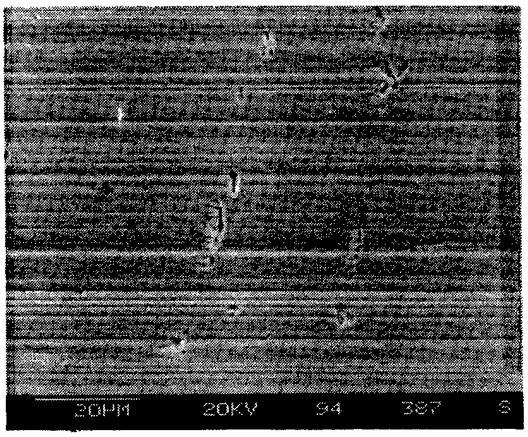

(d)

Figure 41 Typical Pre-Test Surface Condition Of M-50 Steel Races, Bearing B1: (a) Outer Race, General Appearance, (b) Outer Race, Pits Due To Removed Surface Carbides, (c) Inner Race, General Appearance, (d) Inner Race, Pits Due To Removed Surface Carbides. Races Were Sputter-Coated With Pd Prior To Photographing.

Before Testing

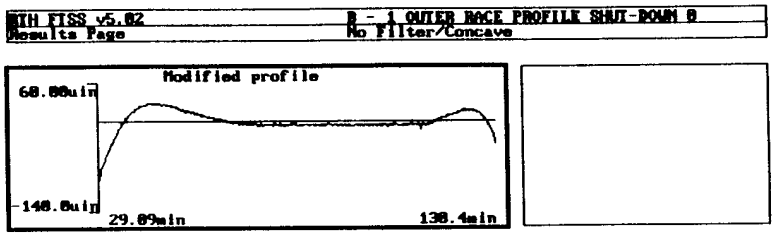

After Testing

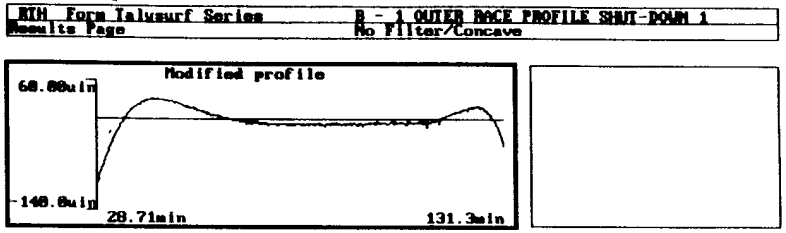

Outer Race

Ra Init = 0.6522 μ in Ra Final = 0.6933 μ in

Rt Init = 6.3518 μ in Rt Final = 5.5501 μ in

Wt. Change +0.0002 gm

Before Testing

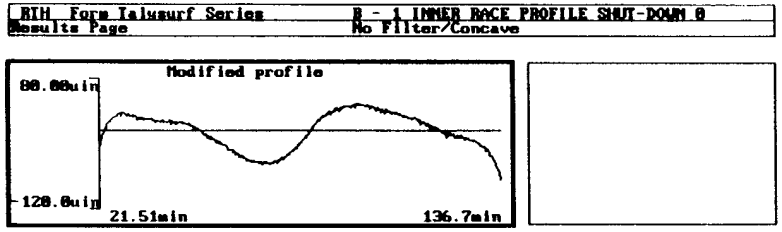

After Testing

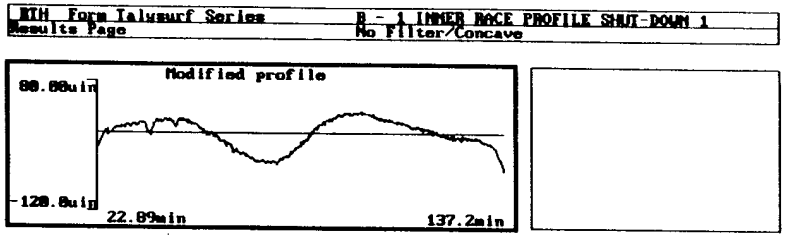

Inner Race

Ra Init = 1.1904 μ in Ra Final = 1.903418 μ in

Rt Init = 8.4074 μ in Rt Final = 23.7645 μ in

Wt. Change -0.0001 gm

Balls

Ra Init = 0.2497 μ in Ra Final = 0.2299 μ in

Rt Init = 2.8114 μ in Rt Final = 3.5322 μ in

Wt. Change 0.0000gm

Test Conditions

300 Hrs. (54 X 10^6 Revs)

2.76 GPa (400 Ksi)

λ = 1.0 T = 60° C (140°F)

Figure 42 Wear Test Results For M-50 Steel Races and Bearing "B-1".

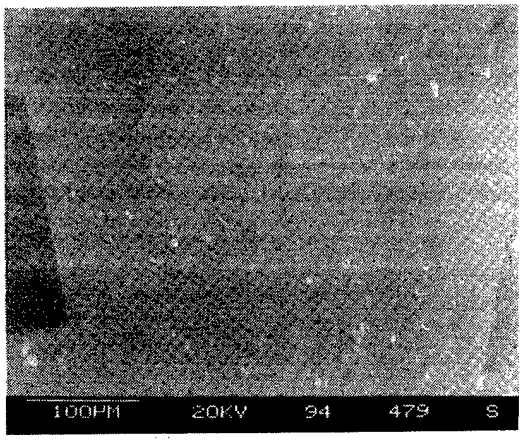

(a)

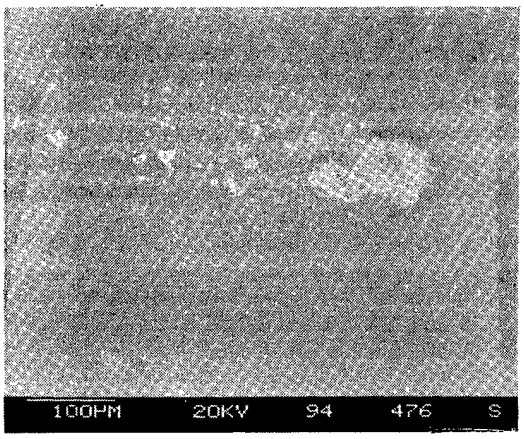

(b)

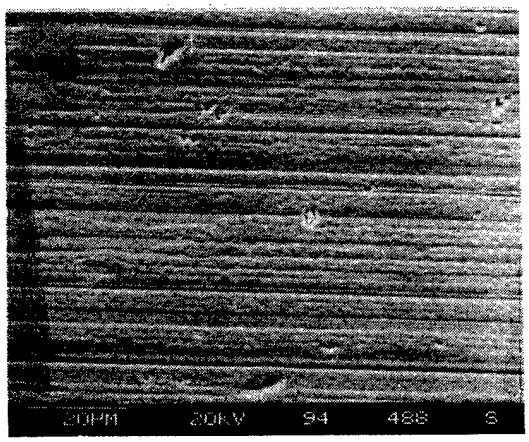

(c)

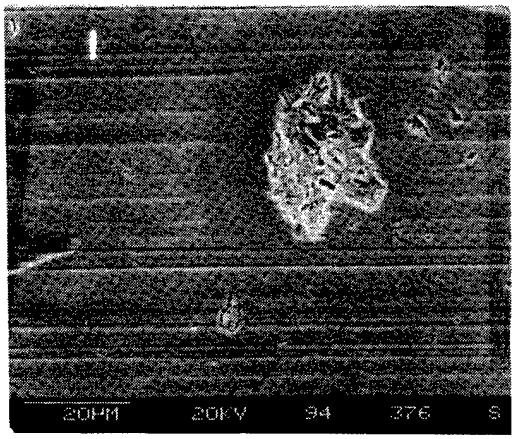

(d)

Figure 43 Post-Test Condition Of Races and Bearing B-1 Run 300 Hrs. At 2.76 GPa (400 Ksi), λ = 1.0: (a) Outer Race, General Appearance, (b) Micro-Spalling On Outer Race, (c) Inner Race, General Appearance, (d) Micro-Spalling On Inner Race.

Before Testing

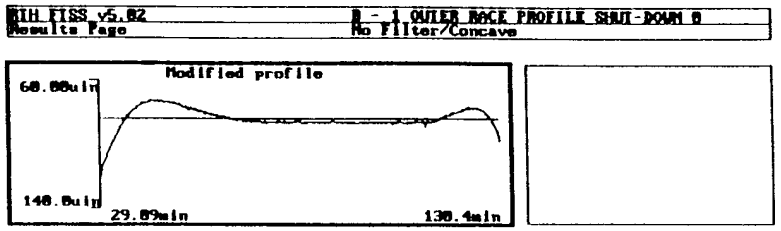

After Testing

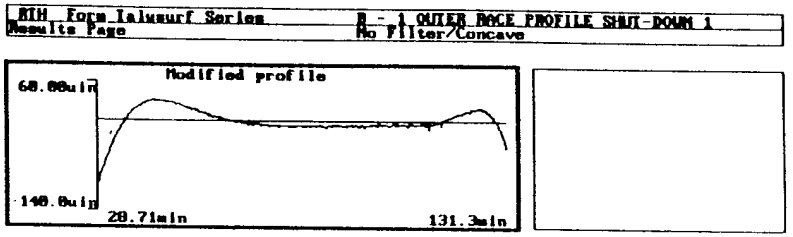

Outer Race

Ra Init = 0.6522 μ in Ra Final = 0.6933 μ in

Rt Init = 6.3518 μ in Rt Final = 5.5501 μ in

Wt. Change +0.0002 gm

Before Testing

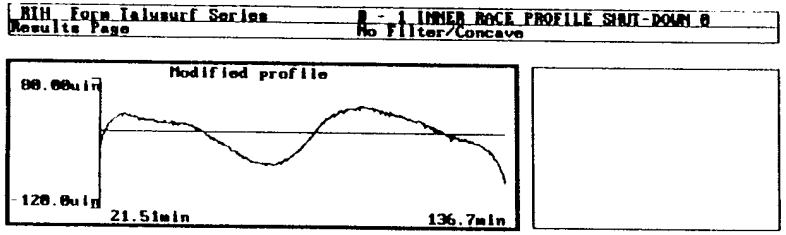

After Testing

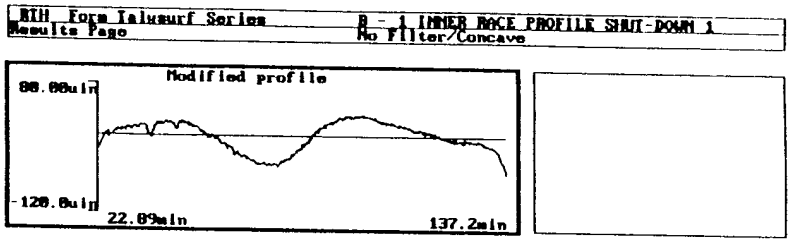

Inner Race

Ra Init = 1.1904 μ in Ra Final = 1.903418 μ in

Rt Init = 8.4074 μ in Rt Final = 23.7645 μ in

Wt. Change -0.0001 gm

Balls

Ra Init = 0.2497 μ in Ra Final = 0.2299 μ in

Rt Init = 2.8114 μ in Rt Final = 3.5322 μ in

Wt. Change 0.0000gm

Test Conditions

300 Hrs. (54 X 10^6 Revs)

2.76 GPa (400 Ksi)

λ = 1.0 T = 60° C (140°F)

Figure 44 Wear Test Results For M-50 Steel Races and Bearing "B-2"

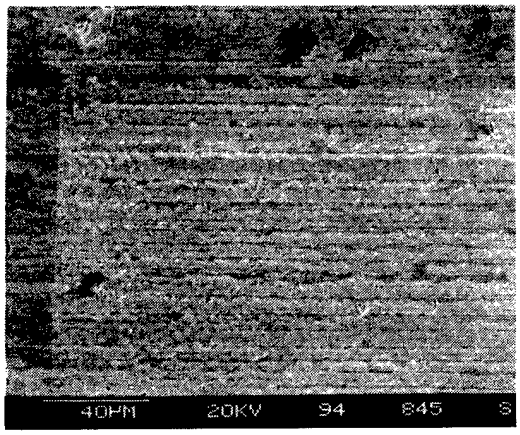

(a)

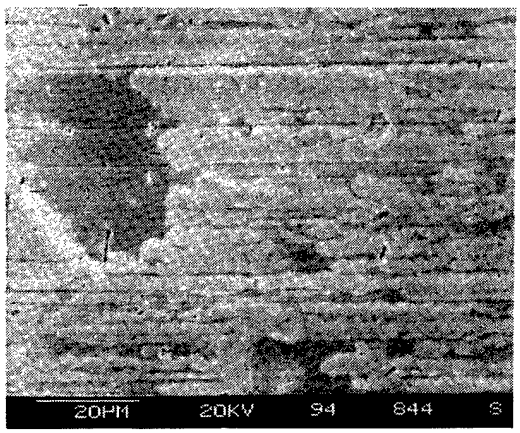

(b)

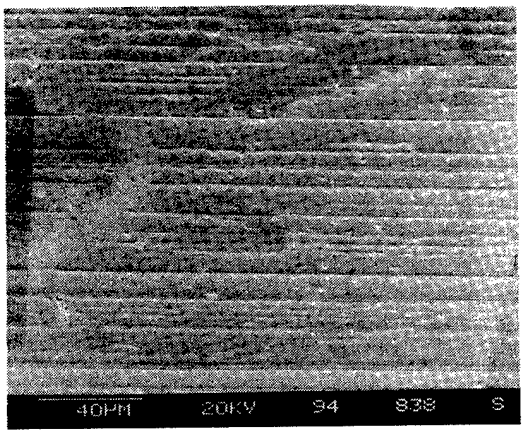

(c)

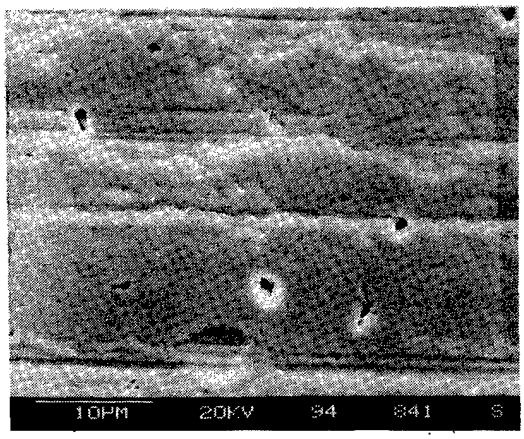

(d)

Figure 45 Post-Test Condition of M-50 Steel Races and Bearing B-2, Run 150 Hrs. At 2.76 GPa (400 Ksi), λ = 0.3: (a,b) Outer Race, (c,d) Inner Race. Races Not Pd-Coated Prior To Photographing Film Appears To Be Unremoved Friction Polymer From Lubricant Degradation.

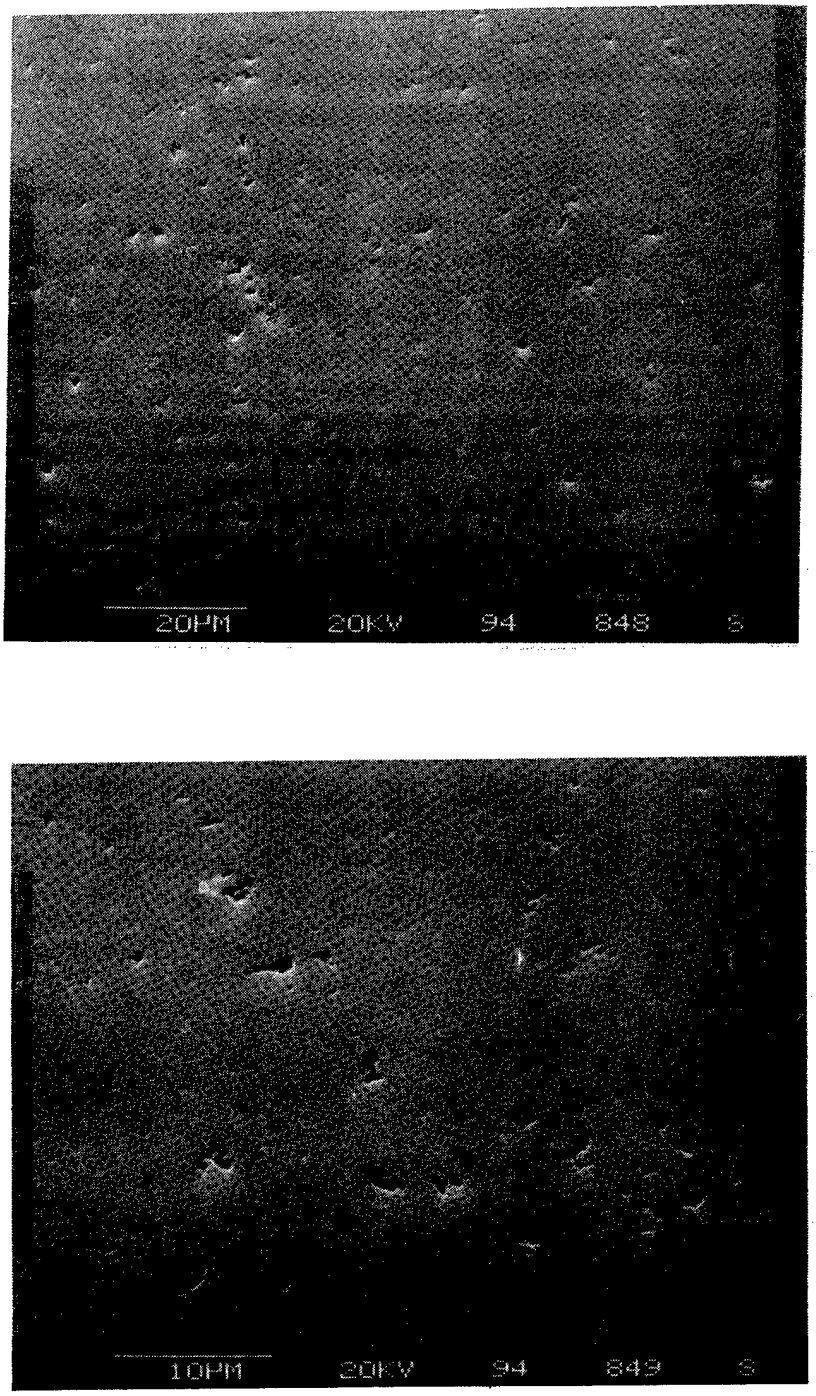

Figure 46 Post-Test Condition Of NBD-200 Ball From M-50 Steel Race and Bearing B2. Two Different Areas On Ball Surface Are Shown. Lubricant Film May Have Filled In Some Surface Grain Pullout.

The final hybrid bearing test was run under a condition of reduced contact stress, to permit running for an extended time under boundary EHD film conditions. Bearing M-50-B3 was run at a maximum Hertzian contact stress of 2.61 Gpa (379 Ksi), calculated to approximately double the expected L-10 life. Although the target was 1000 hours, a slight change in the sound of the bearing running prompted termination of the test at 830 hours, to minimize possible fatigue damage to the bearing. The source of the change in sound was microspalling of the races.

Figure 47 lists the data from the wear test of M-50 steel bearing B3. A slight roughening of the surface of the outer race was measured, while the inner race was unchanged, based on the surface traces. The balls may have become slightly rougher. None of the component weights was changed by a measurable amount. A brown-tinted stain was visible with slight optical magnification on the wear track of the balls.

Figures 48 and 49 illustrate the post-test appearance of the outer and inner races, respectively. The outer race shows numerous microspalls, on the order of 10-15 μm in diameter. A large amount of debris damage from the microspalling, in the form of pitting, dents and apparent polishing-type wear was present. The inner race showed less damage from the circulated debris, but more fatigue micropitting than the outer race. The origins of the fatigue spalling were identified in several instances as alloy carbides (Mo, Cr, Fe) from remnant particles within the spalls. Figure 49d, however, shows a large carbide of this type on the surface within close proximity to a microspall which apparently originated at a cluster of alumina particles instead of at the carbide.

The ball surface appearances inside and outside the wear track are compared in Figure 50. The amount of grain pullout does not show much difference in the two areas. Photo (d) in Figure 50 shows evidence of lubricant degradation and wear products lodged in pores on the ball surface. Figures 51 and 52, from EDAX and wavelength dispersive x-ray analysis, indicate that the products in the wear track of the ball are enriched in phosphorus and zinc from the lubricant additives, iron from the races, carbon from the base oil and oxygen, combined with silicon nitride wear products.

4.4.3 Testing of an All-M-50 Steel Bearing

In the absence of any useful quantitative wear data from the testing of the hybrid bearings, it was decided to test an all-steel bearing as a qualitative comparison to the hybrid bearing performance. A group of 5/32", Grade 5, M-50 steel balls manufactured by Winsted Precision Ball Co. was obtained through MPB Corporation. One set of the remaining M-50 races was assembled with these balls to produce test bearing "X1". This bearing was run under the same load and film thickness conditions as the hybrid bearing B3. Because of the lower elastic modulus of the steel balls compared to silicon nitride, however, the maximum Hertzian contact stress in the steel bearing was lower, 2.27 GPa compared to 2.61 GPa (329 Ksi vs 379 Ksi).

The pretest surface texture of the M-50 balls is shown in Figure 53 to be greatly different from that of the NBD-200 balls (compare to Figure 29). The steel surface was free of the small pores resulting from grain pull-out that characterized the NBD-200 balls. The surface of the M-50 balls was plastically deformed, as well as abraded by the finishing process. Some deeper gouges may have been partially covered over by the plastic flow of the surface. Such areas, even though covered, could still act as spall initiation sites under rolling-contact conditions.

The wear test data for the M-50 steel bearing are shown in Figure 54. The profile traces of the races showed no detectable changes due to running. The surface roughness of the balls and outer race increased slightly from their original values, but the race finishes, after testing in the all-steel bearing, were measurably smoother than those that were shown in Figure 47 for the hybrid bearing M-50-B3. Weight losses of the inner race and the balls were apparently greater than those of the hybrid bearing, even though this bearing was run for only 500 hours, as compared to 830 hours for the hybrid bearing , and at a lower contact stress.

Figures 55 and 56 show, respectively, the post-test appearance of the outer and inner races. Both are marked by numerous microspalls. Note that the race finishes, away from

the spalls, appear much smoother in the all-steel bearing than those in the hybrid bearing illustrated in Figures 48 and 49. The reason for this is not clear. It could be related to some mutual plastic accommodation of the ball and race surfaces or, simply to a greater degree of polishing due to more debris passing through the all-steel bearing in the presence of a greater number of microspalls. At any rate, the effect is minor, in terms of the volume of material removed, compared to that associated with the microspalling.

Figure 57 shows the appearance of the M-50 steel balls after testing. Significant amounts of microspalling occurred on the balls as well as on the races. The unspalled ball surface, also, was smoother than before testing as seen by comparison with Figure 53.

4.4.4 Summary Assessment of Wear Test Results

Taken together, the results of the wear tests described above indicate that, even under severe conditions of boundary lubrication, conventional wear will not be the life-limiting factor in the operation of hybrid ball bearings. In AISI 52100 steel races, the life was limited by race spalling which originated at very small alumina non-metallic inclusions. In M-50 steel races, the life was limited by microspalling which originated at both alumina inclusions and at alloy carbides. Within the lifetime of the races, measurable wear of the bearing components had not occurred. Hybrid bearings have the potential for longer useful lives than all-steel bearings, however, because the steel balls represent an additional bearing element which can be a source of fatigue microspalling. Under these test conditions, no damage to the NBD-200 balls was observed.

Before Testing

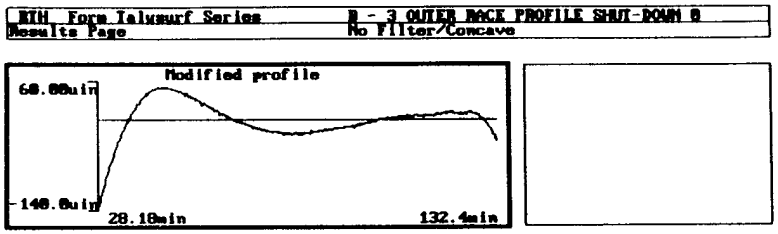

After Testing

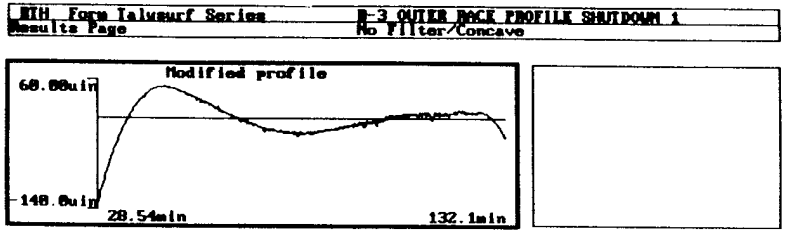

Outer Race

Ra Init = 0.6633 μ in Ra Final = 1.3852 μ in

Rt Init = 5.9824 μ in Rt Final = 12.5259 μ in

Wt. Change +0.0001 gm

Before Testing

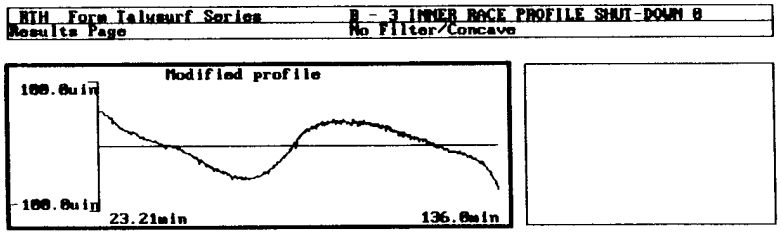

After Testing

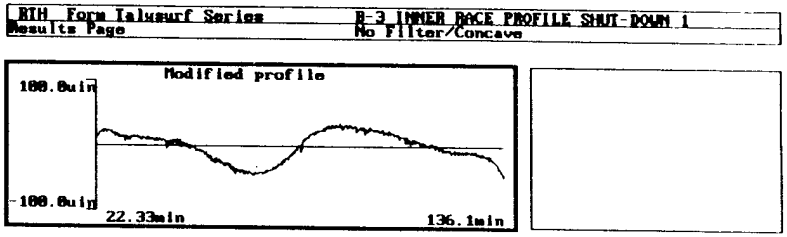

Inner Race

Ra Init = 1.4658 μ in Ra Final = 1.7357 μ in

Rt Init = 22.1750 μ in Rt Final = 18.2926 μ in

Wt. Change -0.0002 gm

Balls

Ra Init = 0.2297 μ in Ra Final = 0.5047 μ in

Rt Init = 2.8114 μ in Rt Final = 5.602 μ in

Wt. Change -0.0001 gm

Test Conditions

830 Hrs. (149.588 X 10^6 Revs)

2.61 GPa (379 Ksi)

$\lambda = 0.3$ T =121° C (250°F)

Figure 47 Wear Test Results For M-50 Steel Bearing "B-3".

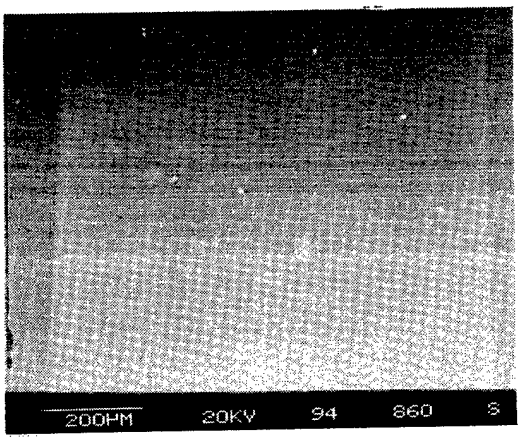

(a)

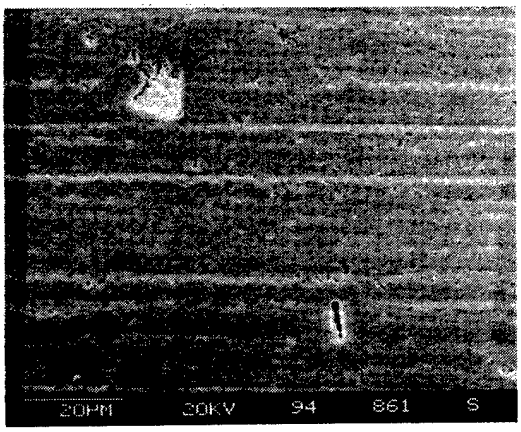

(b)

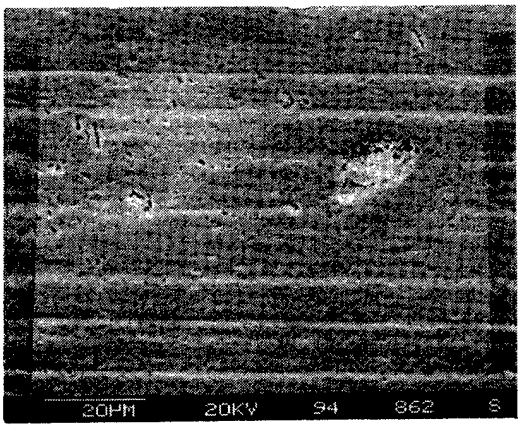

(c)

Figure 48 Post-Test Condition of M-50 Steel Outer Race and Bearing B3, Run 830 Hrs., at 2.61 GPa (379 Ksi), λ=0.3: (a) General Race Appearance with Micropitting, (b) Micropitting and Debris Damage, (c) Additional Micropitting And Debris Damage.

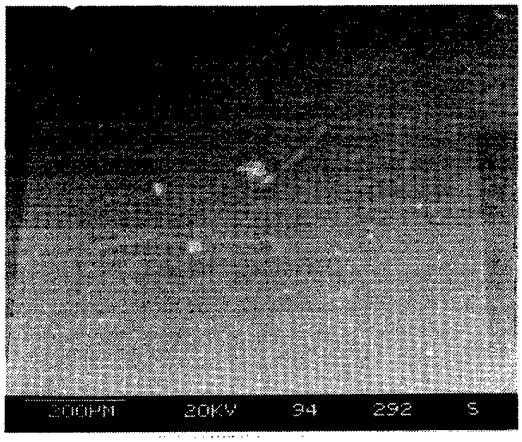

(a)

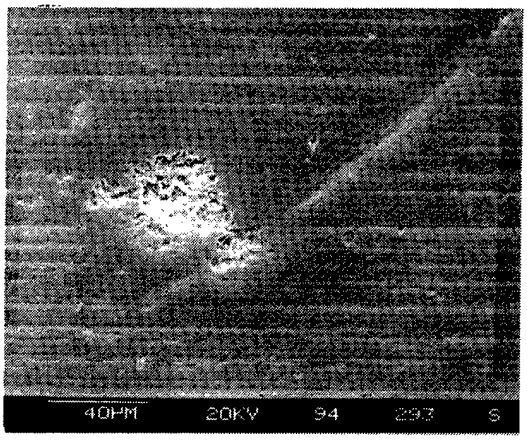

(b)

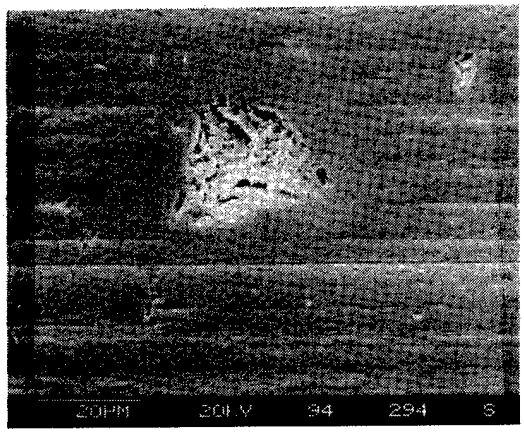

(c)

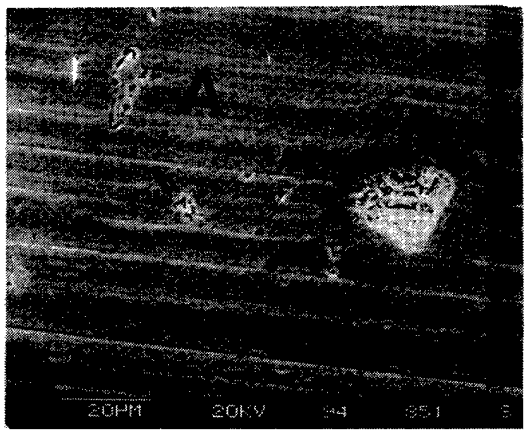

(d)

Figure 49 Post-Test Condition of M-50 Steel Inner Races and Bearing B3 Run 830 Hrs., at 2.61 GPa (379 Ksi), λ = 0.3: (a) General Race Appearance, (b) Micropitting and Debris Gouge, (c) Micropitting And Debris Damage, (d) Micropitting And Debris Damage, Large Carbide At "A".

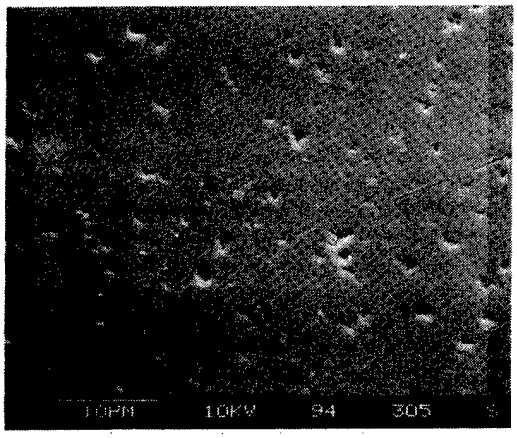

(a)

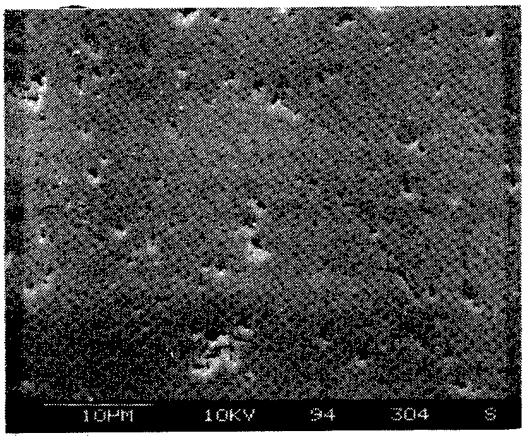

(b)

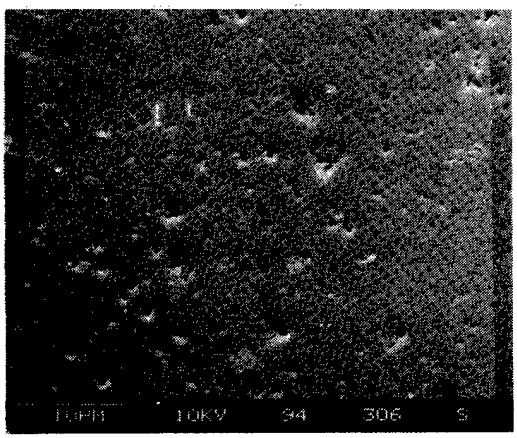

(c)

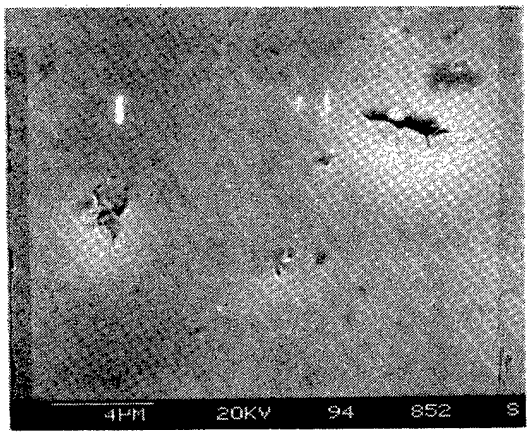

(d)

Figure 50 Post-Test Condition Of NBD-200 Balls From M-50 Steel Races and Bearing B3, Run 830 Hrs., at 2.61 GPa (379 Ksi), λ = 0.3: (a) Appearance Outside of Wear Track, (b) Appearance in Wear Track, (c) Appearance in Wear Track, Second Area, (d) Lubricant Degradation Product in Pits.

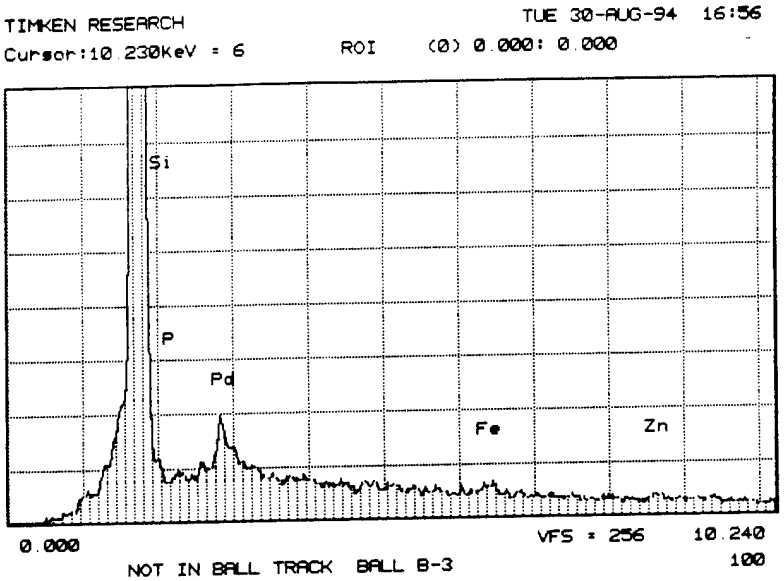

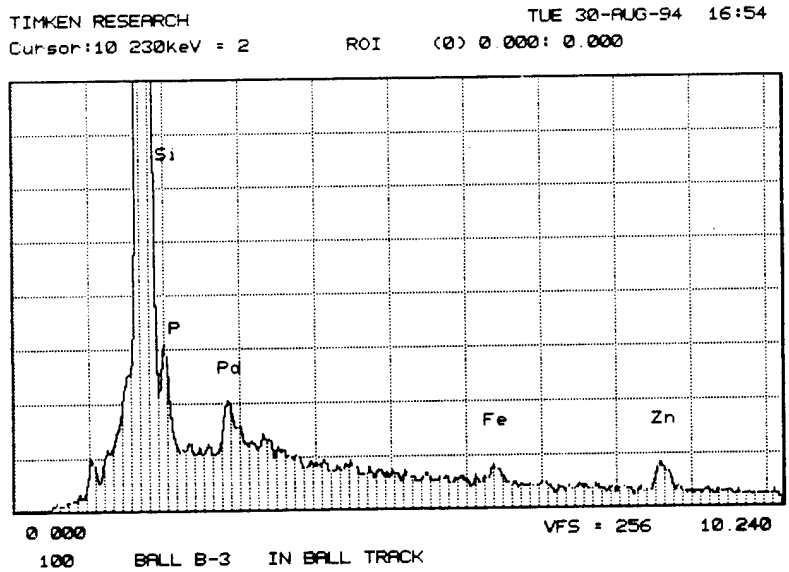

Figure 51 EDAX Analysis of a Post-Test NDB-200 Ball From M-50 Steel Races, Bearing B3. Top: Surface "Outside of" Wear Track, Bottom: Surface "In" Wear Track (Phosphorus, Iron And Zinc Are Indicated).

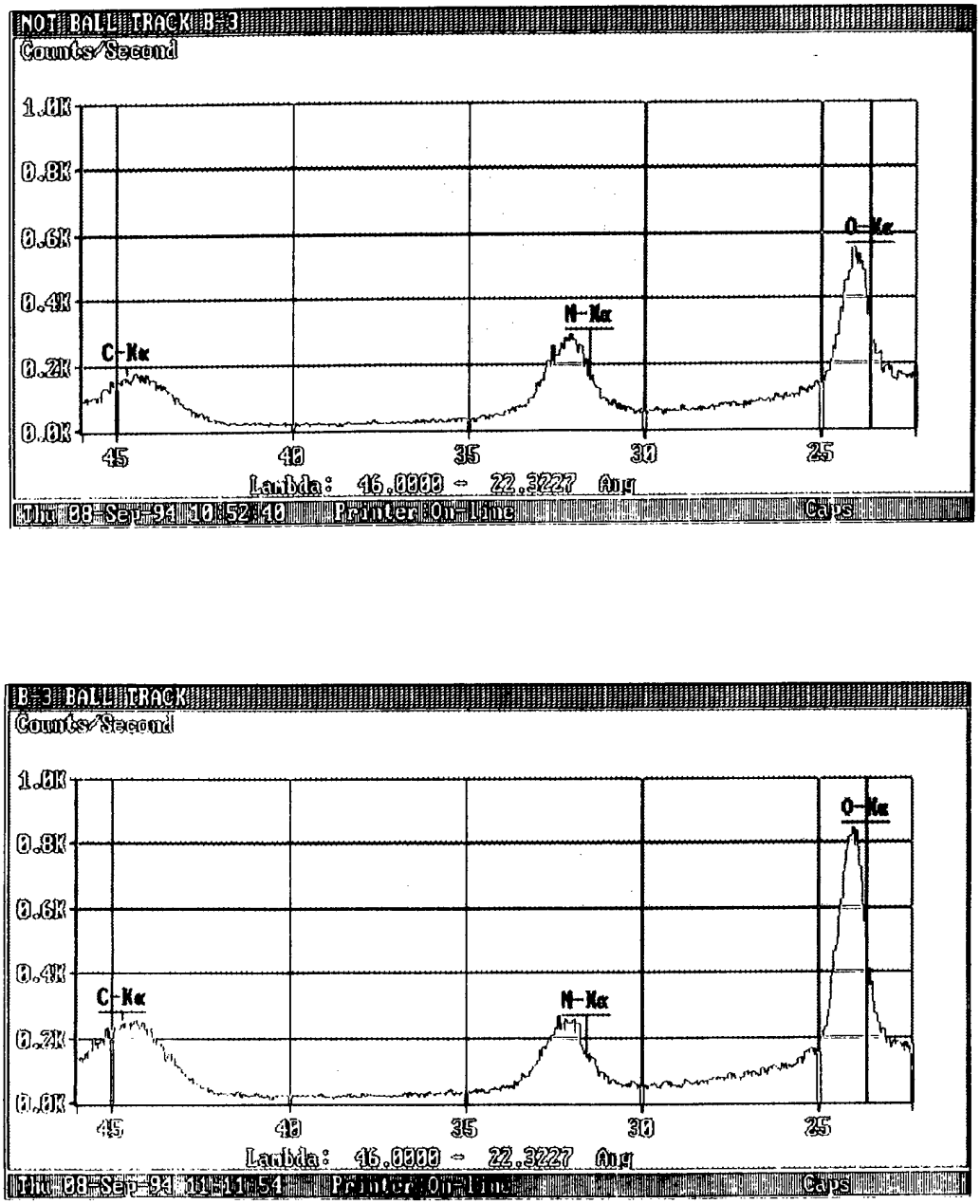

Figure 52 Wavelength Dispersive X-Ray Analysis Of Post-Test NDB-200 Ball From M-50 Steel Race and Bearing B3. Top: Surface "Outside of" Wear Track, Bottom: Surface "In" Wear Track (Pickup of Carbon And Oxygen Is Indicated).

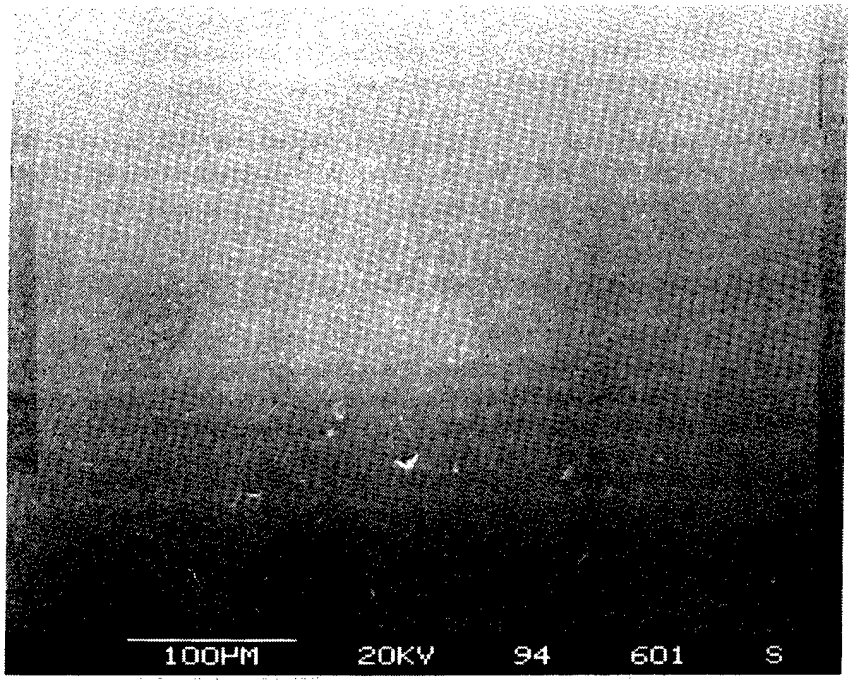

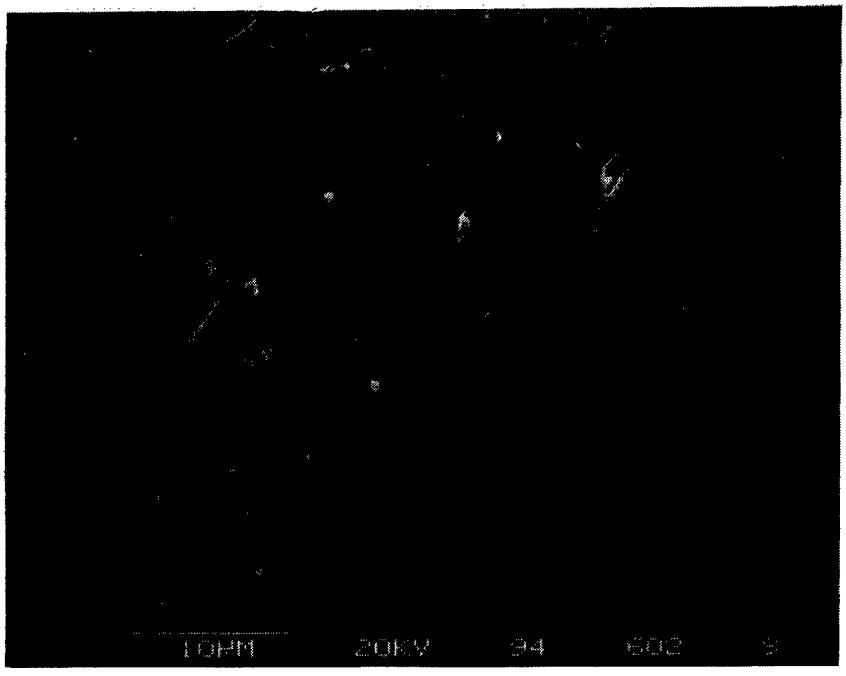

Figure 53 Pretest Surface Condition Of M-50 Steel Balls Tested In M-50 Steel Races and Bearing X1.

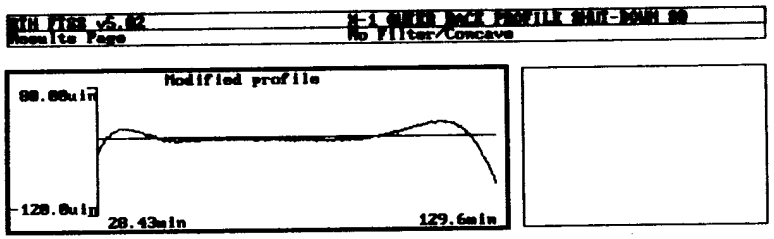

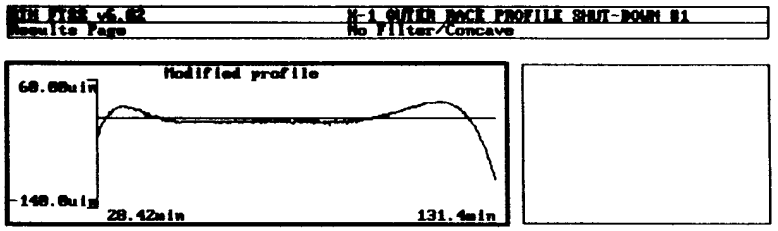

Outer Race

Ra Init = 0.6271 μ in Ra Final = 0.8816 μ in

Rt Init = 8.0135 μ in Rt Final = 9.0259 μ in

Wt. Change 0.0000 gm

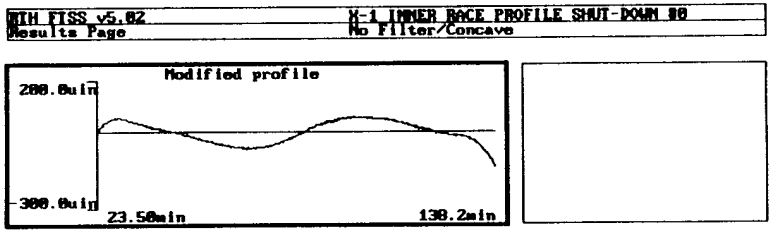

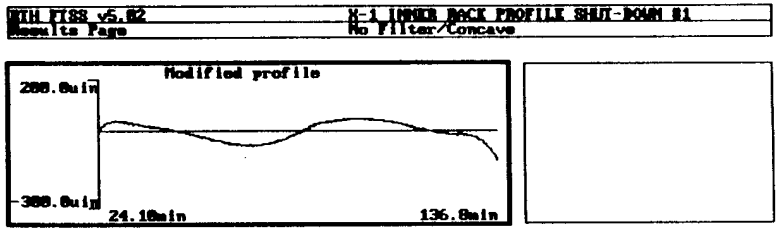

Inner Race

Ra Init = 1.3871 μ in Ra Final = 1.3323 μ in

Rt Init = 13.9130 μ in Rt Final = 10.9004 μ in

Wt. Change -0.0003 gm

Balls

Ra Init = 0.7746 μ in Ra Final = 0.8951 μ in

Rt Init = 5.7508 μ in Rt Final = 7.0121 μ in

Wt. Change -0.0004 gm

Test Conditions

500 Hrs. (90.150 X 10^6 Revs)

2.61 GPa (329 Ksi)

$\lambda = 0.3$ T = 121° C (250° F)

Figure 54 Wear Test Results For All M-50 Steel Races and Bearing X1.

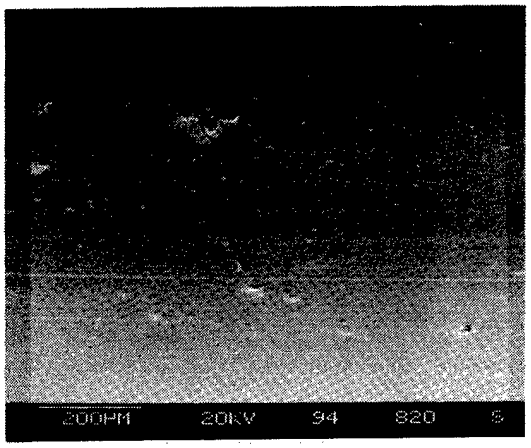

(a)

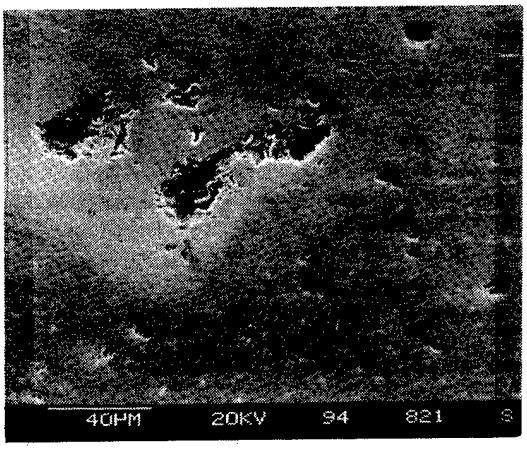

(b)

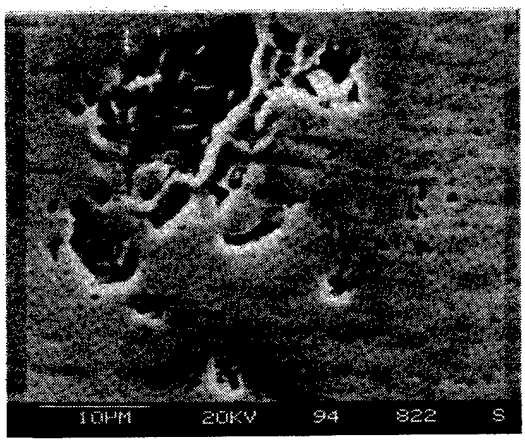

(c)

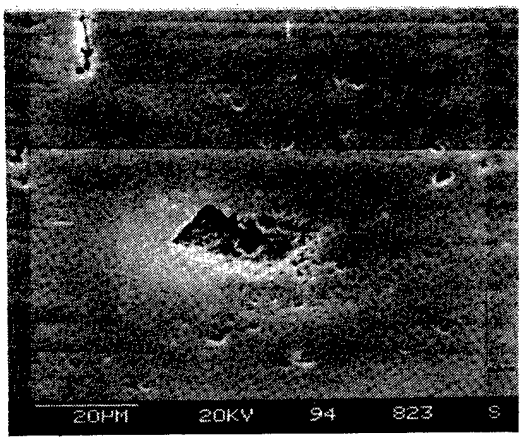

(d)

Figure 55 Post-Test Appearance of M-50 Outer Race, Bearing X1, Run 500 Hrs., At 2.27 GPa (329 Ksi), λ=0.3: (a) General Appearance, (b,c,d) Microspalling.

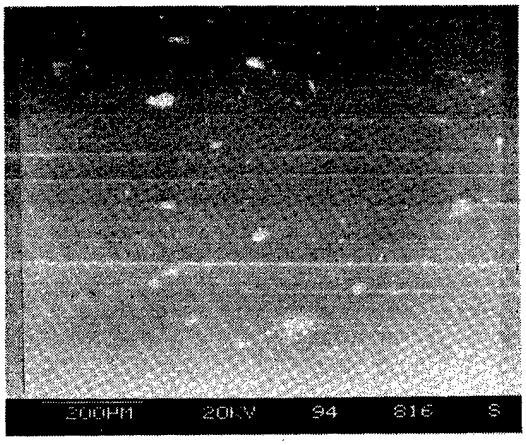

(a)

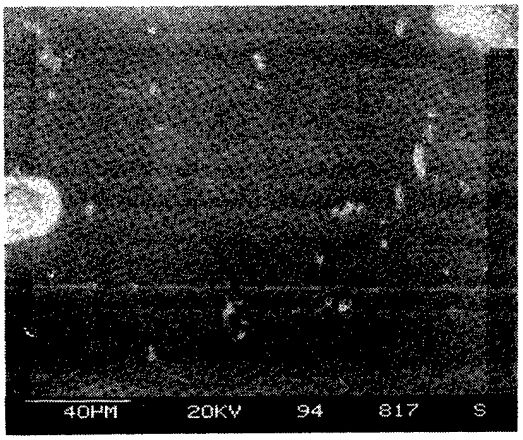

(b)

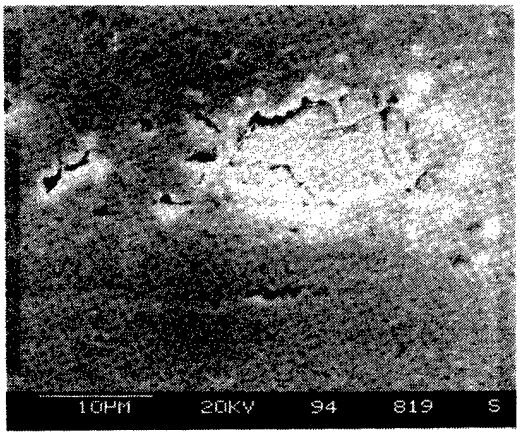

(c)

(d)

Figure 56 Post-Test Appearance Of Inner Race Of All-Steel Bearing M-50-X1 Run 500 Hrs. At 2.27 GPa (329 Ksi) λ = 0.3 (a) General Appearance (b,c,d) Microspalling.

4.4.5 Wear Test Lubricant Analyses

Two independent analytical techniques were used to gain information on bearing wear mechanisms on a scale much finer than that provided by the weight change and metrological measurements described above. Samples of the lubricant removed from the wear test rig and bearings after each test run were subjected to "ferrographic" inspection (Duplex Ferrograph Analyzer by Foxboro Analytical) to characterize the nature of any particles generated during running of the bearings. The used lubricants were also analyzed by Fourier transform infrared spectroscopy (Nicolet 510 FT-IR Spectrometer) to identify any changes in the structure of the lubricant compounds which might have occurred as a result of their bearing exposure.

A direct comparison of the behaviors of the different bearing material systems should, of course, be based on the results of runs made under identical conditions of EHD film thickness, contact stress and running time. Unfortunately, the exploratory nature of finding appropriate test conditions did not produce such an orderly set of data in this program. Table 7 presents the results of the ferrographic studies made on the lubricants from the longest runs made on the AISI 52100 and M-50 hybrid bearings and on the all-M-50 steel bearing. Ferrography is a somewhat subjective technique whose interpretation relies heavily on the skill and experience of the operator. The observations in this program were performed by Ms. Teri R. Reese. Her comments on the nature of the wear particles observed are contained in some detail in Appendix A. In summary, the comparison of the results from the three bearings showed that the lubricant from the hybrid bearing with races of AISI 52100 steel contained more ferrous wear particles than the other two, particularly in the categories of severe sliding wear with striations and bluing, cutting wear, spheres and laminar particles. The hybrid bearing with races of M-50 steel, on the other hand, appeared to show more evidence of wear of the silicon nitride, but less wear of the ferrous components. A direct comparison of the behaviors of the different bearing material systems should, of course, be based on the results of runs made under identical conditions of EHD film thickness, contact stress and running time.

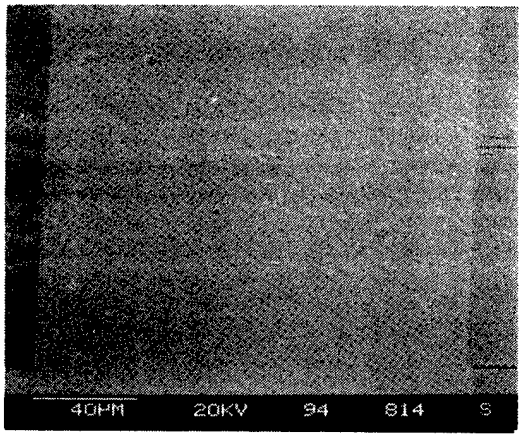

(a)

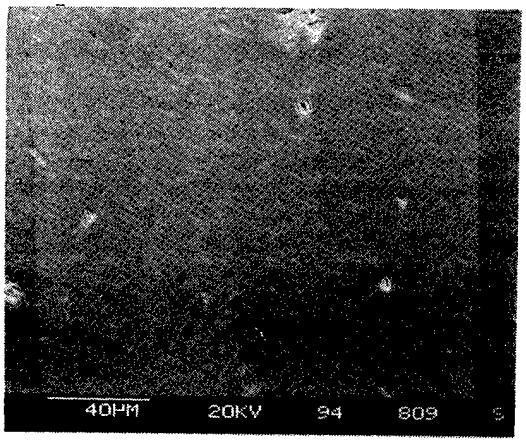

(b)

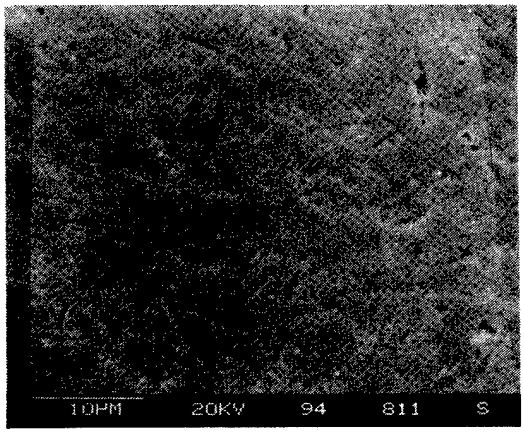

(c)

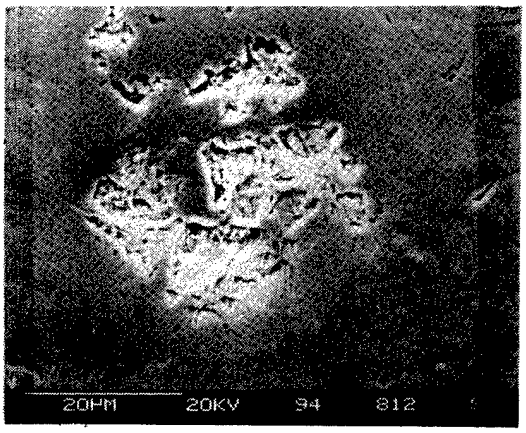

(d)

Figure 57 Post-Test Appearance Of M-50 Balls From Bearing M-50-X1 Run 500 Hrs. At 2.27 GPa (329 Ksi) λ = 0.3: (a) Outside Wear Track Showing Minor Debris Denting, (b) In Wear Track Showing Microspalls, (c) In Wear Track, Smoothing Of Surface Finish, (d) Microspalling.

Unfortunately, the exploratory nature of finding appropriate test conditions did not produce such an orderly set of data in this program. Table 7 presents the results of the ferrographic studies made on the lubricants from the longest runs made on the AISI 52100 and M-50 hybrid bearings and on the all-M-50 steel bearing. Ferrography is a somewhat subjective technique whose interpretation relies heavily on the skill and experience of the operator. The observations in this program were performed by Ms. Teri R. Reese. Her comments on the nature of the wear particles observed are contained in some detail in Appendix A. In summary, the comparison of the results from the three bearings showed that the lubricant from the hybrid bearing with races of AISI 52100 steel contained more ferrous wear particles than the other two, particularly in the categories of severe sliding wear with striations and bluing, cutting wear, spheres, and laminar particles. The hybrid bearing with races of M-50 steel, on the other hand, appeared to show more evidence of wear of the silicon nitride but less wear of the ferrous components. The ferrographic technique appears to be potentially very useful in studying the pre-fatigue mode of damage in bearings. It is much more sensitive to the various wear processes than weight changes or dimensional changes. A limitation of the evaluations in this program was the very small volume of lubricant available for study, less than 3 ml after testing.

FT-IR studies of the unused test oil and of samples from the various wear test runs were conducted by Dr. C. F. Kernizan. A plot of the FT-IR spectrum of unused MobilJet-II, MIL-L-23699 oil is shown, with significant transition peaks identified, in Figure 58. The transitions suggest that the base oil was composed of a dibasic acid ester and a phosphorus-containing extreme-pressure and antiwear agent. The E.P. agent was probably tricresyl phosphate. Samples of the oil from the original wear tests run at 60°C (140°F) showed no detectable change in their FT-IR characteristics. A sample of unused oil was subjected to a differential scanning calorimetry (DSC), (Dupont DSC10) test, to determine what reactions might be expected under conditions of static heating in air.

Table 7
Results Of Ferrographic Analysis
Of Post-Test Lubricants
Bearing 52100-A3 (NBD-200 Balls)
305 Hr., λ=1.0

Types of Particle	None	Few	Moderate	Heavy
Normal Rubbing Wear		X		
Severe Wear		X[a]		
Cutting Wear		X		
Chunks	X[b]			
Laminar	X			
Spheres	X[c]			
Dark Metallo-Oxide	X			
Red Oxide	X			
Corrosive Wear Debris				
Non-Ferrous Metal				
Non-Metallic Birefringent: Inorganic Organic				
Non-Metallic, Amorphous		X[d]		
Friction Polymers	X[e]			
Fibers	X			
Others, Specify				

Note:

[a] Some with striations, some with bluing around edges.

[b] A few extremely large chunks with striations (turn red with filter in reflected light, but don't always line up in rows)

[c] Very rare amount

[d] Silicon nitride

[e] Embedded with ferrous and silicon nitride particles.

Table 7 (continued)
Bearing M-50--B3 (NBD-200 Balls)
830 Hr., λ=0.3

Types of Particles	None	Few	Moderate	Heavy
Normal Rubbing Wear		X		
Severe Wear	X			
Cutting Wear	X			
Chunks				
Laminar	X			
Spheres				
Dark Metallo-Oxide				
Red Oxide				
Corrosive Wear Debris		X		
Non-Ferrous Metal				
Non-Metallic Birefringent: Inorganic Organic				
Non-Metallic, Amorphous			X[a]	
Friction Polymers	X			
Fibers	X			
Others, Specify				

Note:

[a] Silicon nitride particles (rare, very large particles >150 μm).

Table 7 (continued)
Bearing M-50-X1 (M-50 Steel Balls)
500 Hr., λ=0.3

Types of Particles	None	Few	Moderate	Heavy
Normal Rubbing Wear		X		
Severe Wear	X			
Cutting Wear	X			
Chunks				
Laminar	X			
Spheres				
Dark Metallo-Oxide				
Red Oxide				
Corrosive Wear Debris				
Non-Ferrous Metal				
Non-Metallic Birefringent: Inorganic Organic				
Non-Metallic, Amorphous				
Friction Polymers	X			
Fibers	X			
Others, Specify				

All Wear Rating levels are Based on: "Wear Particles Atlas (Revised)" D.P. Anderson, Predict Technologies, (June 1982) For Advanced Technology Office, Naval Air Engr. CTR. Report NAEC 92-163

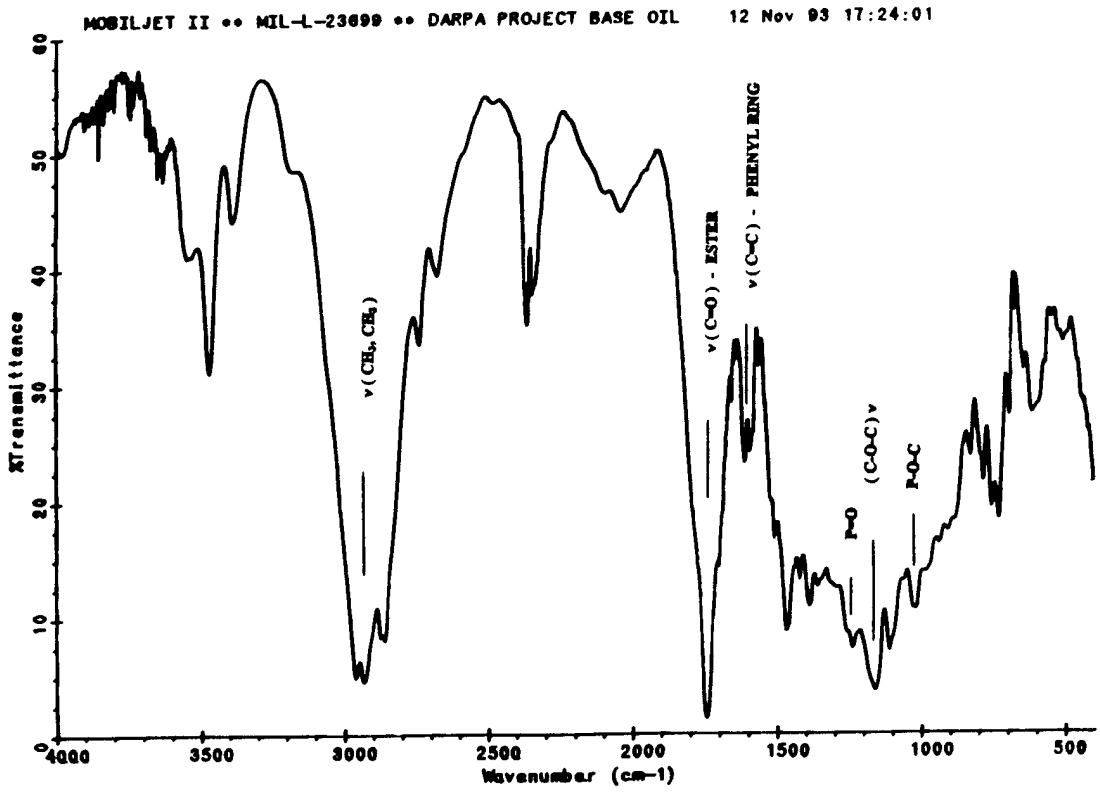

Figure 58 Results Of FT-IR Analysis Of Unused Wear Test Oil. Peak Identification According To: Aldrich Library Of FT-IR Spectra, Charles J. Pouchert, ed. ED. 1, (1985) Aldrich Chemical Co., Inc. Milwaukee, WI.

As shown in Figure 59a, a reaction occurred at 164.5°C (328°F). Based on this information, a sample of the oil was heated to 180°C (356°F) for a period of 3 hours. The FT-IR analysis of this sample showed (Fig. 59b) that decomposition of the phenyl ring <ν(C=C)> bond had occurred, which appeared at wavenumbers 1595 and 1616 cm^{-1} in the new oil. No other changes were evident.

The FT-IR spectra of samples of lubricant from the wear tests of the hybrid M-50 steel bearing "B-3" and the all-M-50 steel bearing "X1" are shown in Figure 60. The unexpected, and unexplained, result is shown (Fig. 60a) that the same <ν(C=C)> bond decomposition occurred in the test of the hybrid bearing at a temperature of only 121°C (250°F) when the influence of the dynamic rolling contact was added. In the lubricant from the all-steel bearing test, however, the phenyl ring <ν(C=C)> bond is still present after running. This observation bears further investigation, since lubricant stability is usually considered to be improved in hybrid bearings, as compared to all-steel bearings. It is possible, based on the measured relatively smoother race finishes of the post-tested, all-M-50 steel bearings, that the contact temperatures were actually lower in this bearing than in the hybrid bearing. The shorter operating time and the lower actual contact stress in the all-steel bearing are, of course, alternative explanations.

4.5 Wear Modeling

One objective of this program, as part of Task 3.3.2, was to describe the wear data from the hybrid bearing tests in terms of a mathematical model. As described in the previous sections, however, "conventional" wear was not observed within the fatigue lifetime of the bearing steels. The measurable wear in these tests was in the form of microspalling of the races and, in cases where the microspalling reached a great enough severity, a secondary shallow material removal from the NBD-200 ball surfaces. Rolling contact fatigue testing performed at The Timken Company, as yet unpublished, has shown that large differences in the resistance to such damage can be found among the various "bearing quality" silicon nitride materials available from different manufacturers today.

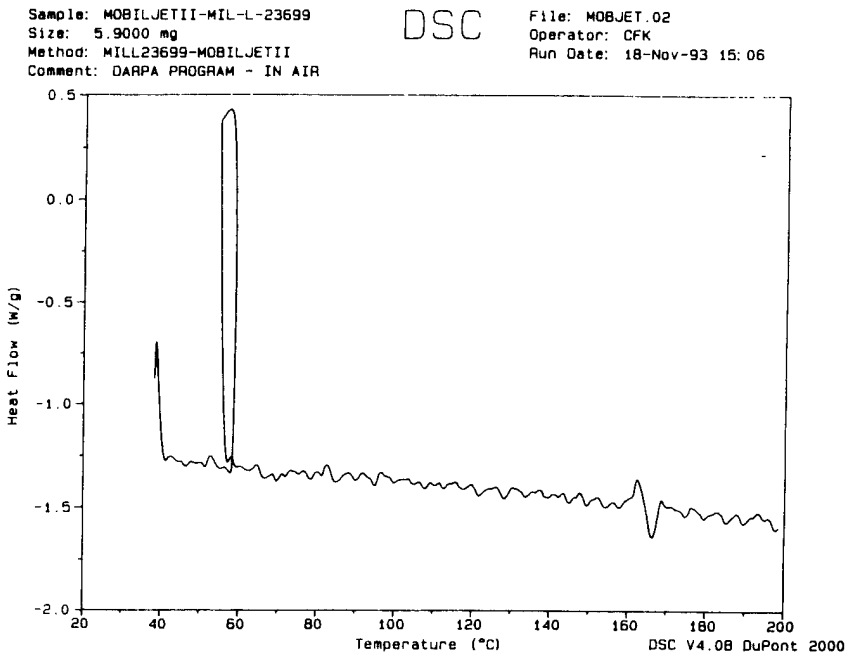

(a)

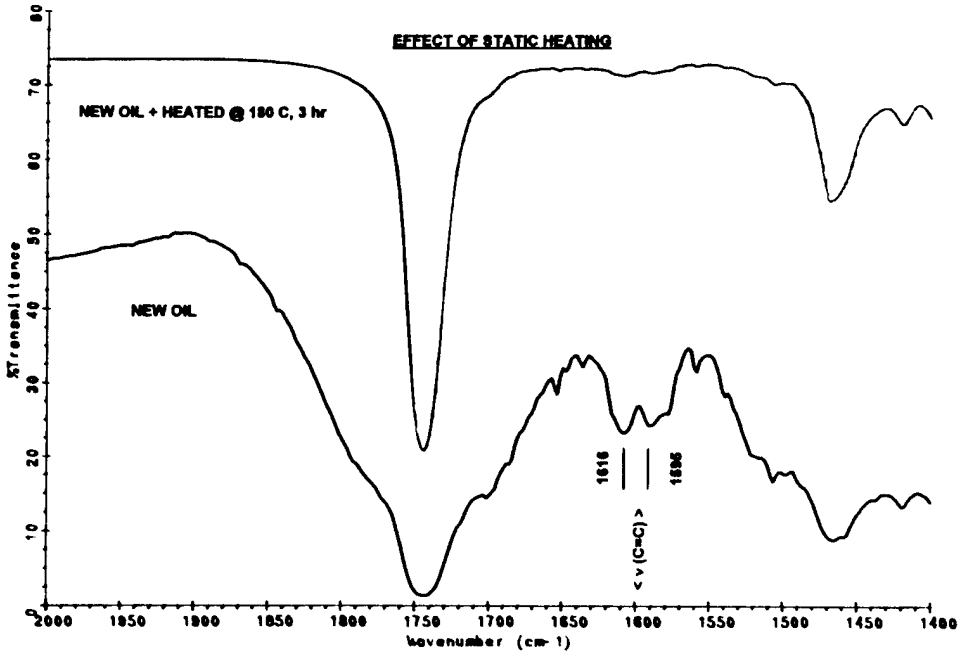

(b)

Figure 59 (a) DSC Scan Of New MobilJet-II Lubricant, Reaction At 164.5° C., (b) FT-IR Comparison Of MobilJet-II Heated 3 Hr. At 180° C., (With Unused Oil. Decomposition Of < υ (C = C) > Bond At 1595 And 1616 cm^{-1}).

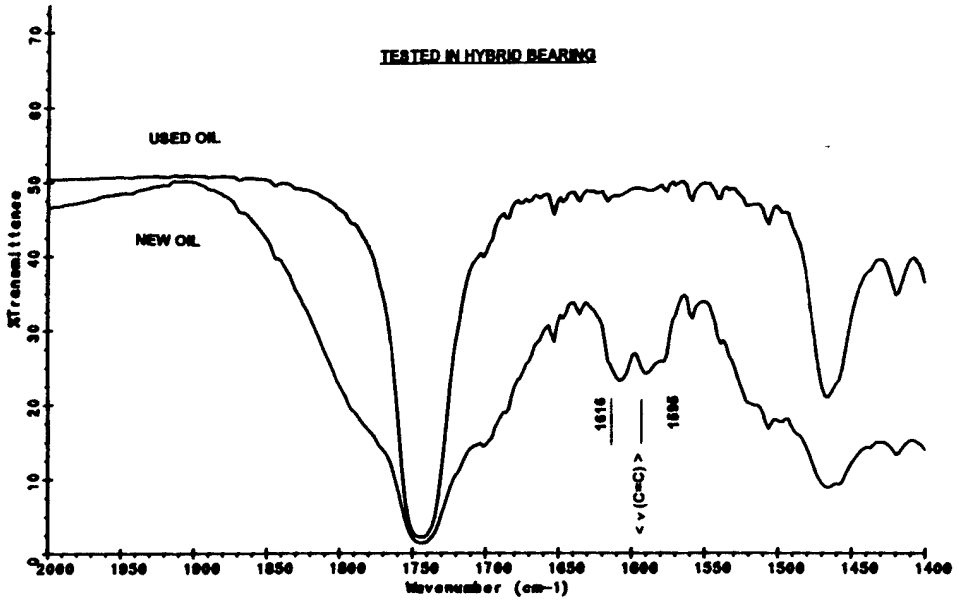

(a)

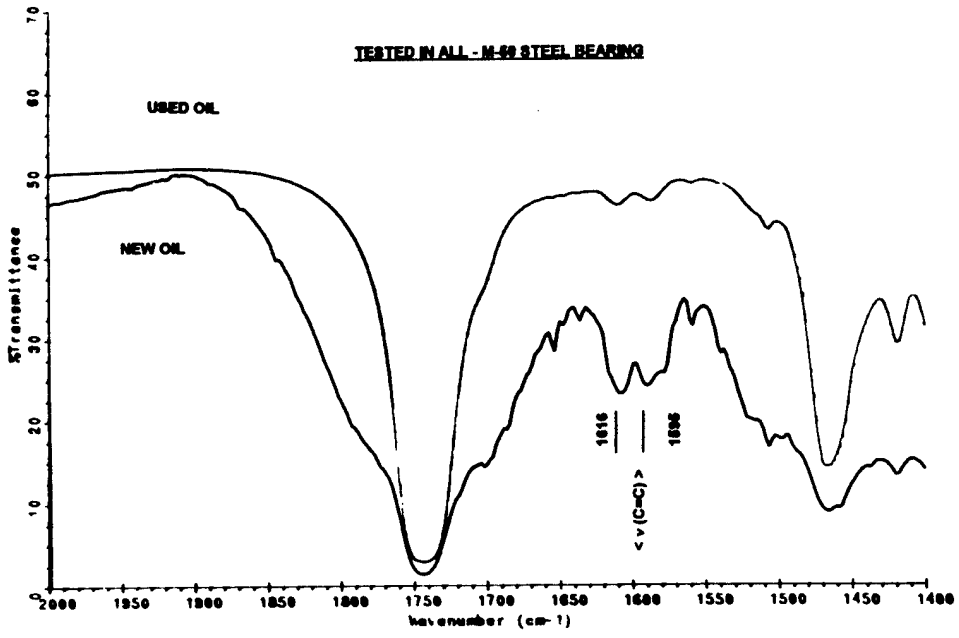

(b)

Figure 60 FT-IR Comparison Of Used And Unused MobilJet-II Oils Tested At 121° C (250° F) In:(a) M-50-B3 Hybrid Bearing 830 Hr., (b) M-50-X1 All-Steel Bearing 500 Hr.

The following comments by M. R. Hoeprich reflect the findings of the literature search on the tribology of silicon nitride, Appendix B, also prepared by Mr. Hoeprich.

4.5.1 Mathematical Wear Model

In lubricated rolling contact, the silicon nitride wear mode is primarily grain pullout (cracked out by grain boundary tensile stress crack development), intergranular fracture, and submicron chipping (section 4.4.1). Some pit spalling from cracks developing along the sides of the wear track due to tensile stresses also added to the wear. If the humidity is high, tribochemical reactions may contribute to the wear.

For the steel raceways, abrasive wear and plastic deformation are expected to be the primary raceway wear modes. There may also be metal transfer to the silicon nitride.

The bearing wear tests conducted in this project were at stress levels significantly lower than rolling contact tests cited above. The film thickness to roughness ratio was 1.0 at the beginning and reduced to 0.3 in subsequent tests (low but not extreme). Consequently, any grain pull-out was likely to be rare. Since the lubricant was heated, no moisture should have been present in these tests which could affect the wear process. It was anticipated that the Archard wear model would have been a suitable starting point. Available wear data indicated that the rate of wear of ball contacts decreased with time (implying exponents would have been appropriate on operating parameters). Of course these data were gathered at high stress levels and it is not known if these same wear mechanisms are operative at the bearing test conditions. It was also likely that other bearing types would wear at other exponential rates.

The following wear coefficient equations were adapted from the Archard wear model for the case of a ball bearing. They could be used if measurable wear of some form was found. Silicon nitride equations of two forms were given depending on whether a wear track was found or only superficial grain pull out was observed.

Archard model: $V/d = k\ W/p_m$

For silicon nitride, let V=Vsn

-With grain pull out V_{sn} = silicon nitride wear volume (mm^3)
$= N(2\pi r)(2a)\ v$
N = number of grains pulled out/mm^2
r = ball radius (mm)
a = half ellipse major axis (mm)
v = average grain volume (mm^3)

-With a wear track $V_{sn} = A_r(2\pi r)$
A_r = cross-sectional area of ball wear track
d = (total inner race revolutions)(πRi)
Ri = inner race radius
W = applied load (N)
p_m = the pressure hardness (kg/ mm^2)
K_{sn} = wear coefficient

For the steel races let V=Vst

V_{st} = steel raceway wear volume (mm^3) (both races) = 2π(Ri Ai+Ro Ao)
Ai = cross-sectional area of inner race wear track
Ao = cross-sectional area of outer race wear track
Ri = inner race radius
Ro = outer race radius
d = (total inner race revolutions)(πRi)n
n = number of balls
W = applied load (N)
p_m = the pressure hardness (kg/ mm^2)
K_{st} = wear coefficient for two steel ball bearing raceways

To determine the wear coefficients, then, required data on the number of pulled-out grains and the size of the wear track in the steel races as a function of running time. The tests performed in this program did not yield the necessary data, since no measurable wear was detected.

5.0 Conclusions

1. Under conditions of full elastohydrodynamic lubrication, and under Herzian contact stresses which significantly exceed those typical of turbine engine mainshaft bearing operation, the fatigue life of standard NBD-200 balls in a hybrid bearing configuration was significantly better than that of all-steel bearings made of CEVM AISI 52100 steel. Within a group of 560 NBD-200 balls tested, none failed within a cutoff limit of five times the L_{10} life of the all-steel bearings.

2. For flaws produced by indenting with a Vickers diamond hardness indentor, the critical crack size for producing rolling contact fatigue failure in NBD-200 balls lies between 61μm and 172 μm. The critical flaw size determined by this technique may be different, however, than that for flaws from other sources, because of the influence of raised material around the indentation, which typically would not be present with other flaw types, such as porosity or inclusions within the silicon nitride material.

3. The Surface Acoustic Wave NDE technique developed at Stanford University was shown to be capable of detecting specific defect types in Volume Two of this report. However, a relationship between the severity of existing compression crack defects and rolling contact fatigue performance was not established by these tests.

4. The Thermal Proof Test developed at the University of Dayton to enhance the detection of defects in NBD-200 balls may have introduced critical defects in balls which otherwise would have performed satisfactorily in subsequent bearing operation.

5. Hybrid bearings combining either CEVM AISI 52100 steel or VIMVAR, M-50 steel races with NBD-200 balls did not show a measurable amount of wear within the fatigue lifetime of the steel races. Fatigue microspalling of the races occurs at nonmetallic inclusions or at larger alloy carbides before conventional wear occurred, even under boundary lubrication conditions with film thickness / roughness ratios on the order of 1.0 and 0.3.

6. Under the conditions of the wear testing performed in this program, no beneficial effect to lubricant stability was shown by the use of hybrid bearings. The FT-IR analyses showed a breakdown of a carbon-carbon bond in the MIL-L-23699 lubricant tested in a hybrid bearing which did not occur in a similarly run all-steel bearing.

6.0 Recommendations

1. Consider the use of NBD-200 balls for extended-life ball bearings. In both the fatigue and wear tests conducted in this program, NBD-200 balls demonstrated useful lives well beyond the accompanying premium bearing steel races.

2. Continue development of a Surface Acoustic Wave type of nondestructive inspection technique as a enhancement to standard inspection techniques. The critical flaw size in NBD-200 balls appeared to be within the inspection capability of the standard techniques, but a reliable, more rapid procedure could potentially contribute to a net cost reduction of the finished balls. Thermal proof testing did not appear to be a desirable technique for inspection of NBD-200 balls.

3. Ferrographic techniques should be included in further investigations of the basic mechanisms of wear in hybrid bearing contacts. These techniques were more sensitive to the early stages of wear and race microspalling than dimensional or gravimetric techniques.

4. Continue the investigation of the wear of hybrid bearings with races made of carburizing grades of steel such as M-50NiL. Existing experience suggested that the resistance to fatigue microspalling of these races should be better than that of the through-hardening grades, while the wear resistance may be inferior. Unfortunately, the bearing configuration which was chosen for testing in this program was not possible to manufacture in silicon carbide because of thin sections.

Appendix A

A DISCUSSION OF VARIOUS TYPES OF WEAR DEBRIS AND APPLICATION TO FERROGRAPHIC EVALUATION OF SELECTED TEST LUBRICANTS FROM THIS PROGRAM

by Teri R. Reese

Normal Rubbing and Break-in Wear

Rubbing wear or normal wear particles are generated as the result of normal sliding wear in a machine and result from the exfoliation of parts of what is known as the shear mixed layer. Typically, rubbing wear particles range from 15 μm down to 0.5 μm. Their surface is smooth and they are very thin. During break-in, these particles, along with larger particles, are generated. The result of this process is a smoothing of the contact surface.

Contamination, such as sand, in a lubricating system can cause an increase in the amount of rubbing wear. This contamination may cause a problem even though this type of particle is considered normal, since over time there will be a build up of particulate material in the lubricating system.

Severe Sliding Wear

Severe sliding wear occurs when the wear surface stresses become excessive due to load and/or speed. The ratio of large-to-small particles depends on how far the surface stress limit is exceeded. The higher the stress level, the higher the ratio becomes. Severe sliding wear particles range in size from 15 μm up. Some of these particles have surface striations as a result of sliding.

Dark Metallo-oxides

Dark metallo-oxides are partially oxidized ferrous wear particles. They indicate the presence of heat during their generation and may signal lubricant starvation.

Cutting Wear

Cutting wear is essentially self explanatory. It is the result of one surface penetrating another. There are two ways of generating these particles A misaligned or fractured component may result in a hard , sharp edge penetrating a softer surface. The other way these particles are generated is by hard, abrasive particles in the lubrication system becoming embedded in a soft wear surface, such as a brass cage. The abrasive particles protrude from the softer surface and penetrate the opposing wear surface.

Rolling Contact Fatigue (Rolling Element Bearings)

There are three distinct types of particles associated with rolling bearing fatigue; fatigue spall particles, spherical particles and laminar particles.

Fatigue spall particles constitute the actual material removed as a pit or spall opens up. The particles are up to 100 μm during the microspalling process.. When the spalling becomes macroscopic and failure occurs, the particle size may increase even further. Spherical particles associated with rolling bearing fatigue are generated in the bearing fatigue cracks. Their presence provides a warning of impending trouble. They usually occur before any actual spalling occurs. Spherical particles can originate from welding debris, but these spheres are typically much larger. The normal sphere associated with fatigue is 1-2 μm in diameter. Laminar particles are very thin free metal particles. They are thought to be formed when a wear particle passes through a rolling contact. They are typically generated throughout the life of a bearing, but their quantity increases with the onset of fatigue spalling. Visually, the particles are very thin and often exhibit holes.

Friction Polymers

Friction polymers are characterized by metal wear particles embedded in an amorphous matrix. They are thought to be created by overstress in a critical contact.

Silicon Nitride

During this analysis the problem of how to identify silicon nitride in a ferrogram arose. To solve this dilemma, two pieces of silicon nitride were rubbed together over a glass slide. The particles that sloughed off due to the scraping were then examined with the Ferroscope. The conclusion was that silicon nitride can look very different depending on its thickness. The thicker, chunkier pieces appear black and amorphous under bichromatic light. The thinner pieces can look very refractile and similar to a friction polymer in the same light. The difference is that under polarized transmitted light, the silicon nitride particles tend to look very shiny white. The friction polymers do not.

DISCUSSION OF FINDINGS FROM THREE FERROGRAMS

Bearing 52100-A3

The lubricant, from sample A3-52100 steel with silicon nitride balls, showed normal rubbing wear, severe wear, cutting wear, chunks, laminar particles, spheres, dark metallo-oxide particles, corrosive wear debris, silicon nitride particles, friction polymers, and fibers.

Possible presence of fatigue could have been indicated by the laminar particles, spheres, and a rare amount of chunks. Keep in mind, though, that only three milliliters of oil were used in the bearing. The A3 lubricant showed more cutting wear particles than the other two lubricants. This could have been related to the Rockwell hardness of the 52100 as opposed to the M-50 steel.

Some of the severe wear particles in this sample showed striations and bluing around the edges. Dark metallo-oxide particles, which were partially oxidized ferrous particles,

were also present. This observation suggested that at some point, there was high temperature, i.e. 120-175°C (250-350°F). in the test bearing.

Bearing M-50-B3

Analysis of the lubricant from B3 indicated the presence of normal rubbing wear, severe wear, cutting wear, laminar particles, corrosive wear debris, silicon nitride particles, friction polymers and fibers. There was a greater amount of silicon nitride particles than normal rubbing ferrous particles present.

This observation suggested that the silicon nitride was wearing at a rate equal to or greater than that of the steel components.

The ratio of severe sliding wear particles to normal rubbing wear suggested possible fatigue. To further substantiate this, note that the ferrous particles present tended to be extremely thin, some with holes.

Bearing M-50-X1

The lubricant from sample X1 , steel on steel bearing, contained normal rubbing wear, severe wear, laminar particles, cutting wear, friction polymers and fibers.

The ferrous particles were for the most part, typical of the type of debris expected in a ball bearing. There was less normal rubbing wear than in, for example, a tapered roller bearing. A rare amount of severe wear and laminar particles were present. This is not an uncommon occurrence, however, in a normal operating system.

Comparison of 52100-A3, M-50-B3 AND M-50-X1

Overall, the lubricants from the bearing tests were slightly to moderately contaminated. The lubricant from A3 showed more of the types of ferrous particles expected in an abnormal condition (i.e.: severe sliding wear with striations and bluing, cutting wear, spheres, and laminar particles). The lubricant from B3 had more silicon nitride particles and

less normal rubbing wear than the lubricants from A3. This led to the conclusion that the wear rate of silicon nitride was higher than ferrous wear in the B3 lubricant. Also, there was a higher wear rate of silicon nitride in B3 than in A3. The lubricant from X1 appeared less contaminated with debris than the lubricant from A3, but about the same as B3, as far as ferrous wear was concerned. Friction polymers were present in all three samples. They were characterized by metal wear particles embedded in an amorphous matrix. They were not completely understood, but were thought to be created by overstress in a critical contact.

Appendix B

A REVIEW OF THE LITERATURE ON WEAR IN SILICON NITRIDE-CONTAINING HYBRID BEARING APPLICATIONS

by Michael R. Hoeprich

Introduction

A number of bearing applications were given by Lucek (1988), in which improved wear resistance was desired. Chemicals, abrasives, adhesion and fatigue could affect the wear involved in applications such as gyroscopes, special chemical applications, conveyors, spindles, and small or large main shaft jet engine bearings (Yust, 1988).

Wedeven provided the following list of considerations in studying wear. These should provide a guideline in setting up tests and evaluating results.

I. Tribo-System: Operating Variables
   a) Load
   b) Kinematics
   c) Temperature
   d) Environment
II. Structural Elements of Tribo-System
   a) Lubricant Film
   b) Surface Film
   c) Near Surface Region
   d) Subsurface Region
III. Tribological Interactions
   a) EHD/Micro-EHD Lubrication
   b) Surface Film Formation
   c) Adhesion
   d) Abrasion
   e) Plastic Flow
   f) Tribochemical Reaction
   e) Fatigue
   f) Wear
IV. Tribo-Induced Property Changes of System Components

It has been verified by Dalal (1974) that EHD films develop with silicon nitride in a manner consistent with the current theory. Ceramic materials also respond to conventional

develop with silicon nitride in a manner consistent with the current theory. Ceramic materials also respond to conventional EP additives in lubricants (Fisher, 1985). However, higher lubricant contact temperatures may develop with ceramics relative to steel because of their lower heat conduction coefficient (Gates). However, degradation of the lubricant may be less with ceramic balls, because the ceramic balls are rounder and smoother than steel balls. Thus, asperity contacts and high stress (normal pressure and shear) excursions will be less (Gardos, 1992).

For this program, the test lubricant was a synthetic lubricant which conformed to military specification MIL-L-23699C. Lubricant viscosities were 5-5.5 centistokes at 98.9°C (210°F) and 25 centistokes at 37.8°C (100°F). For these wear tests, the Central film thickness was 0.053 micrometers and the lambda ratio was 1.

Silicon Nitride Manufacture and Finishing Effects

The Cerbec NBD 200 silicon nitride balls used in this project were formed from hot isostatically pressed powder with MgO as a sintering aid. Ceramics have a propensity for fracture because of slip plane constraints which are much more restraining than for metals. To reduce this tendency to fracture, ceramic materials should be dense, free of cracks, voids, and inclusions which serve as stress risers.

The following should be addressed to improve performance (Yust, 1988):

a) Refine microstructure to reduce residual flaw content.

b) Modify microstructure to minimize initiation and retard crack propagation.

c) Design to minimize the onset of fracture.

The following material properties of NDB-200 silicon nitride are from the NORTON ADVANCED CERAMICS Technical Data Sheet:

Density = 3.2 g/cm^3 (0.117 lb/in^3)

Modulus of elasticity = 310 GPa (46X10^6 psi)

Poison's ratio = .26

Coefficient of thermal expansion = 2.9x10^{-6}/°C (1.6x10^6/°F)

Coefficient of heat conduction = 29.3 W/m-k (203 BTU-in/hr-ft^2-°F), 21.3 W/m-k (203 BTU-in/hr-ft^2-°F)

Hardness = 78 Rc

The finishing processes produced cutting and grinding micro scale surface defects which should have been well characterized (Yust, 1988). Grinding ceramic material could have involved micro-fracture (crushing), plastic deformation (ploughing), micro cracks, and residual compressive stresses (Tönshoff, 1991). Micro-fracture (crushing) causes an irregular surface with isotropic roughness; and horizontal cracks remove flat chips from the ground surface of the workpiece material (Wobker, 1993 verbal). Silicon nitride has a hardened surface layer formed by plastic deformation during grinding. This layer is approximately 15-36 micrometers thick with the most severe material alteration in the first 2-3 micrometers (Tönshoff, 1989).

If grains were found growing from the inside walls of open pores and cracks, these voids were present before testing or machining. The grains grew from the sides of the open pores and cracks during sintering (Tönshoff, 1989).

Tungsten carbide was sometimes present in silicon nitride as an impurity from powder manufacture (NBD-200 does not contain tungsten carbide). Testing indicated tungsten carbide may contribute to surface deterioration through spalling. Tests indicated the presence of tungsten carbide had no detrimental effect on surface wear. Structural integrity of the silicon nitride was the primary factor (Braza,1991; Allen,1993).

Silicon Nitride Wear

Silicon nitride wear occurs via several mechanisms. Fatigue, plastic deformation, tribochemical wear of various types, fracture, and polishing by debris can all play a role. The dominant mechanism of wear depends on whether the contact is lubricated or dry, against ceramic or metal, if moisture is present or not, the finishing process, material integrity, and type of loading (Jahanmir-Summary and Tribology Issues (1991), Fisher (1990), Ajayi (1989), Braza (1991)).

As indicated above, the rate of wear is a complex function of the environment. Wear can increase significantly (approximately two orders of magnitude) if a threshold load level related to surface material fracture is exceeded. The friction force (coefficient of friction) strongly affects this transition to severe wear. A small reduction in the coefficient of friction can result in a substantial reduction in wear or conversely in a large increase in the required transition load. The coefficient of friction can be reduced by hydrocarbon lubricants and polar additives (Jahanmir-Workshop Summary).

Because the conditions in a rolling element bearing are different than in many experimental rigs, the wear mechanisms discussed in the literature may apply to rolling element bearing wear in various degrees. However, all of these mechanisms should be considered in the analysis of bearing wear regardless of their perceived likelihood.

Dry Contact Wear

Unlike metals, the dominant wear mechanism for silicon nitride in dry sliding is micro fracture, not plastic deformation (Fisher, 1990). In the absence of moisture, friction remains fairly constant (around .8) and wear occurs by fracture. Fisher and Tomizawa (1985) found that in a dry atmosphere, silicon nitride wears by two fracture mechanisms. Within one micrometer of the surface, large local stresses exist and cracking is on a very fine scale. At a depth of three to five micrometers, the fracture follows weaknesses in the material, intergranular fracture with transgranular cleavage. No evidence of plasticity was observed.

In sliding wear tests, Ajay and Ludema (1989) observed two wear mechanisms and a transfer film affecting the wear rate. Microfracture from asperity tips accounted for a small amount of wear. Most of the material removal occurred by a surface fatigue mechanism. It was also found that a transfer film formed, which consisted of reattached fine wear debris particles held on by van der Waals forces. The presence of a liquid would reduce these adhesive forces and could prevent formation of a film. The transfer film protects the surface and reduces the wear rate. The film results in greater friction but less wear, because the film may be softer than the substrate.

When brittle fracture is the wear mechanism, it has been observed that facetted particles are produced (Dalal, 1974). Quite possibly, then, higher aspect ratio grains could improve performance because a more tightly interlocked grain structure would be created. This structure would be more resistant to grain pullout and crack development (Allen, 1993). If fracture is present, severe abrasion has most likely occurred; however, a smooth surface indicates the abrasive wear was by fine particles (Fischer, 1990). In a test involving dry contact sliding between silicon nitride and 52100 steel, Gardos and Hardesty, (1992) found the wear mechanism to involve grains being pulled out. This probably involved grains lying parallel to the surface and grain fracture of those lying perpendicular to the surface. Surface analysis showed the silicon nitride surface picked up 6 to 8% iron from the raceway and the steel raceway picked up 5 to 6% silicon.

Though it may be suspected that hardness should not correlate with wear resistance because ceramics wear by micro fracture and not plastically, as for metals. This may not be the case since it has been found that higher hardness does correlate with lower wear. Perhaps this correlation between hardness and improved wear resistance is due to less sintering aid (Fischer, 1990; Lucek, 1990; Katz, 1991). Wear also seems to increase with larger grains (Gates, 1988).

When metals are in contact with ceramics, metals deform plastically in the contact and do not generate high enough contact stresses to induce wear by fracture in the

ceramic. In unlubricated service, metal wear occurs by transfer of metal onto the ceramic surface. The ceramic material wears either by fatigue or by tribochemical reaction with the metal and environment (Fischer, 1990).

Studies on ceramic tool wear indicate increased residual stress from the finishing process reduces wear. However, it is not entirely clear whether the reduction in wear is due to the higher residual stress or the attendant surface hardening due to plastic working (Tönshoff, Wobker).

At high temperatures, oxidation of the primary phase is also observed to contribute to the wear process (Jahanmir-Tribology Issues).

Lubricated Wear

In rolling contact, Braza (1989) found the wear mode to be primarily grain pullout (cracked out by grain boundary tensile stress crack development) for reaction bonded material without sintering aids. For hot pressed or pressureless sintered material, submicron chipping was the dominant wear mode. WC reduces polishing wear in sliding. Lucek (1990) observed lubricated rolling contact wear to occur primarily by intergranular fracture in the compressed zone of the contact. Some pit spalling from cracks developing along the sides of the wear track due to tensile stresses also added to the wear. In highly stressed steel ball-on-rod life tests, Burrier (1995) found silicon nitride wear degradation to vary with material fatigue resistance. Silicon nitride which exhibited the greatest fatigue life (and higher hardness) experienced minor grain pull out. Materials with poor fatigue lives exhibited significant microspalling.

In the lubricated sliding of silicon nitride against steel, the wear mechanism involves a polishing or grinding action due to an Fe(oxide)-Si_3N4 slurry (Braza, 1989 and 1991; Gangopadhyay, 1989). In dry pin-on-disc tests conducted by Tennenhouse (1988) at high temperatures, Mn and Fe were found to combine with Si from the Si_3N_4 to form a tribo material on pins (high temperatures). Silicon nitride oxidation wear decreased with reduced oxygen. At lower ambient temperatures and lubricated sliding, discoloration, which is composed of

wear debris or an oil degradation product and debris mixture, forms along the sides of the wear track (Yust, 1990).

Denape (1992) observed a similar progression of wear in boundary lubrication for silicon nitride rubbing against 52100. Initially, wear occurred through abrasion of the steel (possibly creating grooves) and microcleavages of prominent silicon nitride asperities (providing a polishing abrasive). After an initial period of time, a metallic layer made of iron and chromium carbide (strongly oxidized) forms on the steel. This layer tends to flake off due to delamination. A reaction film (due to high temperature and pressure) can form on the metallic layer. The silicon nitride is polished by the previously generated ceramic debris. As the friction and temperature go down (surfaces smooth up and pressure drops as the pin wears), the reaction film is no longer replenished and it wears off. Jahanmir (Tribology Issues, 1990) states, however, that the details of the boundary lubrication process are not well known, particularly the adsorption mechanism of polar compounds on ceramics.

The strong role iron plays in the formation of the friction polymer is discussed by Klaus, 1990. In a Si_3N_4 on Si_3N_4 system, the addition of iron (iron salt) to the lubricant decreases wear. The iron promotes the oxidation of mineral oils and phosphate esters, which leads to an enhanced production of friction polymer. Thus, wear resistance is best when there is an unlimited supply of iron, such as when a steel surface is present. Klaus also found straight mineral oil to be a better lubricant than tricresyl phosphate; however, 1% tricresyl phosphate in mineral oil was significantly better for Si_3N_4 on Si_3N_4 and about the same as mineral oil for steel on Si_3N_4.

From the wear diagrams given by Jahanmir (Tribology Issues) and the low raceway coefficient of friction, the bearing wear will be a mix of tribochemical reaction and fracture regimes. The large lambda ratio will skew the wear toward tribochemical reactions.

In lubricated pin on disc wear tests, Dalal (1974) noted that the friction was lower when the pin moved perpendicular to the finish rather than parallel to the

finish. This is probably a fluid film thickness effect, since it was noted the friction did not change with finish orientation when the contact was dry. A thicker lubricant film is generated when movement is perpendicular to the finish lay.

Moisture

Moisture has a significant effect on silicon nitride wear whether the moisture is in the test atmosphere or in the lubricant, or if the test is run in water. The wear rate and coefficient of friction go down in the presence of moisture and are a complex function of sliding velocity, load and temperature. In a humid atmosphere or in water, an amorphous protective layer forms, probably a highly hydrated amorphous silicon oxide. Vickers pyramid indentations are 10 to 20% larger in this material than in material adjacent to the wear track. In the presence of moisture, wear debris is predominantly amorphous (silicon oxide) with dispersed fine Si_3N_4 crystallites a few nanometers in size. Dissolved water in a lubricant can do the same thing. Grain boundaries can be attacked, resulting in the removal of entire grains from the surface. In a humid atmosphere, cylinders are rolled from the soft tribo-material which flakes off the surface. These cylinders are 1 to 3 micrometers long and 0.15 micrometers in diameter and can be found laying on the surface. When this Tribochemical material is present, the friction coefficient is around .2 (Fisher, 1985 and 1990; Tomizawa).

There is a balance between tribochemical reactions and the rate of mechanical wear. When the wear rate exceeds the tribochemical reaction rate, wear occurs by fracture and the wear rate increases dramatically. At high temperatures, the friction coefficient is .8 in all atmospheres and wear occurs by fracture (Tomizawa, 1987).

Wear in an intermediate humidity level is a mixture of dry and high humidity modes (fracture and tribochemistry). A tribochemical film forms in this intermediate level of humidity. When this film fractures to form pits, there is an absence of fine fracture cracks in these pits. This observation supports the idea that the tribo film prevents asperity stress concentrations which are most likely responsible for the fine grain fracture found in dry contacts (Fischer, 1985).

Raceway Wear

Abrasive wear and plastic deformation are expected to be the primary raceway wear modes. There may also be metal transfer to the silicon nitride. In steel ring on silicon nitride block wear tests, it was observed that the steel wear occurred through abrasive wear, plastic deformation of asperities, and circumferential wear grooves. The friction coefficient reached a peak value on start-up and rapidly decreased to a steady state value within a few minutes. A chemical reaction occurred between silicon nitride and the chrome in stainless steel carbides, which resulted in excessive wear. However, the lower temperatures in rolling contacts would not initiate this kind of wear (Braza, 1991; Fischer, 1990).

Retainer Wear

Braza (1992) conducted wear tests for silicon nitride with several cage materials and lubricants. There was no perceptible wear of the silicon nitride for any test combination. PEEK with glass fiber fill and PEEK with carbon fiber fill had the lowest friction with no discernible wear. Brass had the most wear and exhibited stick-slip behavior. Dicronite coated aluminum exhibited similar wear behavior as brass. Silver plated 4340 rings wore, but did not loosen from the substrate. Wear was less than for brass or the dicronite coating.

Mathematical Wear Models

Ludema lists various wear models, but suggests that none of the published models is really satisfactory. The first is the Archard model:

$$V/d = KW/p_m$$

where V = wear volume
d = distance of travel
W = applied load
p_m = the pressure hardness
K = wear coefficient

This can also be written as a rate equation:

$$dV/dt = KUW/p_m$$

where U = relative surface velocity

For reaction rate wear: $K = K_m\alpha$, where α = fractional film defect.

Abrasive wear has been fit with the equation:

$$dV/dt = WV/p_m$$

Bhushan uses the following equation to calculate the wear coefficient for ball wear in a rolling four ball tester:

$$k = 0.129(pv)/(sca^3\sigma)$$

where
- p = hardness (kg/mm^2)
- v = volume removed
- s = spin to roll ratio
- c = stress cycles
- a = contact radius
- σ = maximum contact stress

For a ball bearing, the wear life can be calculated from the following equation:

$$L = d(p/k)/(PV)$$

where
- L = bearing life from wear failure
- d = maximum acceptable wear depth
- p = DPH hardness of bearing material
- k = wear coefficient (2E-7 for a dry Si_3N_4 bearing)
- P = nominal load pressure
- V = sliding velocity

Katz uses the following equation for Si_3N_4 RCF wear which considers hardness and fracture toughness:

$$\text{Wear} \approx \text{Load}^{Q}/(K_{Ic}{}^{m}H_{v}{}^{n})\cdot(E/H_{v})^{P}(\text{Distance})$$

where $m \& n \approx 0.5$
$Q \& P \approx (0.8\text{-}1.2)$

Kim gives another relationship for dry rolling contact wear associated with brittle fracture:

$$\text{Wear} = \alpha Sc^{n}$$

where $\alpha = 1.56 \times 10^{-5}$
$n = 5.46$
$Sc = Pm(Rmax)^{.5}/K_{Ic}$
Pm = mean Hertzian pressure
$Rmax$ = mean value of maximum surface roughness of wear groove.

$$K_{Ic} = 0.013(E/H)P^{.5}Cr\text{-}1.5$$

E = Young's modulus
H = vickers hardness
P = indentation load
Cr = length of radial crack induced by vickers indentation

Gardos uses the Evans-Wilshaw wear model:

$$\text{Wear Volume} \approx 1/(K_{Ic}{}^{3/4}H_{v}{}^{1/2})\cdot\Sigma P^{5/4}d$$

However, he suggests there may be problems with using K_{Ic} and H_v as wear determining parameters:

1. Hardness is not a fundamental property; it depends on the elastic and plastic response of material.

2. K_{Ic} depends on the residual stress in the ceramic; and the size, type, and frequency of surface flaws from the finishing process.

3. Are K_{Ic} and Hv sufficient parameters?

4. What happens in high temperature air.

Allen (1992) notes that wear models should be formulated in terms of the microstructure (grain size, grain strength, quantity and strength of grain boundary phase) and applied conditions (stress, test environment, and surface roughness).

Compilation of Published Wear Data

Sliding Contact

Braza , (1989) Si_3N_4 vs. nodular cast iron in mineral oil:

Si_3N_4, $0.6\text{-}2.0\times10^{-9}$ $mm^3/(N\cdot m)$

Denape, (1992) Si_3N_4 vs. 52100 steel pin, boundary lubrication

(Total-Rubia X):

steel, $0.01\text{-}1.0\times10^{-6}$ $mm^3/(N\cdot m)$
Si_3N_4, negligible

Klaus, (1991) Steel on Si_3N_4 and Si_3N_4 on Si_3N_4 exhibit a high wear run in a period of 30 minutes followed by a slow linear wear increase. The wear scar wears about 15% larger than the Hertzian diameter during the initial wear-in.

Yust, (1990) Si_3N_4 pin vs. Si_3N_4 whisker-Si_3N_4 composite disc. Data only from lubricated unidirectional testing will be given here.

Si_3N_4, 7.7×10^{-9} $mm^3/N\text{-}m$
Si_3N_4 whisker-Si_3N_4 composite, not measurable

Wear factors of 1.0×10^{-6} $mm^3/N\text{-}m$ or greater represent severe wear.

Rolling Contact

Braza, (1989), Si_3N_4 vs. nodular cast iron in mineral oil:

Si_3N_4, $.2\text{-}1.2\times10^{-10}$ $mm^3/(N\cdot m)$

Lucek, (1990), Si_3N_4 vs. M50, Wear appears to increase rapidly at start up and then increase very slowly. Stress drops off as wear modifies contact geometry.

steel, 0.2×10^{-2} mm^3

Si_3N_4, 0.03×10^{-2} mm^3

Cleaning Procedures

Specimen cleaning procedures can affect measured coefficients of friction. Improper cleaning has erroneously resulted in ceramics being thought of as low friction materials. To avoid these problems, Gates used the following cleaning procedure:

1. Ultrasonic cleaning with hexane/toluene (9:1) to remove residual polishing oils.

2. Ultrasonic cleaning with acetone to remove polar surface contaminants an residual hexane and toluene.

3. Ultrasonic cleaning with a laboratory detergent (micro at 2% concentration in deionized water) to remove residual organics.

4. Several ultrasonic rinses with deionized water to remove residual detergent.

5. High temperature bakeout when feasible.

Test Method and Considerations

Test methods should be analyzed to prevent unexpected or undiscovered factors from affecting and possibly invalidating

test results. For instance, machine dynamics and ambient vibration are probably often neglected (Yust, 1988). In ball on rod tests, Lucek (1990) found profilometer traces to be acceptable for rod wear measurements. Ball wear scar width was measured optically, but simple micrometers were found to be as accurate and even more repeatable.

The selection of a wear test method should be a function of the following considerations:

wear test = f (geometry, alignment, vibration) . . . . . (inherent to apparatus)

+ g (speed, load, duration, temperature) . . . . . (operator controlled)

+ h (lube, material) . . . . . (mat'l selec. & history)

+ i (atmosphere) . . . . . (environmental aspects)

Expected Silicon Nitride Composite Bearing Wear Mode

In lubricated rolling contact, the silicon nitride wear mode is primarily grain pullout (cracked out by grain boundary tensile stress crack development), intergranular fracture, and submicron chipping. Some pit spalling from cracks developing along the sides of the wear tract due to tensile stresses also add to the wear. If the humidity is high, tribochemical reactions may contribute to the wear.

For the steel raceways, abrasive wear and plastic deformation are expected to be the primary raceway wear modes. There may also be metal transfer to the silicon nitride.

The bearing wear tests conducted in this project are at stress levels significantly lower than rolling contact tests cited above. The film thickness to roughness ratio was 1.0 at the beginning and reduced to 0.3 in subsequent tests (low but not extreme). Consequently, any grain pull-out may likely be rare. Since the lubricant will be heated, no moisture should be present in these tests which could affect the wear process. It is anticipated that the Archard wear model will be a suitable starting point. Available wear data indicates the

rate of wear of ball contacts decreases with time (implying exponents would be appropriate on operating parameters). Of course, these data were gathered at high stress levels and it is not known if these same wear mechanisms are operative at the bearing test conditions. It would also be likely that other bearing types would wear at other exponential rates.

Bibliography

Ajayi, O. O. and Ludema, K. C.,"Formation of Transfer Film During Ceramics/Ceramics Repeat Pass Sliding," Wear of Materials, 1989, vol. I, pp 349-359.

Allen, D. L.,"Effect of Composition and Physical Properties of Silicon Nitride on Rolling Wear and Fatigue Performance", STLE Annual Meeting, Calgary, May 17-20, 1993, Preprint No. 93-am-6f-2.

Bhushan, B. and Sibley, L. B., "Silicon Nitride Rolling Bearings for Extreme Operating Conditions," ASLE Trans., 25, 4, pp 417-428 (1982).

Braza, J. F.,"Tribological Evaluation of Silicon Nitride Against Retainer Materials," SAE Paper 921723, International Off-Highway & Powerplant Congress & Exposition, Milwaukee, WI, Sept. 14-17, 1992.

Braza, J. F. and Braza, P. A.,"Examination of Silicon Nitride in Lubricated Sliding Wear Tests," Advances in Engineering Tribology, Y. P. Chung and H. S. Cheng, Eds., Spec. Publ. No. 31, STLE, Park Ridge, IL, pp. 133-144 (1991).

Braza, J. F., Cheng, H. S., Fine, M. E.,"Silicon Nitride Wear Mechanisms: Rolling and Sliding Contact," STLE Tribology Transactions, Vol. 32 (1989), 4, 439-446.

Burrier, H. I., "Optimizing the Structure and Properties of Silicon Nitride for Rolling Contact Bearing Performance," to be presented at 1995 STLE Annual Meeting in Chicago.

Dalal, H., Chiu, Y. P. and McCool, J. I.,"Surface interactions and Lubrication Response of Silicon Nitride Bearing Elements," Final Report, Naval Air Systems Command Contract No. N00019-73-C-0150, February 1974.

Denape, J., Marzinotto A. and Petit, J. A.,"Roughness Effect of Silicon Nitride Sliding on Steel Under Boundary Lubrication," Wear, 159 (1992) pp. 173-184.

Evans, A. G. and Willshaw, T. R., "Quasi-Static Solid Particle Damage in Brittle Solids -I. Observations, Analysis and Implications," Acta Metallurgica, 1976, Vol. 24, pp.939-956.

Fischer, T. E.,"Friction and Wear of Ceramics," Scripta Metallurgica, Vol. 24, 1990, pp. 833-838.

Fischer, T. E. and Tomizawa, H. "Interaction of Tribochemistry and Microfracture in the Friction and Wear of Silicon Nitride", Wear of Materials, 1985, p. 22 (ASME).

Gangopadhyay, A. K., Fine, M. E. and Cheng, H. S.,"Reduction in Wear Rate of α-Alumina and Silicon Nitride by Diffusional Surface Modification," Mat. Res. Soc. Symp. Proc. Vol. 140, ©1989 Materials Research Society, pp. 293-296.

Gardos, M. N. and Hardesty, R. G.,"Fracture Toughness and Hardness-Dependent Polishing Wear of Silicon Nitride Ceramics," Preprint No. 92-TC-5A-2, Presented at ASME/STLE Tribology Conference in San Diego, CA, Oct. 19-21, 1992.

Gardos, M. N. and Pratt, J. R.,"Effects of Machining and Finishing on Performance," Ceramic Bearing Technology, Proc. NIST/DARPA Workshop on Ceramic Bearing Technology, NIST, Gaithersburg, MD, Special Publ. 824 (1991).

Gates, R. S., Yellets, J. P., Deckman, D. E., and Hsu, S. Considerations in Ceramic Friction and Wear Measurements," Selection and Use of Wear Tests for Ceramics, ASTM STP 1010, Yust, C.S. and Bayer, R. G., Eds., American Society for Testing and Materials, Philadelphia, 1988, pp. 1-23

Jahanmir, S.,"Workshop Summary,"Ceramic Bearing Technology, Proc. NIST/DARPA Workshop on Ceramic Bearing Technology, NIST, Gaithersburg, MD, Special Publ. 824 (1991).

Jahanmir, S.,"Tribology Issues Related to Machining and Performance of Ceramic Bearings," Ceramic Bearing Technology, Proc. NIST/DARPA Workshop on Ceramic Bearing Technology, NIST, Gaithersburg, MD, Special Publ. 324 (1991).

Katz, R. N.,"Effects of Composition, Microstructure, and Processing on Ceramic Rolling Element Bearing Performance," Ceramic Bearing Technology, Proc. NIST/DARPA Workshop on Ceramic Bearing Technology, NIST, Gaithersburg, MD, Special Publ. 824 (1991).

Kim, S. S., Kato, K., Hokkirigawa, K. and Abe, H.,"Wear Mechanism of Ceramic Materials in Dry Rolling Friction," Journal of Tribology, ASME, Vol. 108, Oct. 1986, pp. 522-526.

Klaus, E. E., DUDA, J. L. and Wu, W. T.,"Lubricated Wear of Silicon Nitride," STLE Tribology Transactions, Vol. 47 (1991), 8, 679-684.

Lucek, J. W., "Rolling Wear of Silicon Nitride Bearing Materials," ASME Paper No. 90-GT-165, June 1990.

Lucek, J. W. and Hannoosh, J. G.,"Field Experience in Ceramic Bearings," Engineering Materials For Advanced Friction and Wear Applications, F. A. Smidt and P. J. Blau (eds.), ASM International, pp. 205-208 (1988).

Ludema, K. C.,"Seventy Years of Research on Wear," Achievements in Tribology, Sibley, L. B., and Kennedy, F. E., ed., ASME, 1990, pp. 111-127.

Tennenhouse, G. J. and Runkle, F. D.,"Pin On Disk Wear Tests for Evaluating Ceramic Cutting Tool Materials," Selection and Use of Wear Tests for Ceramics, ASTM STP 1010, Yust, C.S. and Bayer, R. G., Eds., American Society for Testing and Materials, Philadelphia, 1988, pp. 43-57.

Tomizawa, H. and Fischer, T. E., "Friction and Wear of Silicon Nitride at 150 C to 800 C, Tribology of Ceramics, Vol. I, Fundamentals, STLE, 1987, pp. 165-172.

Tönshoff, H. K., and Wobker,"Influence of Surface Integrity on the Wear of Ceramic Cutting Tools," Lubrication Engineering, July 1991, pp. 579-583.

Wedeven, L. D, Pallini, R. A., and Hingley, C. G.,"Systematic Testing of Ceramic Rolling Bearing Elements," Selection and Use of Wear Tests for Ceramics, ASTM STP 1010, Yust, C.S. and Bayer, R. G., Eds., American Society for Testing and Materials, Philadelphia, 1988, pp. 58-73.

Wobker, H. G., Roth, P., and Menz, C."Surface Integrity and Wear Behavior of Ground Ceramics," presented STLE Annual Meeting, Calgary, May 17-20, 1993 (presentation only, not for reference).

Yust, C.S. and Bayer, R. G., Selection and Use of Wear Tests for Ceramics, ASTM STP 1010, American Society for Testing and Materials, Philadelphia, 1988, pp. VII-X.

Yust, C.S. and DeVore, C. E., "The Friction and Wear of Lubricated Si_3N_4/SiC(w) Composites," STLE Preprint No. 90-tc-6A-2, ASME/STLE Tribology Conference Toronto, 1990.

Military Specification MIL-L-23699C dated October 4, 1978.

Tönshoff, H. K., Trumphold H., Brinksmeier E. and Wobker, H. G., "Evaluation of Surface Layers of Machined Ceramics, Annals of CIRP, Vol. 38 (1989) 2, pp. 669-708.